NASA Contractor Report 174745

ION THRUSTER SYSTEM (8–CM) CYCLIC ENDURANCE TEST

C.R. Dulgeroff, J.R. Beattie, R.L. Poeschel, and J. Hyman, Jr.

Hughes Research Laboratories
3011 Malibu Canyon Road
Malibu, CA 90265

October 1984

NAS3-21741

Final Report

20 September 1978 through 31 January 1984

NASA AERONAUTICS AND SPACE ADMINISTRATION
Lewis Research Center
Cleveland, Ohio

National
Aeronautics and
Space
Administration

TECHNICAL REPORT STANDARD TITLE PAGE

1. Report No.	2. Government Accession No.	3. Recipient's Catalog No.
NASA CR-174745		

4. Title and Subtitle	5. Report Date
ION THRUSTER SYSTEM (8-cm) CYCLIC ENDURANCE TEST	OCTOBER 1984
	6. Performing Organization Code

7. Author(s)	8. Performing Organization Report No.
C.R. DULGEROFF, J.R. BEATTIE, R.L. POESCHEL and J. HYMAN, Jr.	

9. Performing Organization Name and Address	10. Work Unit No.
Hughes Research Laboratories 3011 Malibu Canyon Road Malibu, CA 90265	11. Contract or Grant No. NAS 3-21741
	13. Type of Report and Period Covered Final Report 20 September 1978 to 31 January 1984
12. Sponsoring Agency Name and Address NASA Lewis Research Center 21000 Brookpark Road Cleveland, OH 44135	14. Sponsoring Agency Code

15. Supplementary Notes

NASA Project Manager: C. Low
NASA Lewis Research Center

16. Abstract

This report describes the qualification test of an Engineering-Model 5-mN-thrust 8-cm-diameter mercury ion thruster which is representative of the Ion Auxiliary Propulsion System (IAPS) thrusters. Two of these thrusters are scheduled for future flight test. The cyclic endurance test described herein was a ground-based test performed in a vacuum facility with a liquid-nitrogen-cooled cryo-surface and a frozen mercury target. The Power Electronics Unit, Beam Shield, Gimbal, and Propellant Tank that were used with the thruster in the endurance test are also similar to those of the IAPS. The IAPS thruster that will undergo the longest "beam-on-time" during the actual space test will be subjected to 7,055 hours of "beam-on-time" and 2,557 cycles during the flight test. The endurance test was successfully concluded when the mercury in the IAPS Propellant Tank was consumed. At that time, 8,471 hours of "beam-on-time" and 599 cycles had been accumulated. Subsequent post-test-evaluation operations were performed (without breaking vacuum) which extended the test values to 652 cycles and 9,489 hours of "beam-on-time". The Power Electronic Unit (PEU) and thruster were in the same vacuum chamber throughout the test. The PEU accumulated 10,268 hr of test time with high voltage applied to the operating thruster or dummy load.

17. Key Words (Selected by Author(s))	18. Distribution Statement
Electric Propulsion 8-cm Mercury Ion thruster Endurance Test	Unclassified - Unlimited

19. Security Classif. (of this report)	20. Security Classif. (of this page)	21. No. of Pages	22. Price*
Unclassified	Unclassified	149	

*For sale by the Clearinghouse for Federal Scientific and Technical Information, Springfield, Virginia 22151.

FOREWORD

The cyclic endurance test described herein was performed by personnel of Hughes Research Laboratories (HRL), Malibu, California. Modifications made to the electronic components were completed by the Space and Communications Group (S&CG), El Segundo, California. Both of these organizations, are a part of Hughes Aircraft Company. The work at HRL was done in the Plasma Physics Department managed by Dr. J. Hyman, Jr., and the work at S&CG was done in the Power Electronics Department managed by W.E. Michel. All work was supported by the Lewis Research Center under NASA Contract NAS 3-21741; Charles Low was the NASA Program Manager. C.R. Dulgeroff was the HRL Program Manager. Other contributions to this program were made by J.R. Beattie, C.R. Collett, R.L. Poeschel, J. Tyrrell, M. Sawins, S. King, W. Wochna, and HRL Security Department Members.

TABLE OF CONTENTS

LIST OF ILLUSTRATIONS

SUMMARY

This report describes the qualification test of an Engineering-Model 5-mN-thrust 8-cm-diameter mercury ion thruster which is representative of the Ion Auxiliary Propulsion System (IAPS) thrusters. Two of these thrusters are scheduled for future flight test. The cyclic endurance test described herein was a ground-based test performed in a vacuum facility with a liquid-nitrogen-cooled cryo-surface and a frozen mercury target. The Power Electronics Unit, Beam Shield, Gimbal, and Propellant Tank that were used with the thruster in the endurance test are also similar to those of the IAPS. The IAPS thruster that will undergo the longest "beam-on-time" during the actual space test will be subjected to 7,055 hours of "beam-on-time" and 2,557 cycles during the flight test. The endurance test was successfully concluded when the mercury in the IAPS Propellant Tank was consumed. At that time, 8,471 hours of "beam-on-time" and 599 cycles had been accumulated. Subsequent post-test-evaluation operations were performed (without breaking vacuum) which extended the test values to 652 cycles and 9,489 hours of "beam-on-time". The Power Electronic Unit (PEU) and thruster were in the same vacuum chamber throughout the test. The PEU accumulated 10,268 hr of test time with high voltage applied to the operating thruster or dummy load.

SECTION I

INTRODUCTION

A 5-mN-thrust 8-cm-diameter mercury ion thruster has been developed and qualified for flight by Hughes Aircraft Company for the NASA Lewis Research Center (LeRC).[1] Two identical thrusters are part of an Ion Auxiliary Propulsion System (IAPS) developed by the Technology Division of Hughes Space and Communications Group under Contract NAS 3-21055 with NASA LeRC for demonstrating ion-propulsion technology. This system will be evaluated in a flight test on a U.S. Technology Satellite. The IAPS flight test will verify the feasibility of using a mercury ion thruster to satisfy the propulsion requirements for North-South stationkeeping of a geosynchronous satellite. In the scheduled flight test (in a non-synchronous orbit) one thruster will be operated intermittently, while the second thruster will be cycled over a 20-month period. Each of the planned 2,557 cycles will include 2.76 hours of normal thrust operation, resulting in a total thrusting time of 7,055 hours.[2] The cyclic endurance test described in this report was a ground-based test (part of the pre-flight preparation). The purpose of the cyclic test was to verify long-term performance. The test system, results and conclusions will be presented in the following sections. The nomenclature used throughout this report is listed in Appendix A.

SECTION II

TEST SYSTEM DESCRIPTION

The thruster that was tested is an Engineering Model (EM) of the IAPS thruster. The Power Electronics Unit, Gimbal, and Propellant Tank are identical in design to the IAPS hardware. The Digital Interface Unit that was used in this cyclic test differs from the IAPS design in that it does not contain the microprocessor that enables IAPS to operate autonomously for extended periods of time. The cyclic endurance test was successfully concluded after 599 cycles and 8,471 hours of thruster "beam-on-time"; post-test investigations extended these values to 652 cycles and 9,489 hours.

The Engineering Model of the IAPS (EM-IAPS) is comprised of the following four major elements: (1) Thruster/Gimbal/Beam-Shield Unit (TGBSU), (2) Propellant-Tank/Valve/Feed Unit (PTVFU), (3) Power Electronics Unit (PEU), and (4) Digital Interface Unit (DIU). These elements are basically the same as those described in detail by Herron et al[3] and will be functionally described in this section. A layout of these components and a summary of specifications for the EM-IAPS are shown in Figure 1. The actual test configuration, which differs somewhat from that shown in Figure 1, will be described later. The PEU and dummy load bank were modified under this program to approximate those used on the IAPS program. The DIU was also upgraded. All of the Engineering-Model components are similar to the IAPS components except for the Digital Interface Unit. The IAPS uses a Digital Controller and Interface Unit (DCIU), with the major difference being the addition of a programmed microprocessor. During the cyclic endurance test, the DIU Unit was located outside of the vacuum test facility and controlled by manual selection of appropriate set points.

10676-4R3

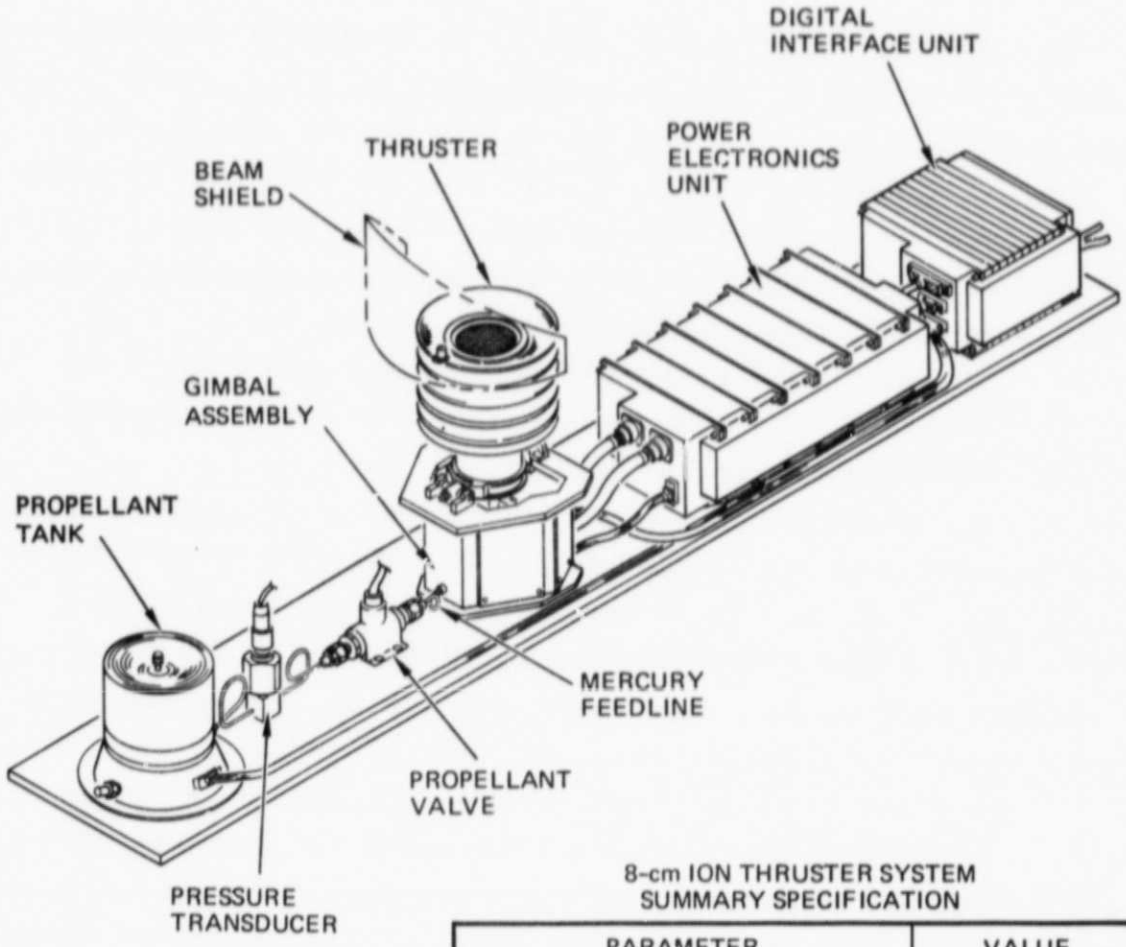

8-cm ION THRUSTER SYSTEM
SUMMARY SPECIFICATION

PARAMETER	VALUE
THRUST LEVEL	5 mN (1.13 mlb)
SPECIFIC IMPULSE	2500 - 3000 sec
SYSTEM INPUT POWER	165 W (TO PPU)
SYSTEM DRY MASS	17.0 kg
MERCURY PROPELLANT CAPACITY	8.60 kg
THRUST DEFLECTION ANGLE	±10 deg
START-UP TIME	⩽30 min

Figure 1. Layout of the Engineering-Model IAPS.

A. THRUSTER/GIMBAL/BEAM-SHIELD UNIT (TGBSU)

The TGBSU is shown in Figure 2. This thruster has a nominal thruster level of 5 mN. The neutralizer can be seen near the center position of the asymmetric beam shield, between the beam shield and the accelerator electrode. This shield was designed to protect the spacecraft from possible interactions during thruster operation. The thruster is attached to a Gimbal Assembly. The Gimbal can re-orient the thrust vector by 10° in any direction from the thruster position shown in Figure 2; the gimbal was also modified under this program. An Engineering-Model TGBSU similar to the one used in the test described in this paper was subjected to a design-verification test at Hughes which included the functional, vibration, and thermal vacuum levels expected during the IAPS flight test.

A cross-section of the thruster is shown in Figure 3. For clarity the thruster is shown in two parts. When assembled the top portion is mounted within the lower portion shown in Figure 3. The callouts in Figure 3 identify the components normally associated with electron bombardment ion thrusters.

B. PROPELLANT-TANK/VALVE/FEED UNIT (PTVFU)

A cross-section of the Propellant Tank is shown in Figure 4. The tank structure consists of a rubber hemisphere which is supported on its exterior by a perforated metal hemisphere and is clamped by a flange that joins it to a matching stainless-steel hemisphere. The mercury propellant is stored in the spherical volume under pressure from nitrogen gas in the volume between the bladder and outer housing. The gas pressure pushes the bladder toward the lower metal hemisphere in Figure 4 as mercury is used by the vaporizer. A pressure transducer is located in the feed line near the tank, and a latching valve is located between the thruster and pressure transducer (see Figure 1). This valve remains closed until the

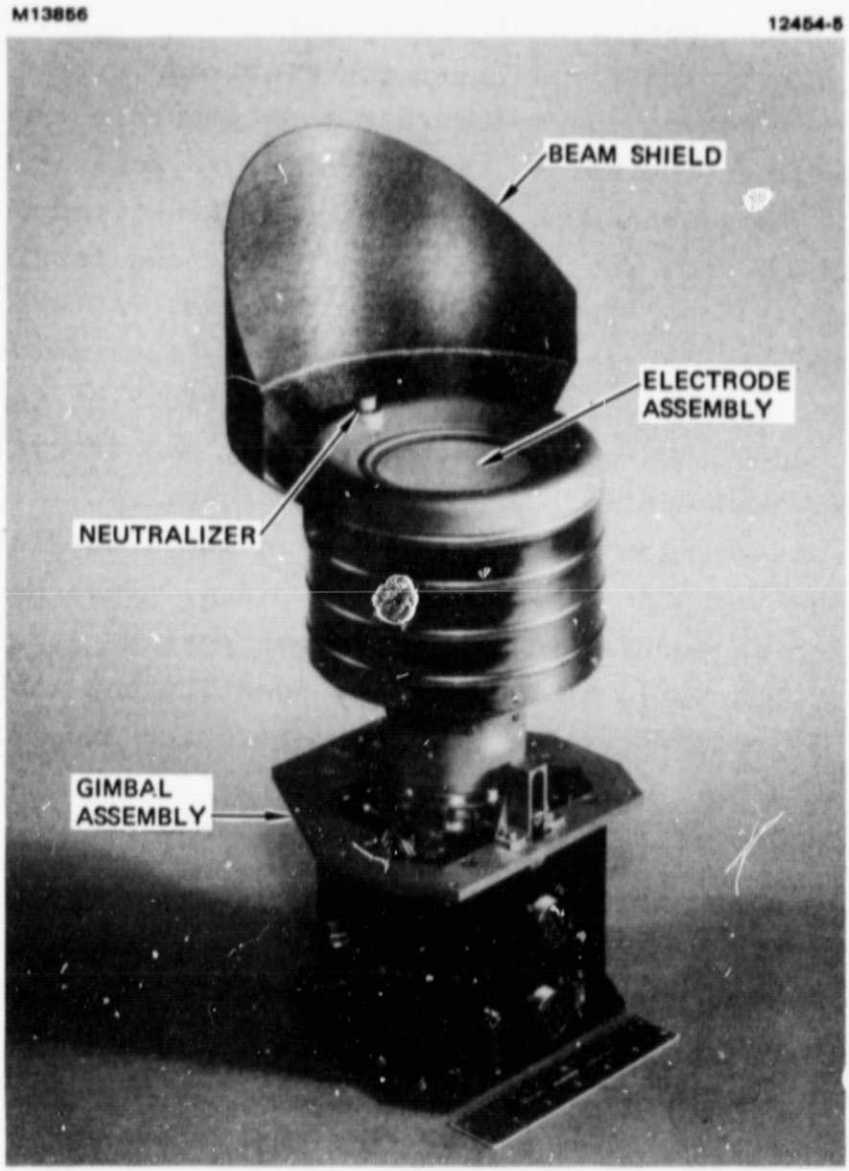

Figure 2. IAPS Thruster/Gimbal/Beam Shield Unit (TGBSU).

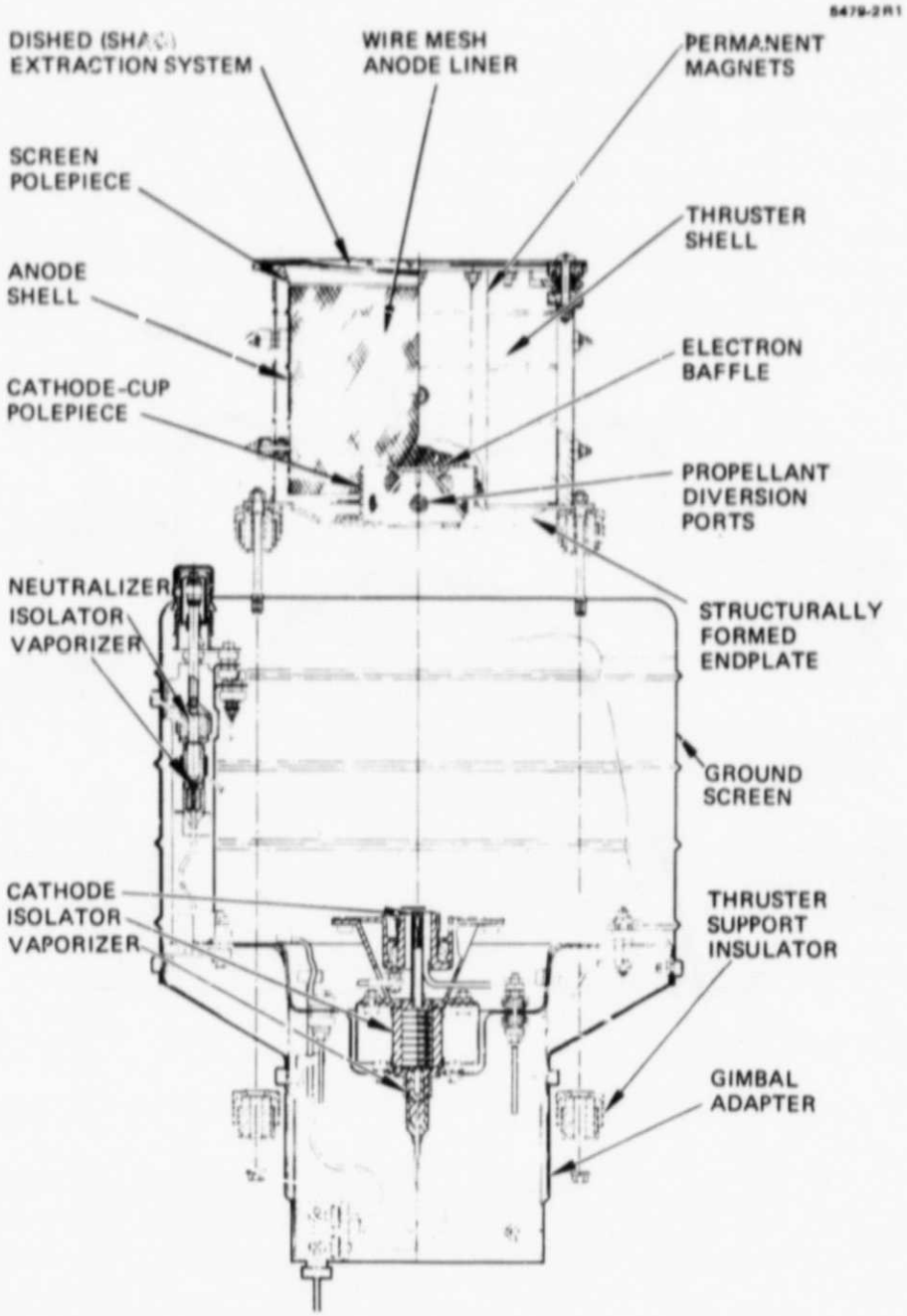

Figure 3. Cross-section of IAPS thruster with discharge chamber elevated from its normal position for clarity.

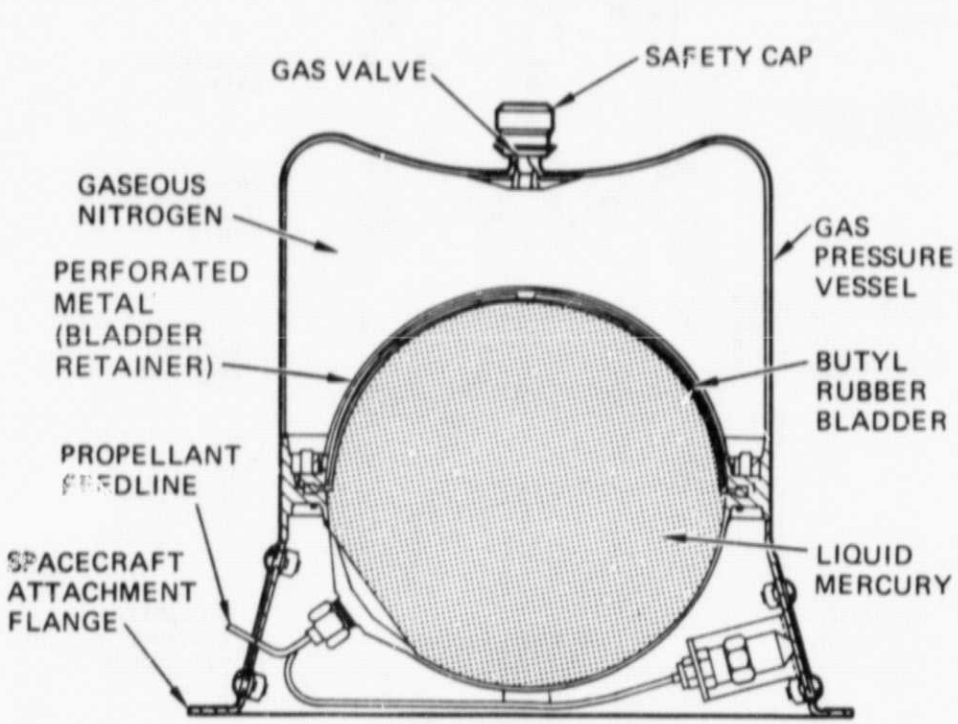

Figure 4. Cross-section of Propellant Tank.

thruster is operated for the first time. Once opened, the vaporizers in the thruster act both as liquid seals and as metering valves; however, the latching valve can be reclosed if required. The pressure transducer provides a means of monitoring the propellant remaining in the reservoir. The tank was filled with 9,217 g of mercury, and then 333 g were off-loaded. The transducer pressure reading was 21.3 psia with 8,884 g in the tank.

C. POWER ELECTRONICS UNIT (PEU)

The Engineering-Model PEU primary power is a 70 ± 20 V-dc power bus. Power at 28 ± 1% V-dc is required by the DIU. A functional block diagram of the EM-PEU is presented in Figure 5. Eleven power supplies, within the PEU, provide power to the thruster. Six of the supplies (heater and keepers) consist of controlled magnetic amplifiers operating from a 96-V-ac distribution bus. The accelerator supply also operates from the 96-V-ac bus. The 96-V-ac power is generated by a 10-kHz transistorized inverter that operates in conjunction with a switching line regulator to provide regulated 48-V-dc power to the inverter. The discharge and screen supplies operate directly from the unregulated primary power and these two supplies provide about 80% of the power required for thruster operation. The control signals for supplying power to the TGBSU from the PEU are furnished by the Digital Interface Unit (DIU).

D. DIGITAL INTERFACE UNIT (DIU)

The DIU issues 0- to 5-V commands to control the PEU. It was designed to be used with a computer capable of operating the TGBSU and supplying the following basic functions:[3]

- Provide storage for the incoming serial digital commands.

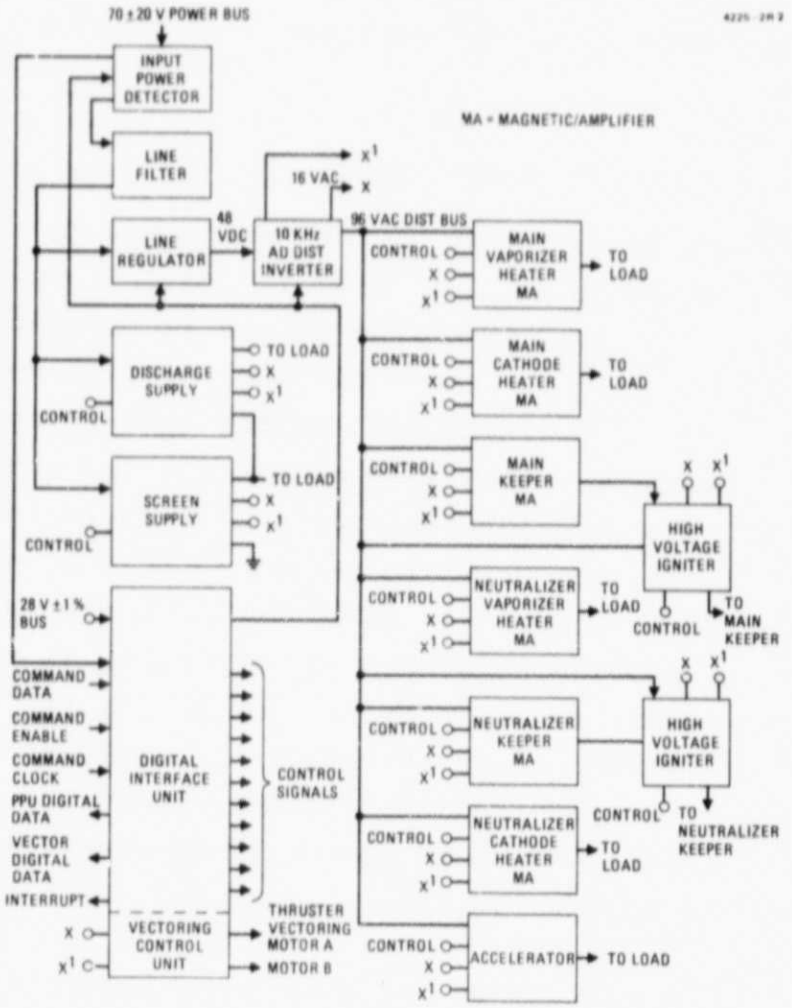

Figure 5. EM Power Electronics Unit (PEU) functional block diagram.

- Convert digital commands to discrete valves or analog reference control signals.
- Turn off the PEU if the input power exceeds ≈ 200 W or if the bus voltage falls below 50 V dc.
- Provide closed-loop control of the two vaporizer supplies to maintain control of thruster operation.
- Provide analog-to-digital conversion of the telemetry signals for use by an external computer.
- Recycle the thruster if a high voltage overload should occur.
- Generate a computer interrupt if an abnormal thruster operating condition should occur.
- Supply power to the gimbal drive motors.

A ground-support test console was used during the cyclic endurance test to provide a manually controlled input to the DIU.

E. TEST FACILITY

A 3.1-m-high by 1.2-m-diameter oil-diffusion-pumped vacuum chamber was used for the test facility of the cyclic endurance test. This life-test facility is shown in Figure 6(a). The chamber is designed to enable the thruster to be mounted so that the ion beam is directed vertically downward toward a frozen-mercury target located at the bottom of the chamber. A liquid-nitrogen-cooled cryoliner near the vertical walls of the test chamber extended from the thruster to the target. The internal thruster support structure and frozen-mercury beam target can be seen in Figure 6(b).

The pumping system has one mechanical roughing pump. Duplicate diffusion pumps and mechanical backing pumps were provided, each with a valve for isolating and/or switching of pumps. Only one diffusion pump and backing pump was operated at one time; however, if either of these pumps malfunctioned it was

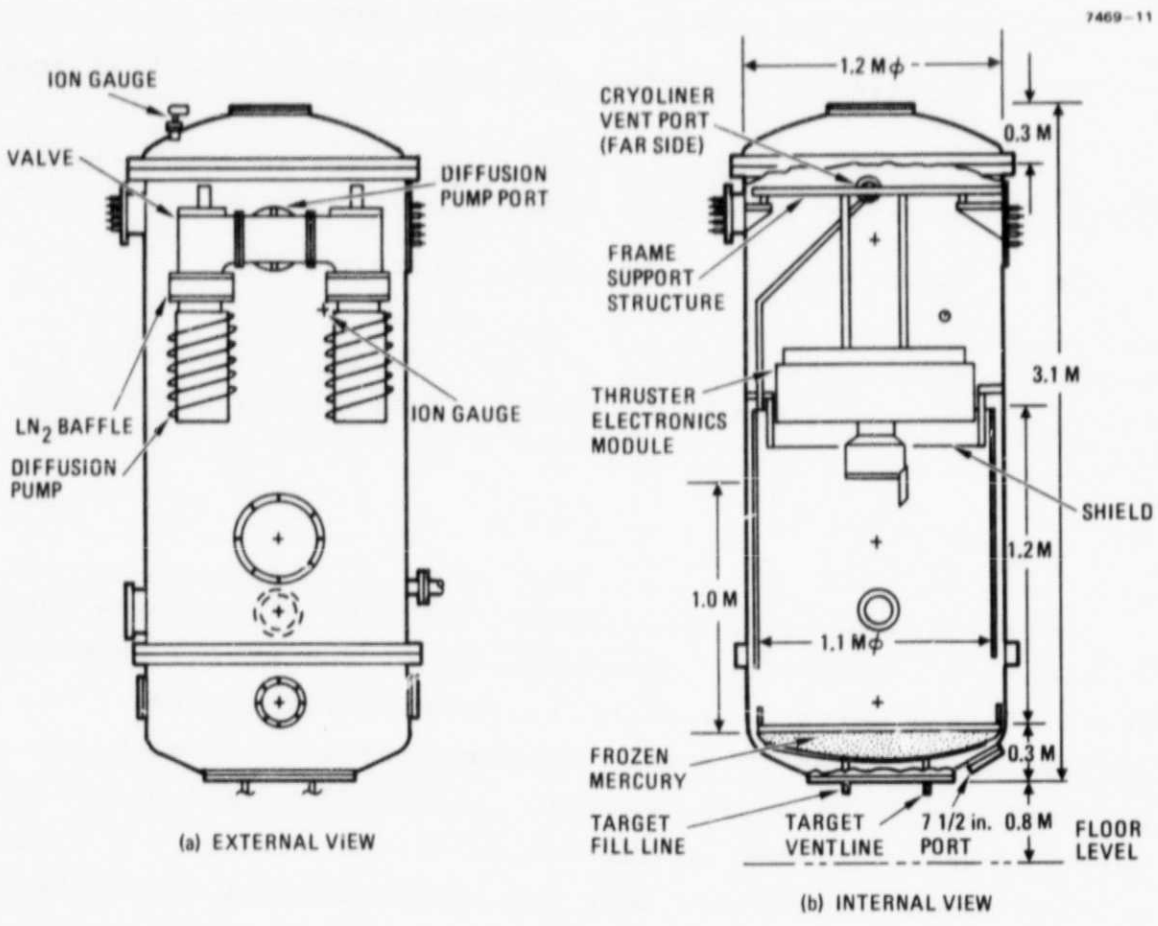

Figure 6. Vacuum life-test facility.

isolated by its valve and a redundant pump would automatically become active and its valve opened. A 12-kW diesel generator provided emergency power for the pumping system. When power outages occurred the diffusion-pump valve would close and the chamber pumping cycle would automatically begin using the emergency power. Power to the thruster would remain "off".

The vacuum obtained was generally 1 to 3 x 10^{-8} Torr (1.3 to 4 x 10^{-6} Pa) with the thruster operating.

F. TEST CONFIGURATION AND INSTRUMENTATION

A test-support mechanical structure was located in the upper part of the vacuum chamber. This test package is located above the test facility in the upper part of Figure 7. The only component that can be seen is the thruster (with beam shield). The PTVFU, Gimbal Assembly and PEU are shown left to right in the electronics module in Figure 8. This photograph was made with the cover of the test fixture removed. Figure 9 is a diagram of the test system. The PEU, TGBSU, and PTVFU were mounted in the electronics module within the vacuum facility. The DIU was located external to the chamber, along with the ground-support test console. An in-line data and recording system was also used. It included two Brush recorders which provided 16 channels of analog recording for the entire test period. A 70-Vdc power supply furnished the primary power to the PEU and a 28-Vdc supply provided the power for the DIU. A third power supply (28-Vdc) was used to activate the latching valve in the feed line. Not shown in Figure 9 are three heaters and their external power supplies. These heaters were mounted under the PEU and Propellant Tank and around the electronics module and were used only if the thruster was not operating for long periods of time to prevent these components from reaching the freezing point of mercury.

M14979

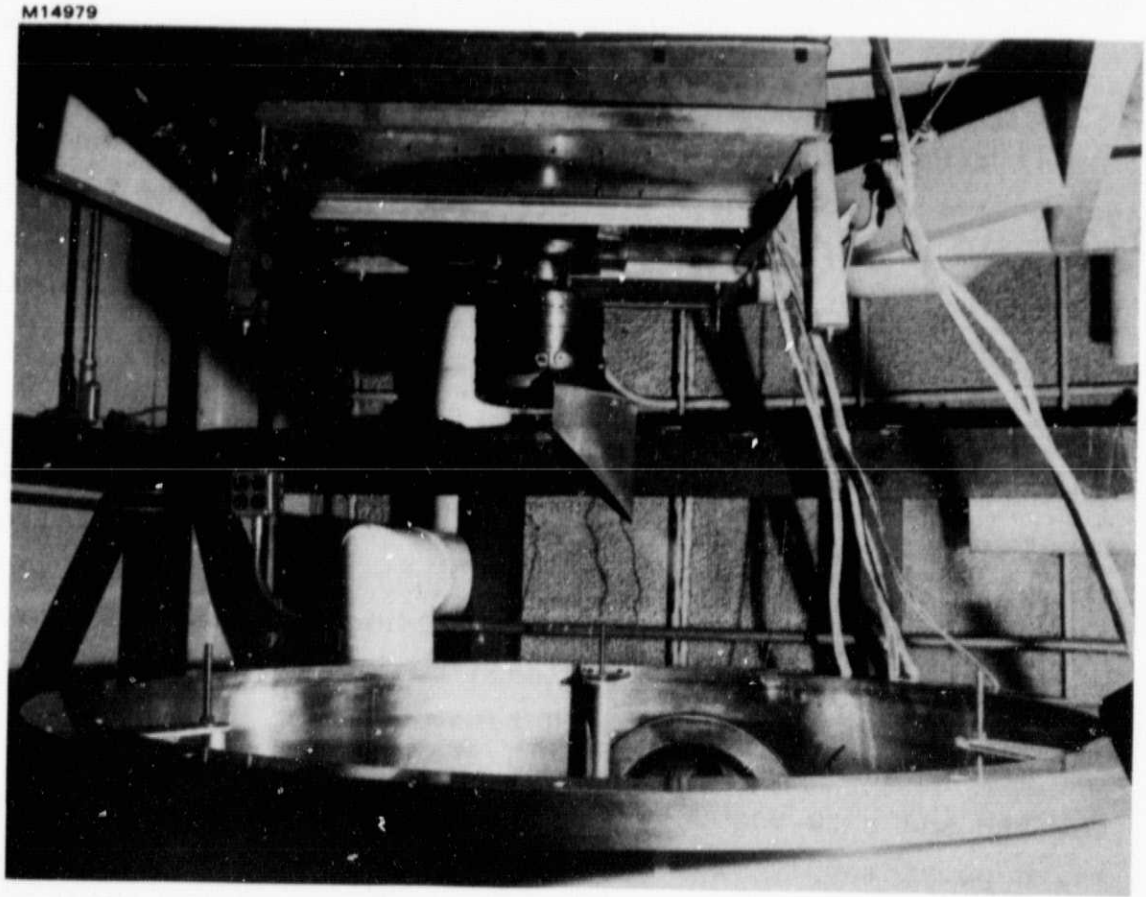

Figure 7. Thruster and electronics module.

M14978

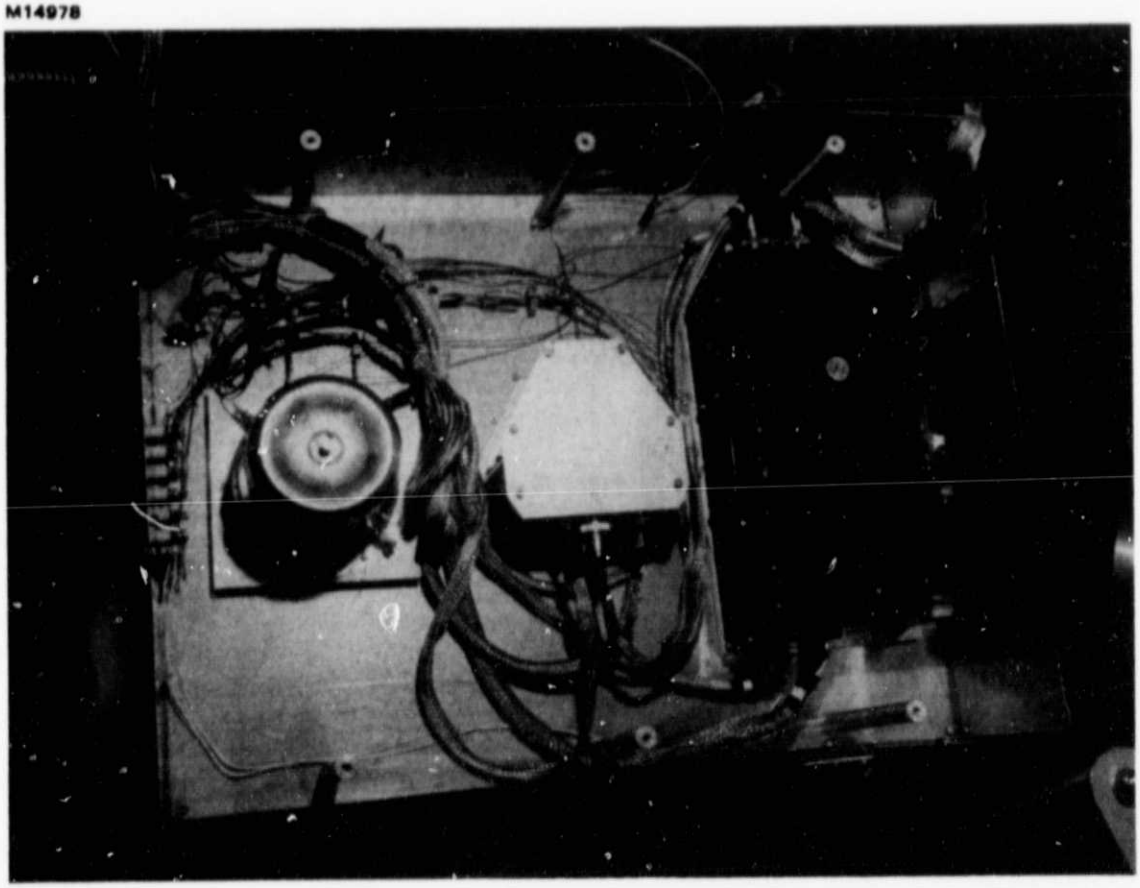

Figure 8. Electronics module with cover removed.

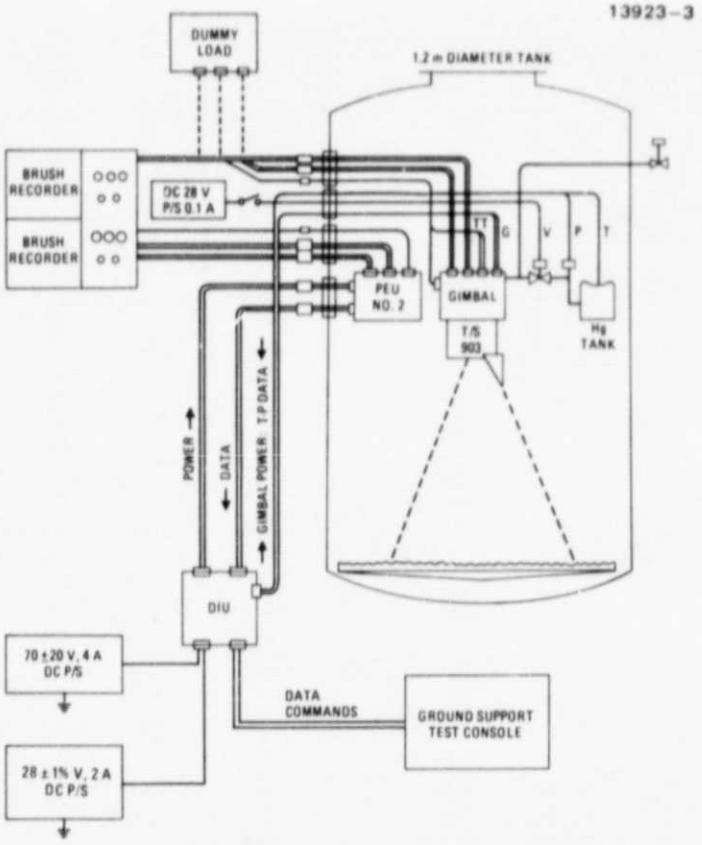

Figure 9. Diagram of cyclic test system.

The ground-support test console was used to provide command inputs to the DIU. The DIU transmitted the signals to control the levels of output power from the PEU. The power from the PEU was then sent through feedthroughs in the vacuum facility to the in-line data system. The power lines returned through the chamber wall to the TGBSU. Thermocouples (not shown) were located on the PEU, Gimbal Assembly and Propellant Tank.

Figure 10 is a photograph of the instrumentation and part of the vertically mounted vacuum facility. Two rack-mounted recorders that can be seen in the left hand side were used throughout the test to monitor thruster parameters and chamber pressure. The third relay rack from the left in Figure 10 contained the in-line analog and digital meters and the bus supplies. The ground support test console and lower portion of the vacuum test facility can be seen on the right hand side of Figure 10.

Since the test was unattended outside of normal working hours, fail-safe protective circuits were used. If the chamber pressure increased to greater than 1×10^{-4} Torr (1.3×10^{-2} Pa) or greater than 2×10^{-5} Torr (2.7×10^{-3} Pa) for 15 minutes, the bus power to the DIU was automatically switched "off". Also, about four months into the test, a protective circuit was added to switch "off" the bus power if the beam level was greater than 76 mA or less than 68 mA (nominal was 72 mA). An alarm box monitored these circuits, and test personnel were notified by the Hughes-Research-Laboratories' Security Department if the alarm box was activated during non-working hours. This alarm box can be seen on the top of the rack-mounted recorder in the extreme left in Figure 10.

M14309

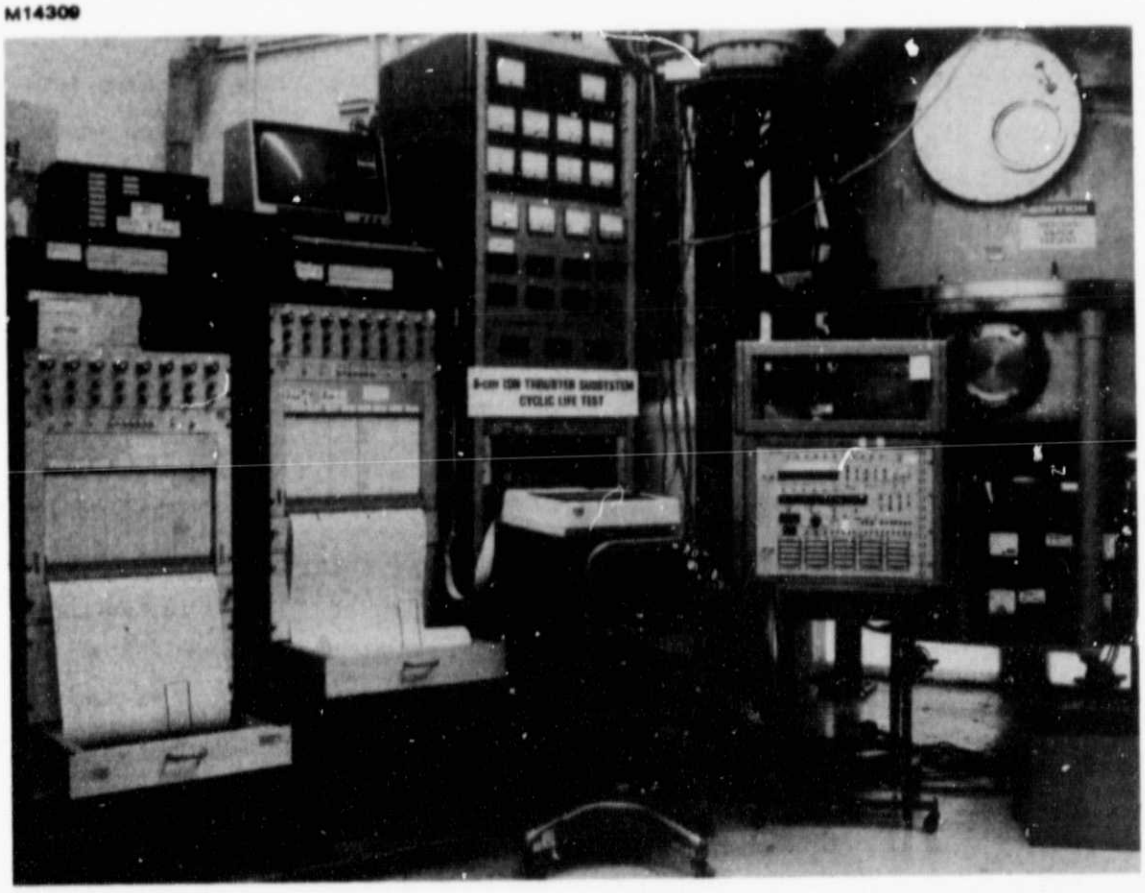

Figure 10. Instrumentation and vacuum facility.

SECTION III

TEST DESCRIPTION AND RESULTS

Prior to the start of the cyclic endurance test, short-term tests were performed to assure that the thruster and associated equipment were functional. Once this was established, the mercury target was filled and the thruster was operated for 48 hours. The cyclic testing began on May 10, 1982, and continued until the mercury in the Propellant Tank was consumed on July 25, 1983. Post-test investigations of the thruster operating characteristics were made without opening the vacuum chamber by using an auxiliary feed system to supply mercury propellant. After those tests the thruster was disassembled for examination.

A. PRE-TESTS

A facility test was performed prior to installing the thruster and electronics module, and filling the target with mercury. This test incuded the following:

- Evacuate the chamber to less than 5×10^{-7} Torr (6.65×10^{-5} Pa) with LN_2 being supplied to the baffle, cryoliner, and target.
- Maintain this condition for 50 hours and obtain a mass analysis scan during this time.
- Allow the cryoliner and target to warm up, close the diffusion pump valve, and vent the chamber.
- Raise and lower the top cover of the chamber.
- Evacuate the chamber to less than 5×10^{-7} Torr (6.65×10^{-5} Pa) with LN_2 being supplied to the baffle, cryoliner, and collector.
- Simulate a power failure to activate the diesel generator.

The pumping sequence was completed in 68 hours (100 hours was the required time). A detailed description of this demonstration test is presented in Appendix B.

When the TGBSU, PEU, and PTVFU were first installed in the test facility, the beam target had not yet been filled with mercury. The next test did not utilize the TGBSU or PTVFU. A dummy load was attached to the power output lines from the in-line data system (see Figure 9). Various tests were performed with different loads and different bus voltages. The only problem encountered with the electronics involved the DIU; it was first noted when the 70-V bus voltage was increased to 90-V and the PEU shut down. This shutdown was caused by failure of a diode in the DIU as a consequence of a wiring error. The diode was replaced, the wiring error was corrected, and the test console DIU, PEU, and in-line data system performed as expected, without further difficulty. A shake-down test of the power processor was performed with the dummy load for 779 hours of accumulated operating time. During this test the chamber pressure was about 2×10^{-7} Torr (2.6×10^{-5} Pa) with liquid nitrogen flowing to the diffusion pump baffle, target, and cryoliner. The results of this test are presented in Appendix C.

After completing these tests, the output lines from the in-line data system were removed from the dummy load and connected to the thruster. The latching valve in the feed line was then opened, and after conditioning the cathodes, the thruster was cycled 10 times and 10 hours of thruster "beam-on-time" was recorded. The operation was judged to be normal and the plan for initiating the cyclic endurance test was implemented.

The target was filled with 591 kg of mercury without opening the vacuum chamber. Following cathode conditioning, the thruster was operated for 48 hours and turned off for 1-1/2 hours; the first cycle of the endurance test commenced on May 10, 1982.

B. CYCLIC TEST

The cyclic sequence for a normal work day is shown in Table 1. Employing this sequence, two thruster "start-ups" were performed during each work day. The thruster was operated at the nominal beam level of 72 mA at all other times, including weekends and holidays. During a normal work week, ten cycles and 148 hours of thruster "beam-on-time" were accumulated.

Table 1. Cyclic Sequence for Normal Work Day

13923-9

TIME	DESCRIPTION
0800	THRUSTER "OFF"
0930	THRUSTER "START-UP"
1000	NOMINAL BEAM LEVEL
1300	THRUSTER "OFF"
1430	THRUSTER "START-UP"
1500	NOMINAL BEAM LEVEL TO NEXT THRUSTER "OFF"

The endurance test began with nominal operating values selected to be close to those of the IAPS thrusters: 72-mA beam current, 1180-V screen voltage, (-)290-V accel voltage, ≈26.5-V difference between discharge and discharge keeper voltages, and 15.5-V neutralizer keeper voltage. The test ran relatively smoothly over the 14-month period. Interruptions were the result of (1) power outages, (2) facility problems, or (3) extinctions of discharge and/or neutralizer.

The vacuum facility performed well. The diesel generator automatically provided power to the pumping system whenever a facility power failure occurred;* however, the protective circuits were designed to turn the bus supplies "off" whenever a facility power failure occurred. The bus supplies were then reactivated and the thruster was restarted manually. Seventeen power failures occurred over the 14-month test period. The liquid-nitrogen-delivery valve malfunctioned twice during the testing period causing the chamber pressure to rise to greater than 10^{-5} Torr (1.3×10^{-3} Pa). Chamber pressure also rose to 0.2 Torr (27 Pa) twice during the test when repairs were being made to a backing pump and a bellows on the backing-pump line. Although these events interrupted the test, they did not appear to affect the thruster performance when the testing resumed following cathode conditioning.

During the test period, interruptions were also caused by neutralizer extinctions, discharge extinctions, or simultaneous neutralizer and discharge extinctions. The history of these interruptions is shown in Table 2.

---

*The Malibu area of Southern California experiences a power failure on the average of 15 times per year

Table 2. Neutralizer, Discharge, and Neutralizer Plus Discharge Extinctions

13923-10

MONTH/ YEAR	NEUTRALIZER	DISCHARGE	NEUTRALIZER PLUS DISCHARGE
MAY/82	1	1	1
JUNE/82	5	1	5
JULY/82	3	0	0
AUG/82	2	1	3
SEPT/82	0	0	1
OCT/82	1	1	5
NOV/82	1	4	0
DEC/82	2	0	1
JAN/83	0	6	1
FEB/83	38	2	2
MAR/83	0	5	2
APR/83	0	9	0
MAY/83	0	8	0
JUNE/83	0	7	0
JULY/83	1	5	0

It can be seen in Table 2 that the greatest number of neutralizer extinctions occurred in February 1983. These extinctions will be discussed later. Discharge extinctions occurred about 1.4 times per week from January 1983 to the end of the test in July 1983, and about once a month prior to that. Neutralizer-plus-discharge extinctions rarely occurred after October 1982. An important abnormality was brought about by extinctions occurring prior to October 1982. (This event is examined thoroughly in the discussion which follows.)

The mercury flowrate through the discharge and neutralizer vaporizers is regulated by closed-loop electronic circuits. These circuits maintain pre-selected voltage setpoints by regulating power to the vaporizers. In the case of the discharge vaporizer, the voltage setpoint is determined by the difference between the discharge-chamber voltage and the voltage of the discharge keeper. For the neutralizer vaporizer, the flowrate is regulated by the neutralizer-keeper voltage.

Whenever an extinction occurs these open-circuit voltages are higher than the setpoint voltage and therefore the heater-power input is automatically increased to the vaporizers, thereby supplying more mercury vapor to the discharge in an effort to decrease the voltage. Whenever the discharges have been extinguished, however, the voltage is not influenced by increasing the mercury-vapor flowrate and therefore full power is supplied to the vaporizers until action is taken by test personnel (prior to mid-October 1982). This sequence is characteristic of the ground-support equipment used in the cyclic test only. Algorithms in the IAPS DCIU should prevent this sequence from occurring during the IAPS flight.

During the cyclic test, both keepers extinguished simultaneously 12 times from May 1982 to the middle of October 1982. On four occasions the condition with full power being supplied to the vaporizers occurred and lasted for periods of between 11 and 16 hours before the condition was detected and the thruster was restarted manually. Start-up of the thruster after one of these events on August 21, 1982 showed an increase of accel current from about 300 μA to 400 μA. The significance of this was not fully appreciated until the cyclic test was completed. Figure 11 shows the accel current as a function of time. The increase in accel current following the event on August 21, 1982 is indicated in Figure 11. There appears to be a slight increase in the accel current during the remainder of the test. In October 1982, it was recognized that full power to the vaporizers for long periods constitutes an abnormal and undesirable mode of operation, so a protective circuit (mentioned earlier) was devised and installed to turn "off" the bus power one minute after a discharge or neutralizer extinction. The circuit also turns "off" the bus power one minute after the accel current exceeds 1 mA. This preventive measure eliminated the possibility of operation with runaway vaporizer power.

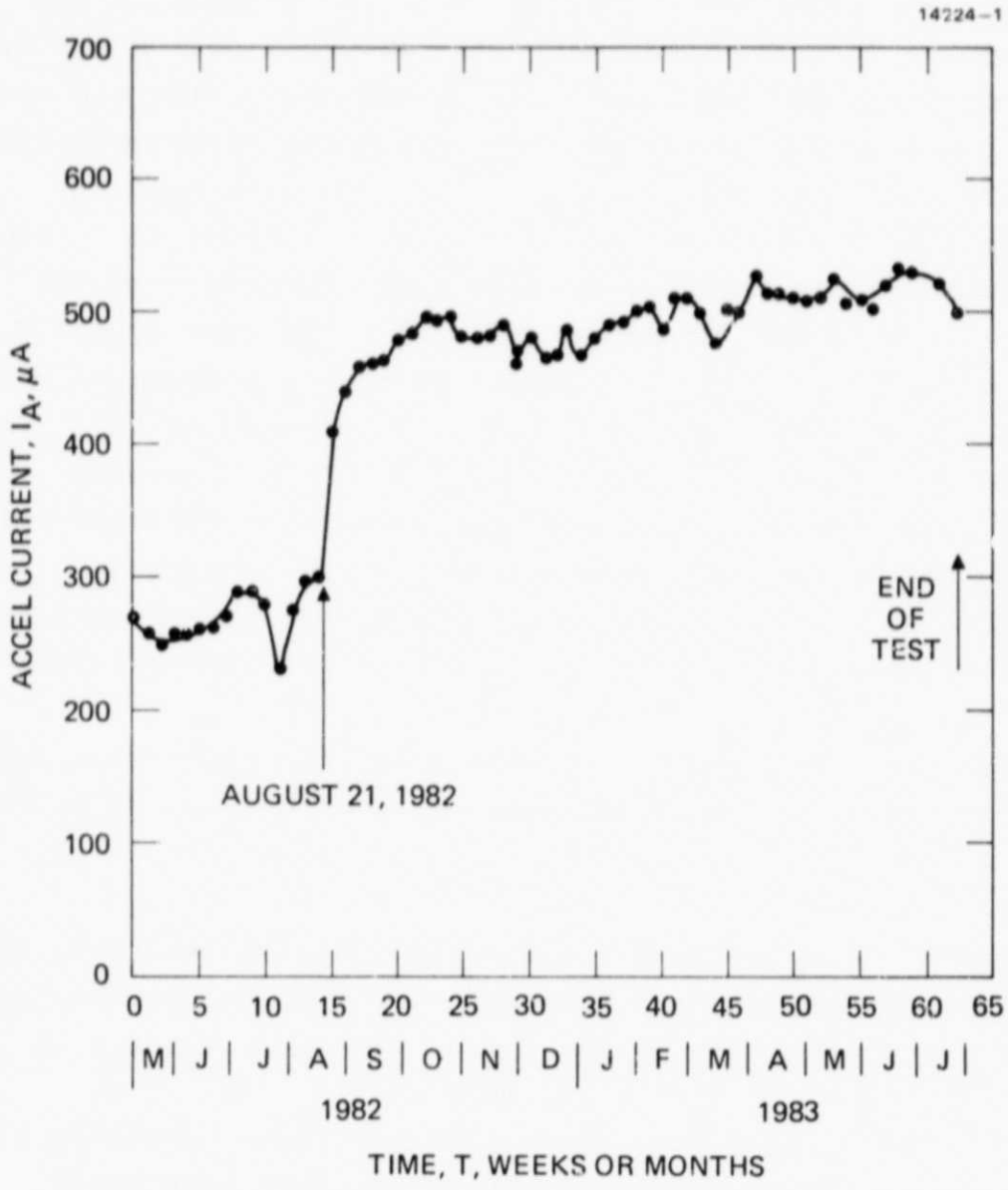

Figure 11. Accel current, I_A, as a function of cyclic test time.

Except for a period when there was an unanticipated high incidence of neutralizer extinctions, the test continued without operational difficulties until the propellant was consumed on July 25, 1983. At that time, 599 cycles and 8,471 hours of "beam-on-time" had been accumulated during the cyclic test. Typical values of thruster parameters throughout the test are shown in Table 3, where it is apparent that V_D decreases with time. This is a result of keeping the value of V_δ constant while the keeper voltage decreased during the test. Although the specified value of V_δ was set at ≈27 V, post-test meter calibration indicated that the measured value of V_{DK} was incorrect and the actual value of V_δ at the end of the test was ≈25 V. The V_δ values shown are the actual values noted during the test using the post-test calibration for V_{DK}. Other notable examples of operating characteristics that changed during the test are neutralizer keeper voltage and current. Neutralizer performance will be addressed later.

An increase in accel current (mentioned earlier) which followed one of the vaporizer-runaway events is noted in Table 3 for August/1982. The variation in coupling voltage that is evident in Table 3 is associated with the neutralizer variations. A total of 436 automatic recycles occurred, with the majority taking place early in the test; the recycle count rate changed after August 21, 1982. There was about a 2% variation in thruster power throughout the test.

Figure 12 shows that the coupling voltage varied by 5 V, the keeper voltage maintained the setpoint voltage until January 1983, and the flowrate deceased (as indicated by the vaporizer flowrate/temperature calibration). This decrease in flowrate was initially believed to be a change in the vaporizer-flowrate-versus-temperature calibration rather than a real effect, since a direct measurement of neutralizer-flow could not be made during the test and because the coupling voltage did not change significantly (hence, there was no reason to expect a change in neutralizer flowrate).

Table 3 Cyclic Test Thruster Operating Values

Date	5/10/82	5/14/82	5/29/82	6/30/82	7/30/82	8/31/82	9/30/82	10/29/82	11/20/82
Cycle Number	1	10	30	73	113	159	199	242	289
"On-time", hrs	50	195	491	1157	1710	2312	2930	3455	4074
V_D, V	38.5	37.9	37.8	37.0	36.6	36.5	36.4	36.2	36.4
I_D, mA	402	402	412	412	412	413	415	414	417
V_{DK}, V	13.4	13.0	12.8	12.1	12.2	11.6	11.5	11.3	11.4
I_{DK}, mA	73	75	75	70	75	75	75	78	78
V_δ, V	25.1	24.9	25.0	24.9	24.4	24.9	24.9	24.9	25.0
V_{DH}, V	3.12	3.12	3.09	3.16	3.16	3.16	3.15	3.16	3.15
I_{DH}, A	1.13	1.13	1.13	1.13	1.13	1.14	1.14	1.14	1.14
V_{DV}, V	5.5	5.60	5.60	5.58	5.00	5.37	5.34	5.39	5.35
I_{DV}, A	1.42	1.42	1.51	1.50	1.33	1.43	1.43	1.43	1.45
V_{NK}, V	15.4	16.2	15.5	15.5	15.3	15.3	15.3	15.3	15.3
I_{NK}, mA	468	465	465	465	465	465	467	467	470
V_{DH}, V	3.83	3.82	3.81	3.82	3.80	3.80	3.81	3.81	3.82
I_{NH}, A	1.28	1.28	1.28	1.29	1.28	1.29	1.29	1.29	1.29
V_{NV}, V	2.82	2.4	3.01	2.90	2.85	2.67	2.62	2.58	2.50
I_{NV}, A	.59	.49	.64	.61	.59	.55	.54	.52	.50
V_S, V	1177	1177	1178	1178	1178	1182	1181	1182	1181
V_B, V	1199	1200	1200	1197	1196	1206	1205	1204	1202
I_S, mA	72.6	72.6	72.8	72.9	72.8	72.8	72.8	72.8	72.8
V_A, -V	290	289	289	289	289	287	286	287	287
I_A, mA	.272	.255	.261	.280	.240	.450	.492	.498	.480
V_C, -V	16.5	15.2	15.8	17.7	18.4	13.0	12.8	13.4	15.8
T_{DV}, °C	280	282	278	278	254	267	261	264	261
T_{NV}, °C	276	253	276	276	264	260	257	252	254
Total Recycles	0	35	75	284	351	359	361	362	365
Total Power, W	130.3	129.8	130.9	130.4	128.5	129.9	129.4	128.4	129.4

(cont'd)

Table 3. (Continued).

Date	12/31/82	1/31/83	2/28/83	3/31/83	4/30/83	5/31/83	6/30/83	7/25/83
Cycle Number	327	363	403	448	489	532	575	599
"On-time", hrs	4714	5279	5813	6346	6922	7530	8100	8471
V_D, V	36.5	36.7	36.5	36.2	36.3	36.3	36.2	36.5
I_D, mA	422	417	417	424	425	425	428	425
V_{DK}, V	11.5	12.0	11.5	11.2	11.1	11.2	11.0	12.2
I_{DK}, mA	75	78	78	78	78	78	79	80
V_δ, V	25.0	24.7	25.0	25.0	25.2	25.1	25.2	24.3
V_{DH}, V	3.15	3.16	3.16	3.17	3.16	3.17	3.16	3.13
I_{DH}, A	1.14	1.14	1.14	1.14	1.14	1.14	1.14	1.13
V_{DV}, V	5.40	5.05	5.00	5.10	5.08	5.05	5.20	5.05
I_{DV}, A	1.45	1.3	1.33	1.34	1.33	1.32	1.38	1.32
V_{NK}, V	15.3	15.3	10.8	10.4	10.3	10.3	10.5	10.7
I_{NK}, mA	475	470	560	558	559	559	559	559
V_{NH}, V	3.80	4.87	3.78	3.78	3.77	3.78	3.76	3.74
I_{NH}, A	1.29	1.67	1.29	1.29	1.29	1.29	1.24	1.28
V_{NV}, V	2.55	1.18	3.42	3.50	3.23	3.53	3.46	3.30
I_{NV}, A	.51	.23	.73	.75	.68	.76	.74	.70
V_S, V	1181	1181	1179	1179	1179	1180	1179	1178
V_B, V	1203	1186	1185	1188	1187	1186	1182	1179
I_S, mA	72.8	72.8	72.8	72.8	72.8	72.8	72.8	72.8
V_A, -V	287	280	280	282	282	282	280	282
I_A, mA	.480	.504	.520	.522	.508	.513	.528	.502
V_C, -V	15.0	32.0	30.9	27	28	30	34	35
T_{DV}, °C	259	252	248	256	253	250	250	252
T_{NV}, °C	245	231	286	286	279	279	282	286
Total Recycles	366	366	368	383	399	409	425	436
Total Power, W	121.8	130.7	128.2	128.4	127.9	128.4	128.8	127.3

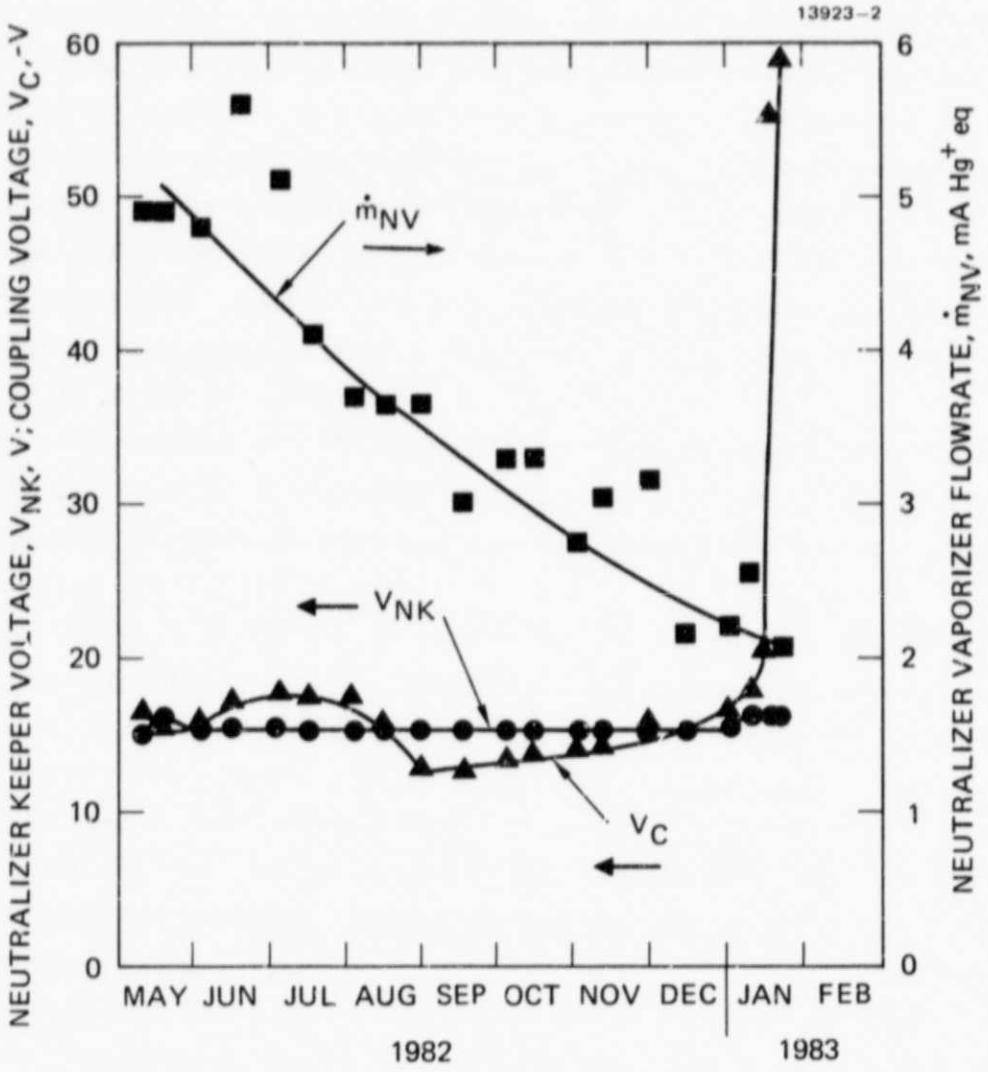

Figure 12. Neutralizer-keeper voltage, V_{NK}, coupling voltage, V_C, and neutralizer-vaporizer flowrate, $\dot{m}_{NV}$, as a function of time.

After December 1982, the coupling voltage could not be kept below 30 V with a keeper voltage of less than 16 V; to correct this condition, two changes were made. The first was to increase the neutralizer-keeper current and the second was to increase the neutralizer cathode power. Increasing the neutralizer-keeper current caused the accel current to increase and become noisy; increasing the neutralizer-tip heater power from 4.9 W to 8.1 W brought the coupling voltage to below 30 V. This improvement in coupling voltage was short-lived however. The next change was to decrease the mercury-vapor flowrate. This change also brought about a short-time decrease in coupling voltage. Throughout these changes, maintaining stable operation of the neutralizer after start-up became a problem and many neutralizer extinctions occurred before a stable condition was established. The coupling voltage was finally restored to $V_C \approx -30$ V by maintaining 4.9-W of tip heat to the cathode, and increasing the neutralizer-vaporizer flowrate to about 7 mA (equivalent). This flowrate value was achieved by maintaining keeper reference voltage at 10 V (approximately 5 V below its value early in the test). Also, although the flowrate was nearly the same as it was at the start of the test, the coupling voltage was higher. Post-test examination revealed that the neutralizer-cathode-orifice diameter had increased, and the keeper aperture diameter had decreased from their nominal values. This explained the poorer coupling characteristics. The reason that the sputtering occurred is attributed to operation of the neutralizer at what was later realized to be a very low (≈2-4 mA) value of mercury flowrate.[4]

At the start of the cyclic test, the selection of the neutralizer-keeper voltage was determined from the tests performed on the thrusters from the IAPS program. This value was approximately 15 V when the keeper current was 500 mA and

cathode-tip-heater power was at 4.9 W, which corresponded to a 6-mA (equivalent) mercury flow. A control loop maintains this predetermined neutralizer-keeper voltage by regulating the mercury flowrate through the vaporizer. At any time during the cyclic test, the actual value of the mercury flowrate can be determined from the temperature/flowrate calibration of the neutralizer vaporizer. A plot of the neutralizer-keeper voltage, V_{NK}, the coupling voltage, V_C, and neutralizer-vaporizer flowrate* is shown in Figure 12 as a function of time up to the time when the coupling voltage increased. It is clear that the actual value of the neutralizer-vaporizer flowrate was decreasing continuously during that period even though the control parameter, V_{NK}, was held constant. The detailed results of the neutralizer study are given in Appenix D.

C. POST-TEST INVESTIGATIONS

As mentioned earlier, the cyclic endurance test ended after 599 cycles and 8,471 hours of thruster "beam-on-time." This value exceeds the 7,055 hours of "beam-on-time" planned for the IAPS flight. The thruster "beam-on-time" for the cyclic test was expected to be greater than 10,000 hours; however, this was based on the amount of mercury in the reservoir at the time that the cyclic test began, the IAPS total propellant utilization of $\eta_{Hg} = 0.71$, and estimates of the amount of mercury used in the start-up and shut-down periods for each cycle.

---

* Calculated from the measured vaporizer temperature.

An investigation was made to determine why this time discrepancy occurred. A calibration of the in-line data-system meters revealed that the discharge-keeper-voltmeter values were about 1.7-V lower than the actual values. This meant that the V_δ-control value was about 25 V rather than 27 V. It is estimated that operating an IAPS thruster at V_δ ≈25 V drops the utilization to $\eta_{Hg} = 0.68$, still above the value $\eta_{Hg} = 0.55$ experienced during the cyclic endurance test. Supplementary tests and analyses were made to determine the reason for this lower-than-expected utilization. These included flowrate measurements and inspection of thruster components. The discussion that follows will identify the probable cause of the performance changes.

1. Tankage Measurement

An indirect measurement of the volume of mercury in the Propellant Tank can be made from the transducer pressure readout. The relationship used is

$$P_T = P_i \left(\frac{V_i}{V_i + \Delta V} \right) + P_{head}$$

where

P_T is the transducer pressure

P_i is the initial gas pressure

V_i is the initial gas volume

ΔV is the mercury consumed

and

P_{head} is the head pressure generated by the mercury in the reservoir.

When the Propellant Tank was filled to capacity with 680 cc of mercury, the gas volume was 831 cc. After 25 cc of mercury was off-loaded, the gas volume was 856 cc. The initial pressure was determined at this time from the transducer pressure using the relationship

$$P_i = P_{T_i} - P_{head} \quad ,$$

where P_{T_i} was the first transducer pressure measurement made. The value of the head pressure is a function of the volume of mercury in the Propellant Tank and was approximated by assuming that the mercury formed a sphere in the Propellant Tank. The calibration curve then could be written as

$$P_T = 17.93 \left[\frac{856}{856 + \Delta V_{Hg}}\right] + P_{head} \quad .$$

At this time, prior to opening the propellant tank valve, the volume of mercury in the reservoir was 655 cc. The calibration curve is plotted in Figure 13. It can be seen that when the calculated transducer pressure fell below 10.2 psia, the reservoir would be empty. Figure 14 shows the actual transducer pressure values throughout the test. The data indicated that the reservoir was empty on July 8, 1983. However, the test continued until July 25, 1983. This is only a 3% error. The calibration curve shown in Figure 13 is a post-test curve.

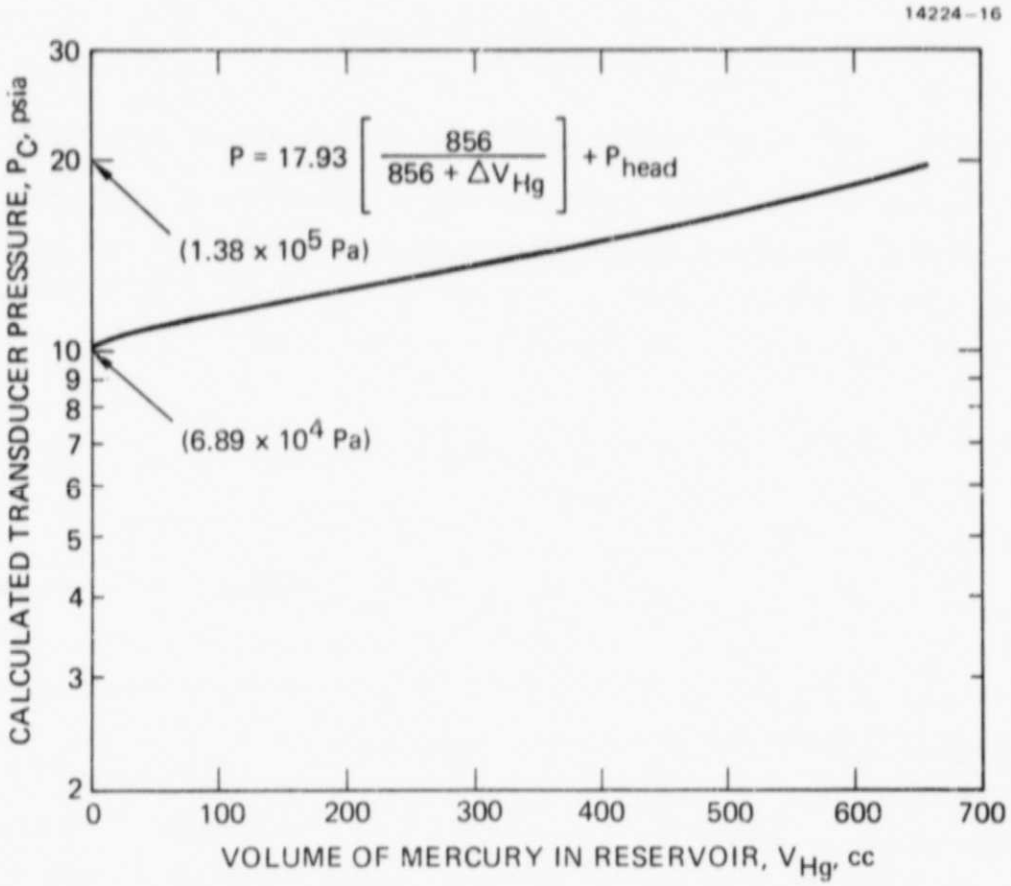

Figure 13. Calculated transducer pressure as a function of mercury in the Propellant Tank.

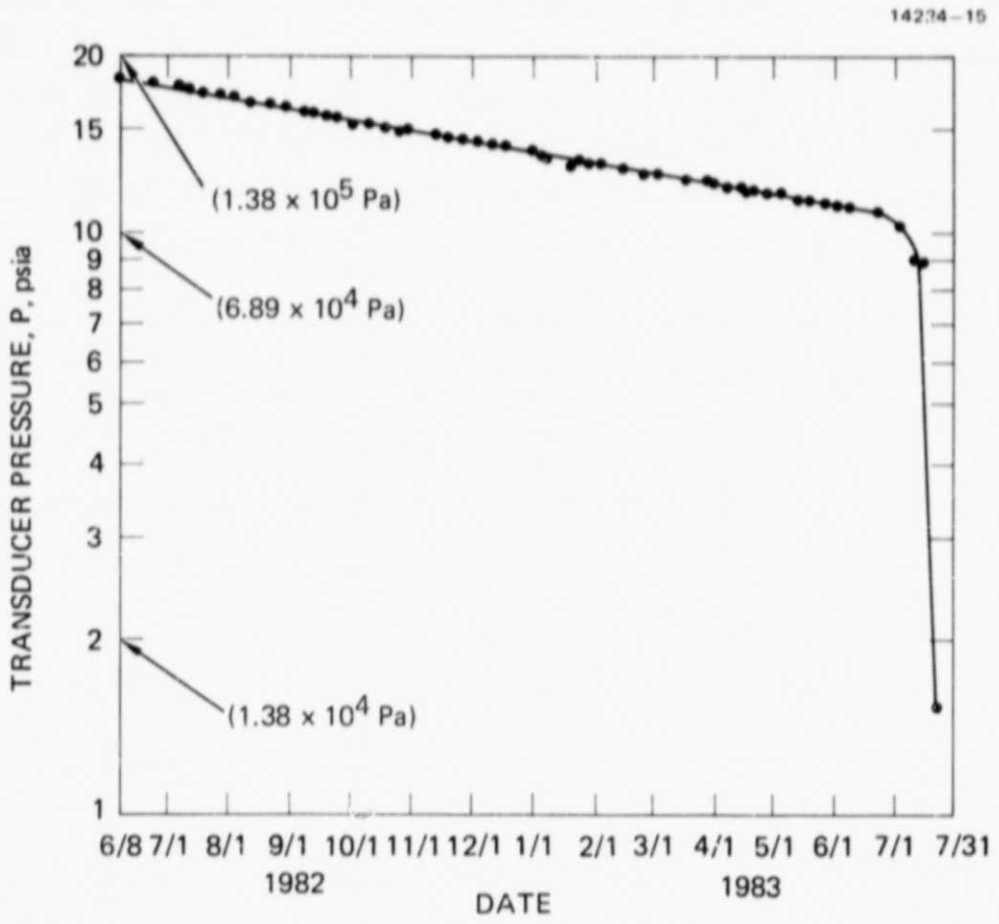

Figure 14. Measured transducer pressure as a function of time.

2. Flowrate Measurements

The first post-test flowrate measurements were made (without opening the vacuum chamber) by connecting a glass burrette feed system to the valve near the top of the chamber, as shown in Figure 9. The valve between the Propellant Tank and thruster was closed so that mercury only flowed to the thruster, and total flowrate could be measured. Total utilization values were obtained as a function of V_δ for I_B = 72 mA. These results are plotted in Figure 15. It can be seen that η_{Hg} = 0.56 at V_δ = 25 V.

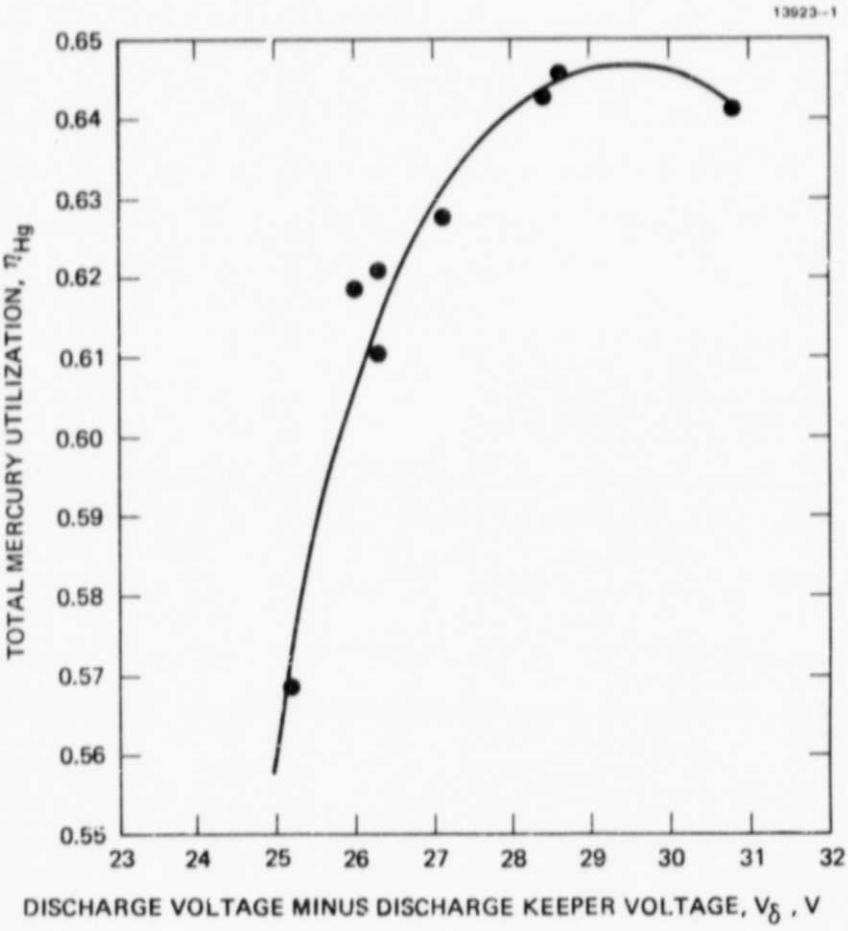

Fig. 15. Total mercury utilization as a function of V_δ for I_B = 72 mA.

If one assumes that η_{Hg} remained constant throughout the 8,481 hours of "beam-on-time", the total utilization value is calculated to be $\eta_{Hg} = 0.55$, which is in agreement with the measured value. However, if one assumes that the pre-test utilization value ($\eta_{Hg} = 0.74$ at $V_\delta = 25$ V) changed during the events on August 21, 1982, the new calculated value would be $\eta_{Hg} = 0.50$ (for $V_\delta = 25$ V) to account for the mercury believed to be consumed after that date to the end of the test. This total utilization value is about 9% lower than the measured value.

Both of the calculated η_{Hg} values are subject to error, since the value for the amount of mercury used during the "beam-on-time" is an estimate based on the following rationale. It is known that the volume of mercury in the Propellant Tank at the start of the cyclic test was approximately 633 cm^3. We estimated the mercury that was used when the beam was "off" by using temperature-flow calibrations and typical time-temperature recordings to calculate the mercury consumed during start-up, cool-down, discharge "on" without extracting a beam, and discharge and neutralizer "off" with full power being supplied to the vaporizers. Of these operating conditions the last is most subject to error because it is believed that liquid mercury was trapped in the isolator of the CIV assembly during the period of full power being supplied to the discharge-vaporizer and it is probable that the temperature-flow calibration for the discharge vaporizer shifted during this time. In other words, even though the temperature of the discharge vaporizer was known, the actual amount of mercury consumed is questionable. This type of behavior could explain the difference between the η_{Hg} calculated value obtained for the period following the event on August 21, 1982 and the η_{Hg} measured value at the end of the test.

In the initial disassembly, the Cathode-Isolator-Vaporizer (CIV) assembly was not removed from the thruster endplate, so this component could not be examined in detail. Consequently,

a test was performed to determine whether the leak was occurring in the vaporizer or isolator. Two ionization gauges were installed on the TGBSU for measuring pressure during thruster operations. One was mounted on the rear of the gimbal pointing toward the vaporizer; the other was mounted in the thruster ground screen pointed in the direction of the isolator. These results were compared to those obtained with an IAPS-type thruster, and the pressure inside the ground screen was about 20 to 30-times higher for the thruster used in the cyclic life test (for equivalent flowrates).

3. Thruster Disassembly and Inspection

Post-test disassembly was conducted in stages. In particular, the isolator inspection was the last to be performed, but will be discussed first because of its significance. Only the components that showed wear will be discussed; however, a complete chronological description of the disassembly and inspection is presented in Appendix E.

a. Isolator

Since the ionization-gage pressure-test results pointed toward a faulty isolator, the CIV was removed from the thruster and its shield was removed. Figure 16 shows part of the upstream braze joint between the ceramic isolator housing and metal flange. The ball of material which is visible has a granular, copper-colored appearance. Except for this, the rest of this braze joint looked normal. Approximately 1.3 cm of the downstream braze joint had material of the same appearance but in lesser volume. The assembly was pressurized internally to about 7 psi (4.8×10^4 Pa) of argon and a leak was detected at the ball of material shown in Figure 16. The material on the downstream braze at first appeared not to leak at this pressure; but, after sealing the upstream leak, the downstream joint was found to leak when checked with a leak detector.

M15923

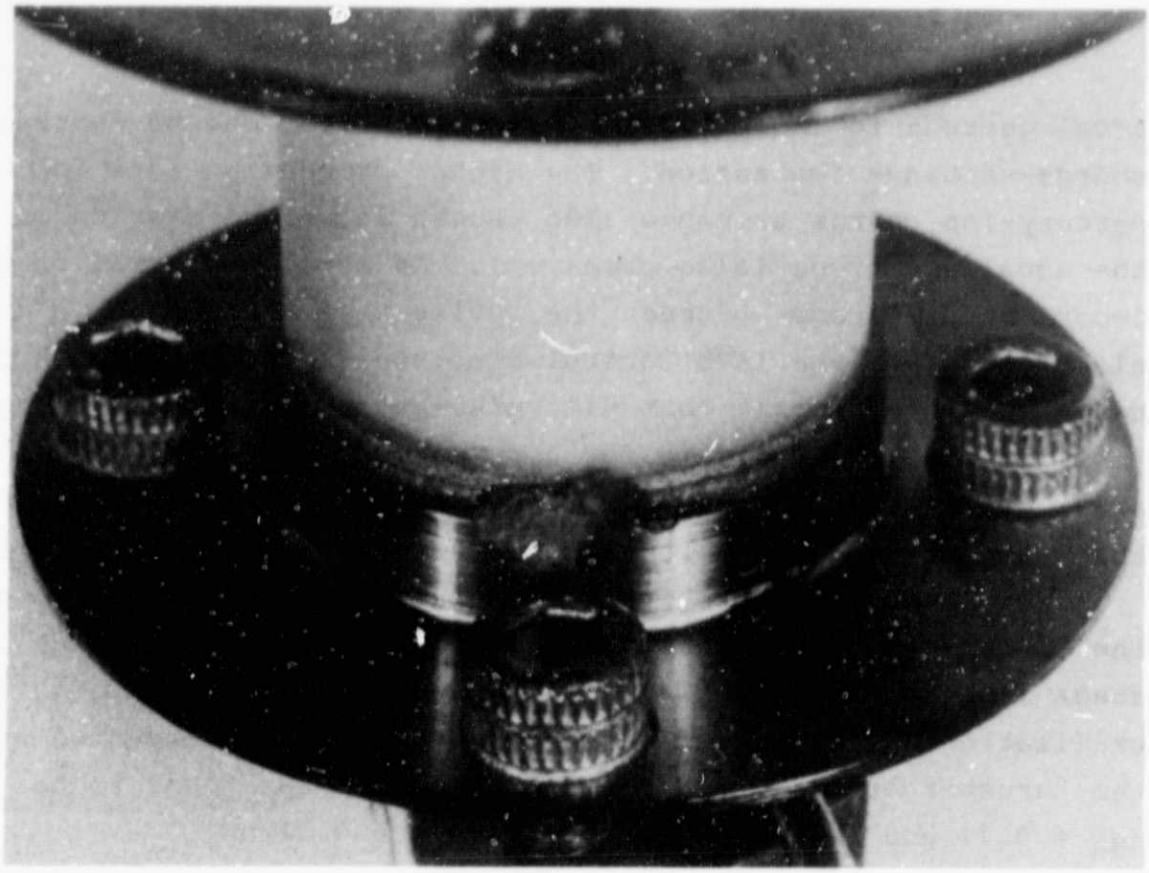

Figure. 16. Braze joint of isolator to flange.

This type of copper-braze failure has never been observed on 5-cm or 8-cm thrusters. This leads one to believe that the isolator on the cyclic life test thruster had experienced an extremely abnormal environment. We know that both vaporizers were operated at full power on four occasions for periods between 11 and 16 hours without a thruster discharge because of a deficiency in the ground-test equipment. Furthermore, the accel current increased following one of these excursions early in the test. One can postulate that mercury condensed in the isolator and that liquid mercury contacted the braze joints during these events and subsequently amalgamated with the copper braze to form the material observed on the joints. A leak developed in the braze and thereby reduced the propellant utilization. The only paths out of the thruster from the isolator leak are around the neutralizer keeper and via the lip of the ground-screen mask which leads either through the interelectrode region or downstream of the accel electrode. The higher vapor density in this region apparently caused the

accel current to increase (which was observed) due to increased charge-exchange ionization. The higher production rate for mercury-ion charge exchange also caused increased erosion of the accel electrode (also observed). As mentioned earlier, an important difference between the cyclic-test control electronics and the IAPS control electronics is that the IAPS has a software program that will prevent the full power being supplied to the vaporizers for long periods of time. Hence, we are confident that the IAPS will never be exposed to the events that caused the leak in the isolator described above.

The leaks in the isolator were sealed with an epoxy, and the CIV assembly passed a helium leak test. To assure that these leaks were the cause of the lower total mercury utilization and higher accel current, a test was conducted with the thruster at V_δ = 27 V. The utilization was found to be η_{Hg} = 0.77 and the accel current was I_A = 0.21 mA. These values are very close to the pre-test acceptance test values of η_{Hg} = 0.78 and I_A = 0.23 mA. This result is important because it demonstrates that the thruster performance did not change significantly after approximately 10,000 hours of "beam-on-time".

b. Electrode Assembly

The major wear on the electrode assembly occurred in the accelerator grid. There are two sets of hole diameters in the accel grid. The centrally located holes had diameters of 0.045 in. (0.114 cm) at the start of the test, and they increased to a range of 0.046-to-0.050 in. (0.117 cm to 0.127 cm) in diameter. The outer holes had diameters of 0.033 in. (0.084 cm) at the start of the test, and they increased to 0.034 in. (0.086 cm) in diameter; the small holes near the edge had become non-circular. The post-test accel grid is shown in Figure 17. This increase in hole size decreases the

utilization by only 2 to 3%. Much more apparent on the downstream side of the accel grid are the triangular charge-exchange-ion-erosion pits located between the apertures of the accel electrode. In some cases, in the central position of the accel grid, these pits actually penetrate through the accel grid. Because of this high erosion rate and deposition on the screen grid there was a build-up of material near one of the holes in the center of the grid assembly. Eventually (during the post-test-evaluation testing) this material flaked off and shorted the grids.

This abnormally high erosion rate was brought about by two abnormal conditions: (1) operation at V_δ = 25 V, and (2) the passage of leaking mercury vapor across the downstream surface of the accel grid. These two abnormal conditions should not exist on the IAPS flight.

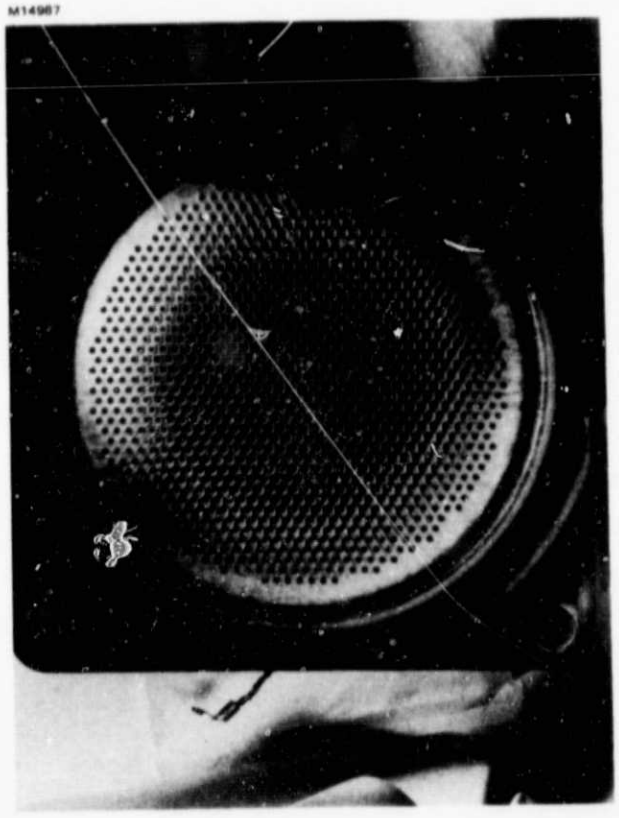

Figure 17. Post-test appearance of the accelerator grid.

c. Neutralizer Assembly

The neutralizer keeper was removed from the assembly and measurements were made of the cathode tip. The hole in the tip had increased from a 0.010-in. (0.025-cm)-diameter hole to about 0.035 in. (0.089 cm). Sharp edges were rounded off and the 45° countersink in the tip showed severe erosion (Figure 18). There are three possible causes for the neutralizer-tip erosion. One cause is that the neutralizer was operating at abnormally low flowrates.[4] Another is the higher-than-normal mercury vapor (from the isolator leak) around the neutralizer keeper. This would permit more mercury ions to be generated around the keeper hole, and some of these ions could strike the neutralizer cathode. The last possible cause is related to a high coupling voltage. Since the neutralizer cathode itself is at the coupling-voltage potential (neutralizer common), any ions near the neutralizer keeper and at ground potential would strike the cathode with more energy as the coupling voltage increases. Sixty percent of test time the coupling voltage remained constant near $V_C \approx -15$ V; however, the rest of the time the magnitude of the coupling voltage increased to a value of $V_C \approx -30$ V. The erosion of the cathode tip is the result of a combination of these three causes.

The material eroded from the tip had apparently deposited on the circumference of the keeper hole, decreasing its diameter from 0.070 in. (0.178 cm) to 0.056 in. (0.143 cm). We know (from previous studies[5]) that the neutralizer coupling may become degraded for keeper holes smaller than 0.070 in. (0.178 cm) in diameter for the 3-cm thruster. This reduction in the keeper-hole diameter is probably the best explanation for the increase in coupling voltage that was observed during the test.

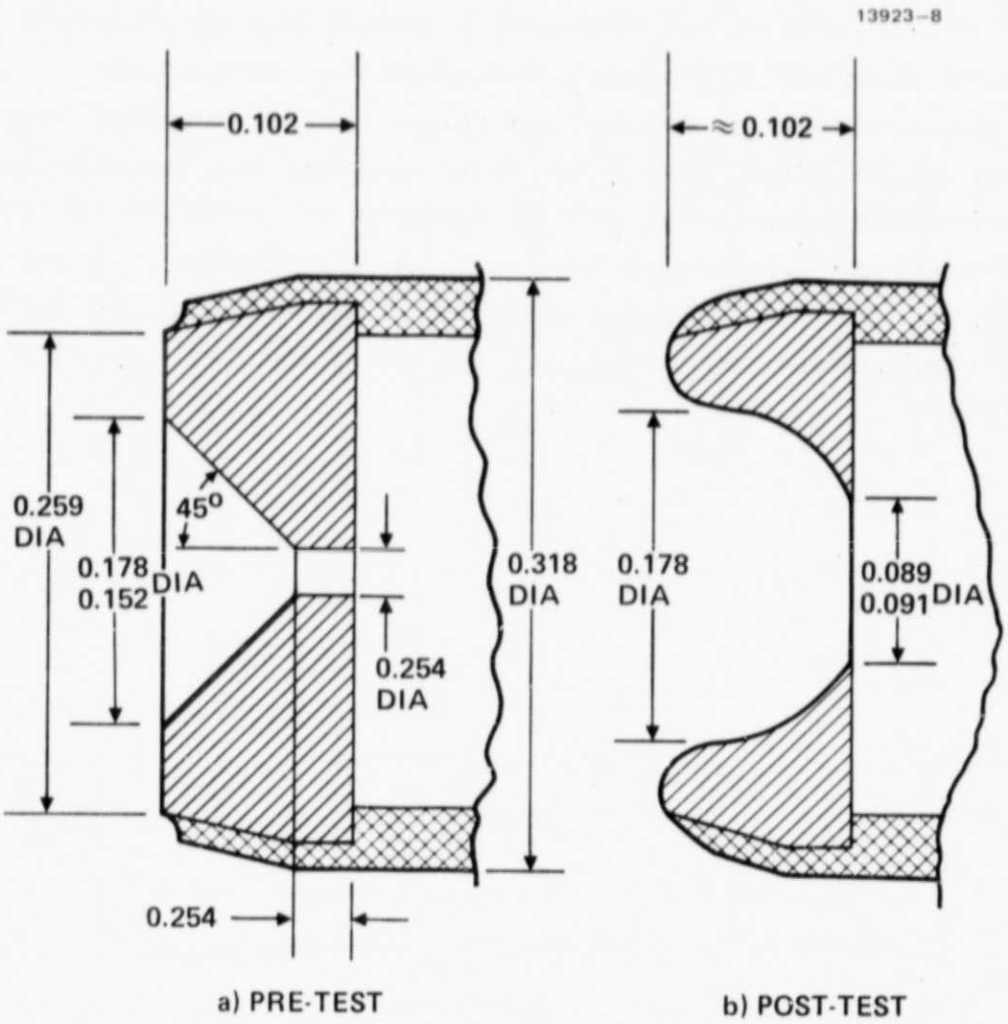

Figure 18. Cross-section of neutralizer cathode orifice (dimensions in cm).

Since the neutralizer-cathode erosion was chiefly caused by low mercury flowrates, the obvious way to avoid the problem is to avoid operation at flowrates below 6 mA (equivalent). Periodic performance mapping, which includes neutralizer characteristics, can be made during a flight program to guard against this undesirable operation.[6] This will provide neutralizer keeper and coupling voltage as a function of mercury flowrate throughout the mission. Should the neutralizer-vaporizer flowrate (based on performance mapping) appear to be lower than 6 mA (equivalent), the neutralizer-keeper-voltage setpoint can be lowered to increase the flowrate to the appropriate value (i.e., 6 mA equivalent). Between the mappings, the neutralizer-vaporizer flowrate will be inferred from temperature readouts, and the coupling voltage will be monitored.

SECTION IV

CONCLUSIONS

The EM-IAPS cyclic endurance test exceeded the required IAPS mission life of 7,055 hours by more than 1,400 hours. The PEU accumulated 10,268 hours of operation with the high voltages "on" during the dummy load testing and thruster "on" testing. The PEU and thruster shared the same vacuum environment during the accumulation of these test hours. The overall test was highly successful and brings about a high level of confidence in the IAPS flight hardware.

The mercury-vapor leak that developed in the cathode-isolator braze material is attributed to insufficient automation of the ground-support equipment at the beginning of the test that led to condensation of mercury within the isolator. Flight software such as that developed for the IAPS can control the power electronics to prevent the condition that led to condensation of mercury in the isolators preventing long periods of full power being supplied to either vaporizer. Appropriate interlocks for ground-support equipment were also successful in preventing the condition during the majority of the life test period.

The basic thruster performance was not altered after nearly 10,000 hr of "beam-on-time". A comparison of the first performance acceptance test (prior to the cyclic endurance test) and the most recent test (following the cycle endurance test and sealing the cathode isolator leaks) is made in Table E-4 of Appendix E.

The grid erosion that was experienced during the cyclic test was greater than expected. However, the increased erosion rate can be attributed to high charge-exchange rates (caused by the isolator leak); this condition is not anticipated in the IAPS flight or any other flight environment. The

charge-exchange rate at the nominal operating point of the IAPS will be considerably lower for the following reasons:

(1) A value of V_δ = 26.5 V will be used instead of the value V_δ = 25 V used inadvertently in the cyclic endurance test.

(2) The leak-tight IAPS isolator will eliminate the cause of a supplementary supply of mercury vapor which was delivered to the charge-exchange ion-production volume during the cyclic test.

Operation of the neutralizer with a flowrate of less than 6 mA (equivalent) can be avoided in life tests or flight applications by periodic mapping and corrective procedures. This should eliminate any low-flow contribution to the neutralizer-tip erosion experienced during the cyclic test.

The results of this test have provided useful information for the IAPS flight, which from all indications should meet its lifetime goal with no difficulties.

REFERENCES

1. C.R. Collett, and J.L. Power, "Qualification Test Results," AIAA Paper No. 82-1954, New Orleans, Louisiana, November 17-19, 1982.

2. J.L. Power, "Planned Flight Test of a Mercury Ion Auxiliary Propulsion System I - Objectives, Systems Descriptions, and Mission Operations,"

3. B.G. Herron, J. Hyman, Jr., and D.J. Hopper, "Development of an 8-cm Engineering Model Thruster System," AIAA Paper No. 76-1058, Key Biscayne, Florida, November 14-17, 1976.

4. A.J. Weigand, "Operating Characteristics of a Hollow-Cathode Neutralizer for 5- and 8-Centimeter-Diameter Electron-Bombardment Mercury Ion Thrusters," NASA X-3209, March 1975.

5. B.G. Herron, J. Hyman, Jr., D.J. Hopper, W.S. Williamson, C.R. Dulgeroff, and C.R. Collett, "Engineering Model 8-cm Thruster Subsystem," NAS 3-18917, June 1978.

6. J.L. Power, Private Communication

APPENDIX A

THRUSTER NOMENCLATURE

Abbreviation	Description
DCIU	Digital Controller and Interface unit
DIU	Digital-Interface Unit
EM	Engineering Model
I_A	Accel Current
I_B	Beam Current
I_D	Discharge Chamber Current
I_{DH}	Discharge Heater Current
I_{DV}	Discharge Vaporizer Current
I_{DK}	Discharge Keeper Current
I_{NH}	Neutralizer Heater Current
I_{NK}	Neutralizer Keeper Current
I_{NV}	Neutralizer Vaporizer Current
IAPS	Ion Auxiliary Propulsion System
PEU	Power Electronics Unit
PTVFU	Propellant-Tank/Valve/Feed Unit
T_{DV}	Discharge Vaporizer Temperature
T_{NV}	Neutralizer Vaporizer Temperature
TGBSU	Thruster/Gimbal/Beam-Shield Unit
V_A	Accel Voltage
V_B	Beam Voltage $(V_S+V_D-\|V_C\|)$
V_C	Coupling Voltage
V_D	Discharge Chamber Voltage

V_{DH}	Discharge Heater Voltage
V_{DK}	Discharge Keeper Voltage
V_{DV}	Discharge Vaporizer Voltage
V_{NH}	Neutralizer Heater Voltage
V_{NK}	Neutralizer Keeper Voltage
V_{NV}	Neutralizer Vaporizer Voltage
V_S	Screen Voltage
V_δ	V_D minus V_{DK}
η_{Hg}	Total Mercury Utilization

APPENDIX B

FACILITY DEMONSTRATION TEST

The following paragraphs describe the facility demonstration test and the results of a residual-gas-analyzer scan performed during the demonstration test.

A block diagram of the pumping system for the vacuum facility is shown in Figure B-1. The initial state of the facility was (1) all power was off and (2) the chamber was at ambient pressure. The power was turned on and the chamber was rough-pumped. One of the two diffusion pumps was then used for continued pumping. After the chamber had been at a pressure of less than 5×10^{-7} Torr (6.67×10^{-5} Pa) with liquid nitrogen in the liner and target for 50-hr, the liner and target were allowed to warm for 13 hours. The chamber was then vented and the top cover of the chamber was raised to break the "O" ring seal. The top cover was then reseated and the chamber was pumped to a pressure of less than 5×10^{-7} Torr (6.67×10^{-5} Pa). A gas analysis was made approximately 22 hours after the start of the 50-hour period. A chronological sequence of the test is listed in Table B-1. It can be seen that the demonstration test took 68 hours; this was 32 hours less than the 100-hr requirement.

The pressures measured during the rough pumping are shown in Figure B-2. Approximately one hour was required to reach $p = 40$ μ (5.23 Pa), the pressure at which the diffusion pump valve was opened. The chamber pressure recorded after the diffusion pump valve was opened is shown in Figure B-3. The 50-hour test started about three hours after the start of the rough pumping.

Throughout the 50-hour test, the pressure was monitored with two ion gauges. These pressures are shown in Figure B-4. An increase in pressure was noted after 22 hours. This increase was caused by the heating of the filament in the gas analyzer.

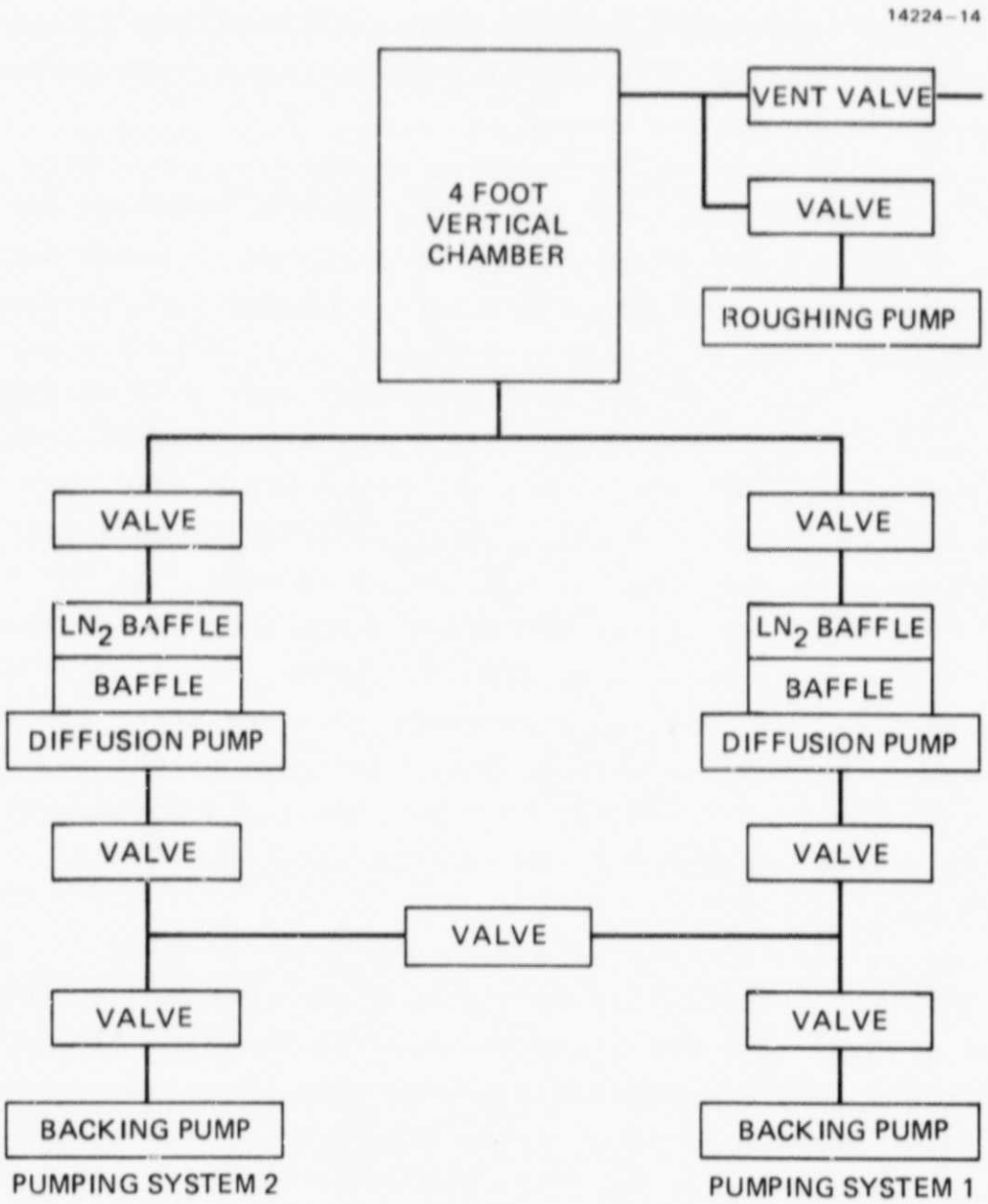

Figure B-1. Block diagram of pumping system

Table B-1. Sequence of Events for Facility Demonstration

Time	Description
Initial Condition	All power off, chamber vented.
0	Start rough pumping, valve to diffusion pump (D.P.) closed. Backing pump No. 1 on, diffusion pump No. 1 on, LN_2 to diffusion pump baffle No. 1.
1 hr, 4 min.	Open D.P. valve to chamber p = 40 μ (5.32 Pa).
2 hr, 3 min.	LN_2 to liner and target p ≈ 8 x 10^{-6} Torr (1.07 x 10^{-3} Pa).
2 hr, 34 min.	Start 50-hr period p < 5 x 10^{-7} Torr (6.67 x 10^{-5} Pa).
24 hrs	Take gas analysis data p ≈ 1 x 10^{-7} Torr (1.33 x 10^{-5} Pa)
52 hrs, 34 min.	End 50-hr test. LN_2 off.
65 hrs, 30 min.	End warmup period. Vent chamber.
66 hrs	Remove top cover and reseal top cover.
66 hrs, 10 min.	Start rough pumping.
67 hrs, 3 min.	Open D.P. valve p ≈ 45 μ (5.99 Pa).
67 hrs, 47 min.	LN_2 to liner and target p ≈ 9 x 10^{-6} Torr (1.2 x 10^{-3} Pa).
68 hrs, 0 min.	p < 5 x 10^{-7} Torr (6.67 x 10^{-5} Pa). End of demonstration test.

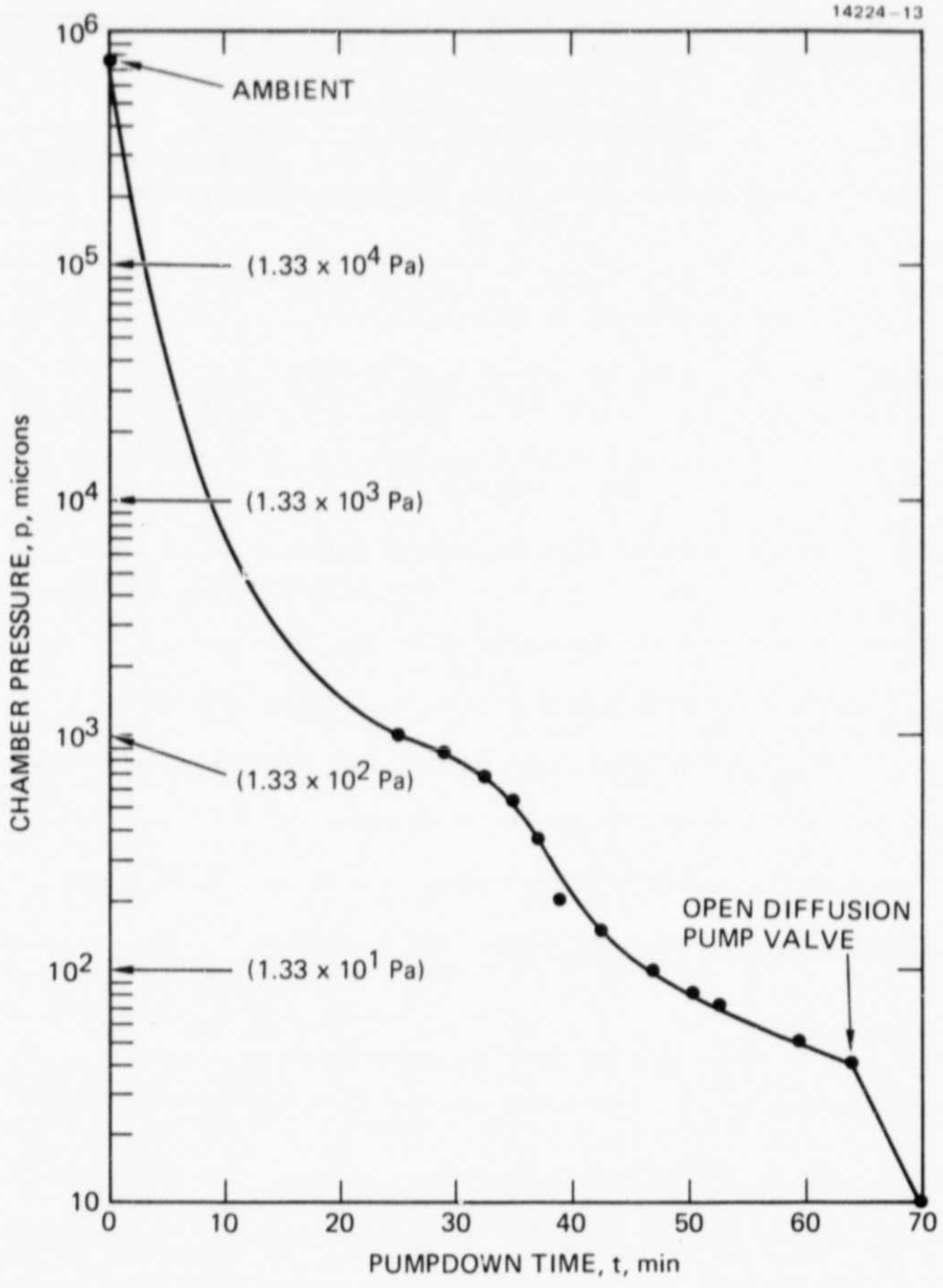

Figure B-2. Chamber roughing pressure

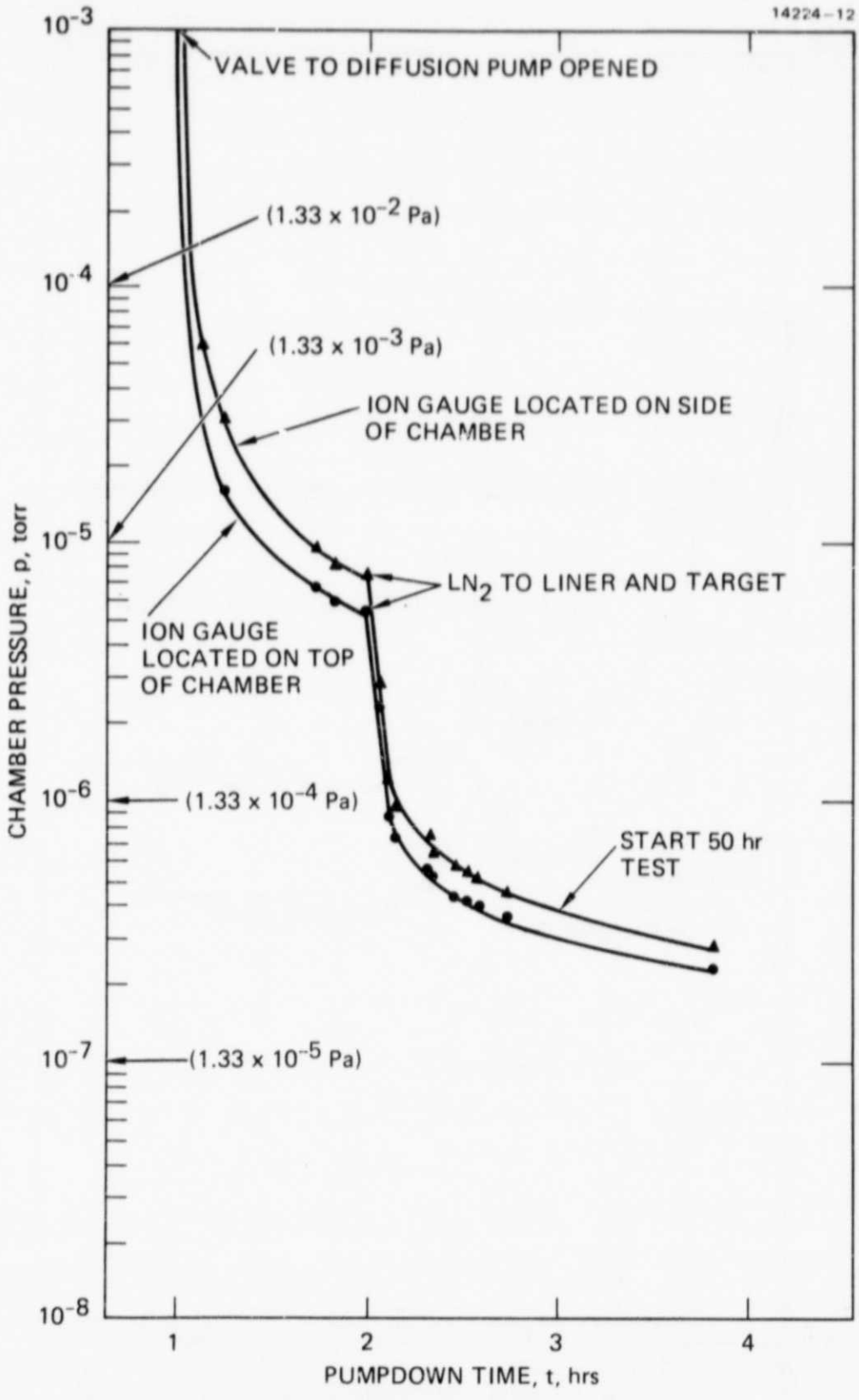

Figure B-3. Diffusion pumped chamber pressure.

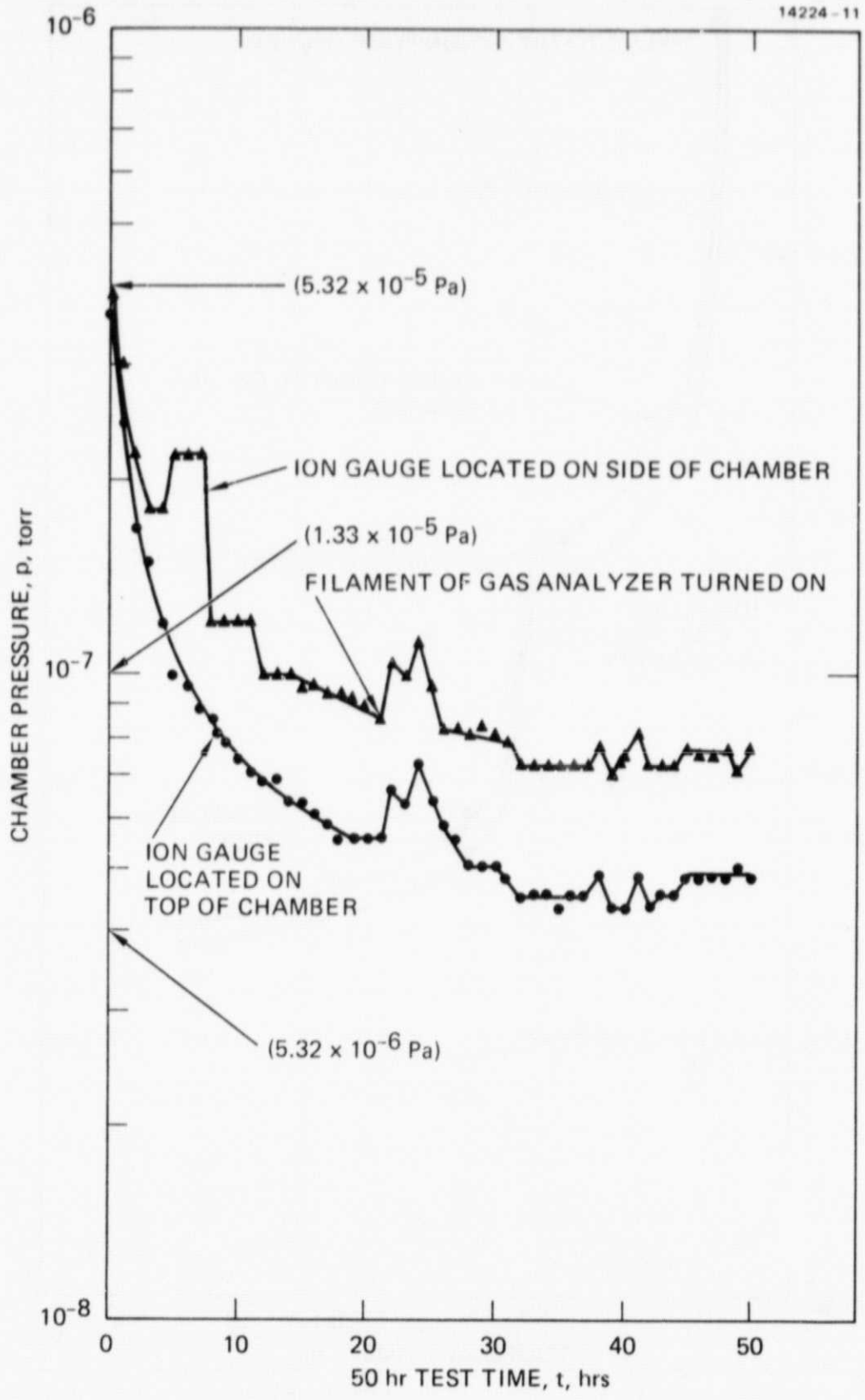

Figure B-4. Chamber pressure during 50 hr test.

Temperature sensors were located on the target and cryoliner. The output of the temperature sensors during the entire demonstration test are shown in Figure B-5. In a pre-test calibration, the output for the sensors at LN_2 temperature was about 1.4 V. Figure B-5 shows that the collector output was 1.8 V at near LN_2 temperature.

As mentioned before, a gas analysis was made 22 hours after the start of the 50-hr test. One of the scans made with the gas analyzer is shown in Figure B-6. The scan extends to AMU greater than 200, and the relative abundance is shown as a function of AMU. Scans were also taken with the relative-abundance sensitiviy 10 times greater so lesser peaks could be identified. Figure B-6 also shows the relative transmission for various AMU. This correction was applied to relative abundances when the partial pressures were calculated. The partial pressures greater than 1×10^{-9} Torr (1.33×10^{-7} Pa) are listed in Table B-2 where the values account for 72% of the total pressure. The remaining 28% is attributed to AMU not listed in Table B-2 and whose partial pressure is less than 1×10^{-9} Torr (1.33×10^{-7} Pa). In addition to the nitrogen and water vapor present in the chamber, there were traces of mechanical pump oil and the solvent used for cleaning the chamber.

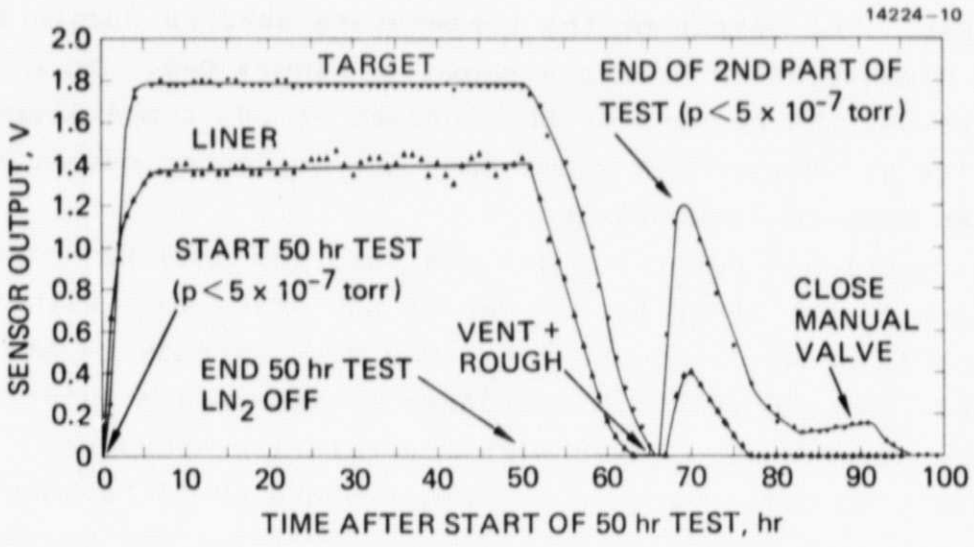

Figure B-5. Output of temperature sensors.

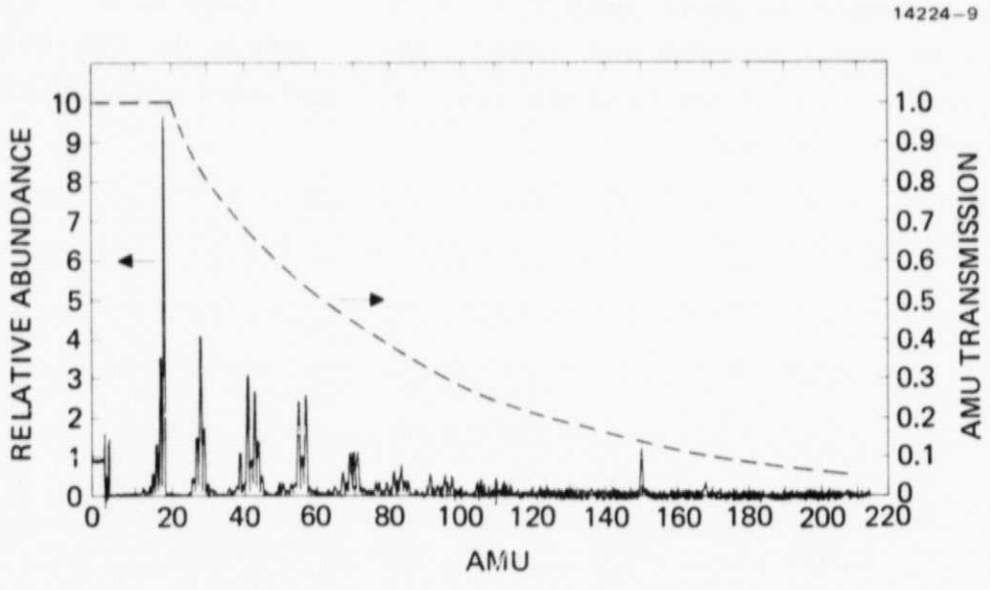

Figure B-6. Gas analyzer plot.

Table B-2. Partial Pressures Greater than 1 x 10^{-9} Torr (1.33 x 10^{-7} Pa)

AMU	Partial Pressure, Torr (x 10^{-9})	Comment
2	1.31	H_2^+
16	1.15	O^+
17	3.27	OH^+
18	8.90	HOH^+
27	1.63	
28	4.60	CO^+, N_2^+
29	1.95	
39	1.48	M.P. Oil
41	4.30	M.P. Oil
42	1.26	M.P. Oil
43	3.75	
44	1.98	CO_2
55	4.01	M.P. Oil
56	1.70	M.P. Oil
57	4.40	M.P. Oil
67	1.25	
69	2.23	
70	2.27	Cl_2
71	2.35	
81	1.53	M.P. Oil
83	1.91	M.P. Oil
91	1.61	
95	1.50	C Cl_2 FC Cl F_2 Fragments
97	1.46	
150	7.94	
151	1.25	
168	3.31	

APPENDIX C

TESTING WITH DUMMY LOAD

Engineering Model Power Electronics Unit No. 2, Thruster/Gimbal/Beam-Shield Unit S/N 903, and Propellant Tankage/Valve Feed Unit were installed in the 4-foot (1.2 m) vertical chamber. The DIU was external to the chamber. At this time the latching valve between the propellant tank and thruster had not yet been opened.

The PEU, thruster, and feed system had been under vacuum for more than two weeks while preparing for the test. A dummy load was attached to the power output lines from the in-line data system. A 70-V dc supply provided the primary power. The ground support test console was used to send commands to the Digital Interface Unit. In-line data was obtained from the instrumentation furnished by NASA. Two eight-channel recorders were used to record the parameters shown in Table C-1.

A chronology of tests and test conditions is shown in Table C-2. Table C-2 shows that from 2/24/82 to 2/25/82 the PEU temperature was increased to a maximum temperature of 48°C to enhance outgassing. The high voltage was turned on after a cooldown period on 2/25/82. On 2/27/82 the PEU was inadvertently turned "off" (while unattended) when a door interlock switch tripped. The PEU was "off" for 7 hours before this was discovered. The temperature of the mercury reservior reached -5°C at this time. The reservior reached -20°C before the power from the PEU started to increase the reservior temperature.

In addition to the 506 hours of testing up to 3/19/82 with a nominal load, and buss voltage, V_{70} = 70 V, test time was accumulated at (1) V_{70} = 52V (33 hr); (2) V_{70} = 90V (27 hr); and (3) $T_{Baseplate}$ = 55°C (25 hr).

Table C-1. Parameters Monitored by the Recorders

Channel Number	Description
1	Discharge Voltage, V_D
2	Discharge Current, I_D
3	Discharge Keeper Voltage, V_{DK}
4	Discharge Keeper Current, I_{DK}
5	Discharge Heater Current, I_{DH}
6	Discharge Vaporizer Current, I_{DV}
7	Temperature Sensor for Discharge Vap, R_{DV}
8	Neutralizer Keeper Voltage, V_{NK}
9	Neutralizer Heater Current, I_{NH}
10	Neutralizer Keeper Current, I_{NK}
11	70 Volt Supply Current, I_{70}
12	Neutralizer Vaporizer Current, I_{NV}
13	Temperature Sensor for Neutralizer Vap, R_{NV}
14	Screen Current, I_S
15	Accel Current, I_A
16	Chamber Pressure, P_C

Table C-2. Chronology of Testing with Dummy Load

Date	Time	Description	Total Power to Load, W
02/04/82		System installed in chamber	
02/05/82		Chamber pump down	
02/08/82		Chamber pressure = 2×10^{-5} Torr (2.67×10^{-3} Pa)	
02/09/82		Chamber pressure = 4.6×10^{-6} Torr (6.13×10^{-4} Pa)	
02/17/82		Chamber pressure = 3.9×10^{-6} Torr (5.20×10^{-4} Pa) Thermocouple circuit check	
02/18/82		LN_2 to liner and target Chamber pressure = 2.4×10^{-7} Torr (3.2×10^{-5} Pa)	
02/19/82		Cooling characteristics of components obtained	
02/23/82	1049	Power to PEU. All loads used except high voltage loads	47.2
02/24/82	0901	11.7 W to PEU heater. Maximum temperature of PEU = 48°C	47.2
02/25/82	0752	PEU heater turned "off"	47.1
	1458	PEU loads removed (1st turnoff)	0
	1536	High voltage loads used	81.3
	2053	All loads used	105.5
02/26/82		Same as 02/25/82 - 2053	105.5
02/27/82	0630	Lost bus power from tripped door interlock switch (2nd turnoff)	
	1725	Start power to loads	
	1851	Power to all loads	104.6
02/28/82		Continual load testing. Maximum temperature of PEU = 37°C. Total "on-time" with all loads = 64 hr.	105.7
03/01/82	0000	Continuation of load testing (V_{70} = 70 V, V_{28} = 28 V	105.7
	0851	Increase I_D to 500 mA, I_{DH} to Setpoint 2, I_{NH} to Setpoint 2	121.2

Table C-2. (Continued)

Date	Time	Description	Total Power to Load, W
03/02/82	1400	V_D to 40.5 V, I_D to 420 mA	126.3
03/03/82	0826	I_{DV} to Setpoint 1	125.7
03/19/82	1003	PEU shutdown for no apparent reasons. Total running time with HV on was 506 hrs.	
03/19/82	1127	PEU restart	127.6
03/22/82	0810	$V_{/0}$ set to 80 V. PEU would trip off at $V_{/0}$ > 84 V	127.5
	1122	$V_{/0}$ to 52 V for low buss test	127.5
	1701	PEU shutdown from backing pump failure. Pressure did not exceed 5×10^{-5} Torr (6.7×10^{-3} Pa). Total running time with HV on was 585 hrs.	
	2122	Diffusion pump valve open to chamber	
	2140	Unable to turn PEU on. Turned off LN_2 to liner and target	
03/23/82	1456	Defective DIU was replaced. Testing resumed on 03/25/82	
03/25/82	0823	LN_2 to liner and target $V_{/0}$ = 70 V. PEU turned on.	128.6
03/26/82	0801	$V_{/0}$ to 52 V	128.6
03/27/82	1105	$V_{/0}$ to 90 V	128.6
03/28/82	1307	$V_{/0}$ to 70 V	128.6
03/29/82	1058	Power to PEU heater (1.65 W)	128.6
03/30/82	0753	Power to PEU heater to 7 Ω. $T_{BAseplate}$ = 52°C	128.9
03/31/82	0815	Power to PEU heater to 9 W. $T_{Baseplate}$ = 55°C	128.9
04/01/82	1240	PEU heater off	
04/02/82	1017	PEU off. End of test. Total time with HV on was 779 hrs.	

The testing of the PEU with the dummy load was completed with only a few minor problems. The failure of the backing pump on 3/22/82 was the result of a low oil level in the pump. The PEU shutdown on 3/19/82 and the inability to operate at V_{70} = 90 V on 3/22/82 was attributed to a faulty diode in the DIU. The diode probably failed early in the test as a result of an 8.3-Ω resistor being used in the overpower circuit instead of an 8.3-kΩ resistor. The unit would operate with a bus voltage, V_{70} = 70 V, but would shut down at the high bus voltages in the DIU. This circuit in the DIU was repaired and the test continued until 779 hours were recorded.

APPENDIX D

NEUTRALIZER PERFORMANCE

By February 23, 1983, the cyclic endurance test had undergone 395 cycles and 5,700 hours of operation at the nominal operating point. The scope of this appendix is to describe the neutralizer behavior during the first nine months of operation. It appeared that the characteristics of the neutralier had changed during the first nine months of the test. The effect of this change was that the absolute magnitude of coupling voltage increased while the neutralizer keeper voltage was kept constant (under closed-loop control). The coupling voltage was lowered in February 1983 to an acceptable value of varying the neutralizer-keeper-voltage set-point.

The remaining parts of this appendix describe the sequence of events that led to the corrective measures taken to restore the coupling voltage to an acceptable level that remained until the cyclic test was completed.

Selection of Parameters for Neutralizer Operation

At the start of the cyclic test, the selection of the neutralizer-keeper voltage was determined from the tests performed on the thrusters from the IAPS program. This value was approximately 15 V for a 6-mA Hg^+ eq. mercury flow. A control loop maintains a predetermined neutralizer-keeper voltage by regulating the mercury flow through the vaporizer. The flow can be determined from the temperature/flow calibration of the neutralizer vaporizer. A plot of the neutralizer-keeper voltage, V_{NK}, the coupling voltage, V_C, and neutralier vaporizer flowrate is shown in Figure D-1 as a function of time up to the time when the coupling voltage increased.

Figure D-1 shows that the coupling voltage varied by 5 V, the keeper voltage maintained the set-point voltage, and the flow decreased. This decrease in flow was initially believed to

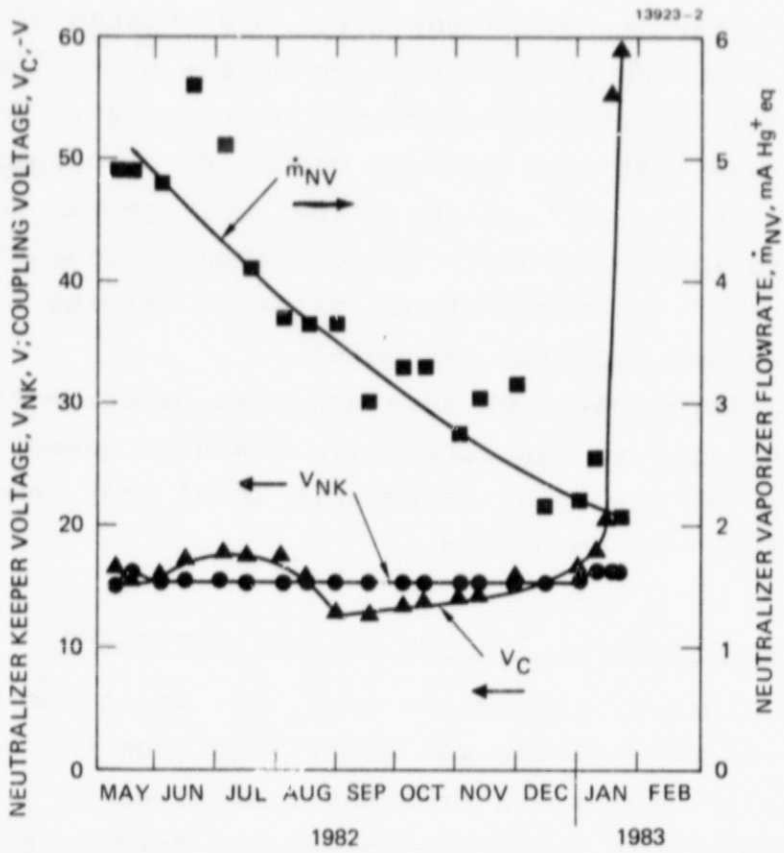

Figure D-1. Neutralizer-keeper voltage, V_{NK}, coupling voltage, V_C, and neutralizer-vaporizer flowrate as a function of time.

be a change in the vaporizer calibration rather than a real effect. Since absolute neutralizer-flow measurement could be made during the test and because the coupling voltage did not change significantly, this was a reasonable assumption.

When the coupling voltage could not be kept below 30 V with a keeper voltage of less than 16 V, the NASA Program Manager was informed of the problem. Two changes were agreed on at that time. The first was to increase the neutralizer-keeper current and the second was to increase the neutralizer tip heat. Increasing the neutralizer keeper current caused the accel current to increase and become noisy; increasing the neutralizer-tip-heater power from 4.9 to 8.1 W brought the coupling voltage to below 30 V. This improvement in coupling voltage was short-lived. The next approved change was an increase in neutralizer-keeper voltage. This change also brought about a short-time decrease in coupling voltage. Throughout these changes, maintaining stable operation of the neutralizer after start-up became a problem and several extinctions usually occurred before a stable condition was established.

With the concurrence of the NASA Program Manager, data were obtained to determine the variation of neutralizer-keeper voltage vs. vaporizer flowrate in order to better understand the problem being encountered. The curves obtained are shown in Figures D-2 and D-3, for two different values of tip-heater power. The flowrates listed were those obtained from the original vaporizer calibration curve. Using these results, it was decided to operate at a keeper voltage of 17 V to maintain a coupling voltage below 30 V. At this time, it was still believed that the flowrates were higher than those listed for the reason mentioned before, i.e., a change in the vaporizer calibration. As time went on, the coupling voltage went higher than 30 V. In an effort to raise the neutralizer-keeper voltage by decreasing the mercury flow, the neutralizer was extinguished This was the first indication that the flowrate measurements

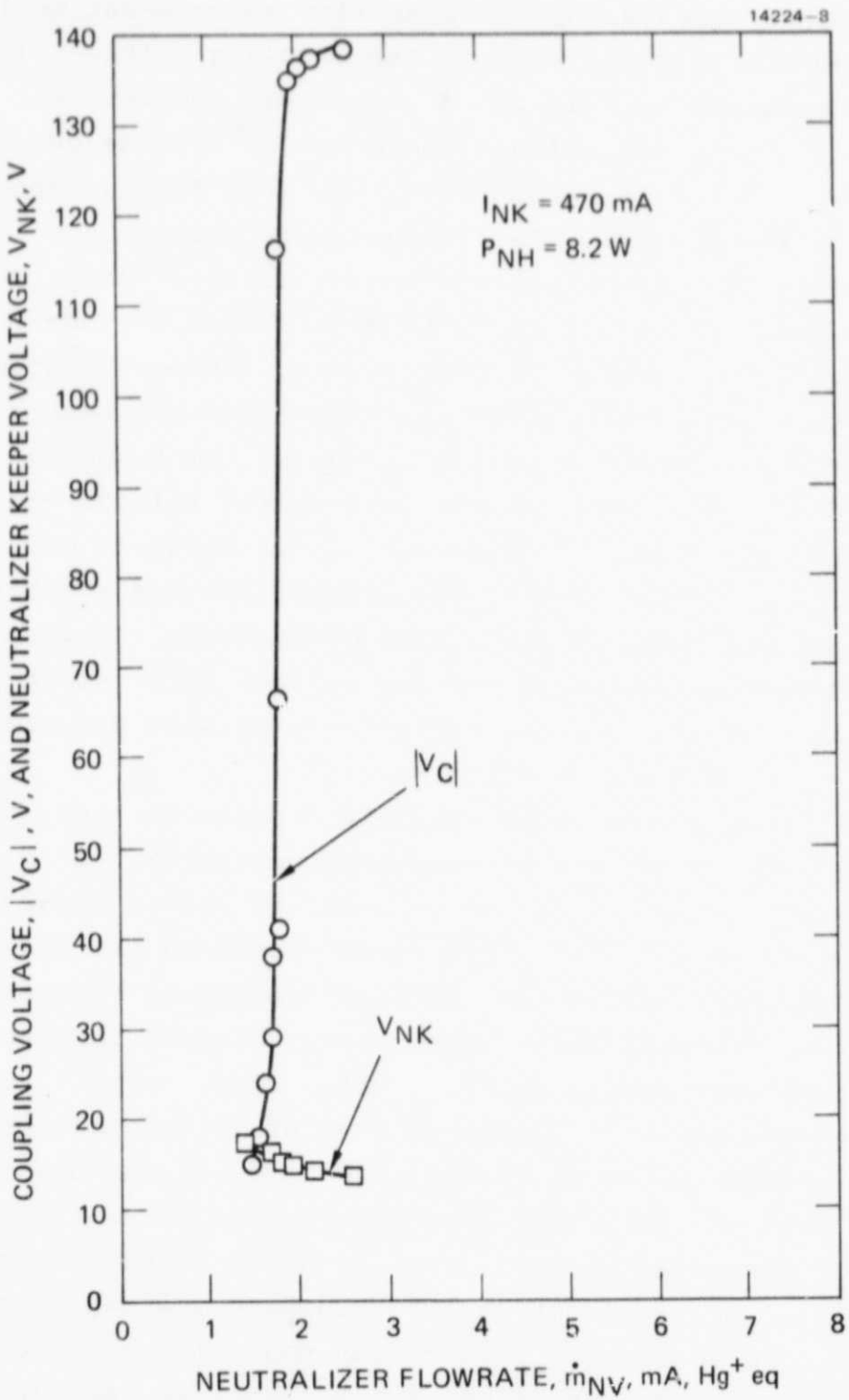

Figure D-2. Neutralizer-keeper voltage, V_{NK}, and coupling voltage, V_C, versus neutralizer-vaporizer flowrate (P_{NH} = 82 W).

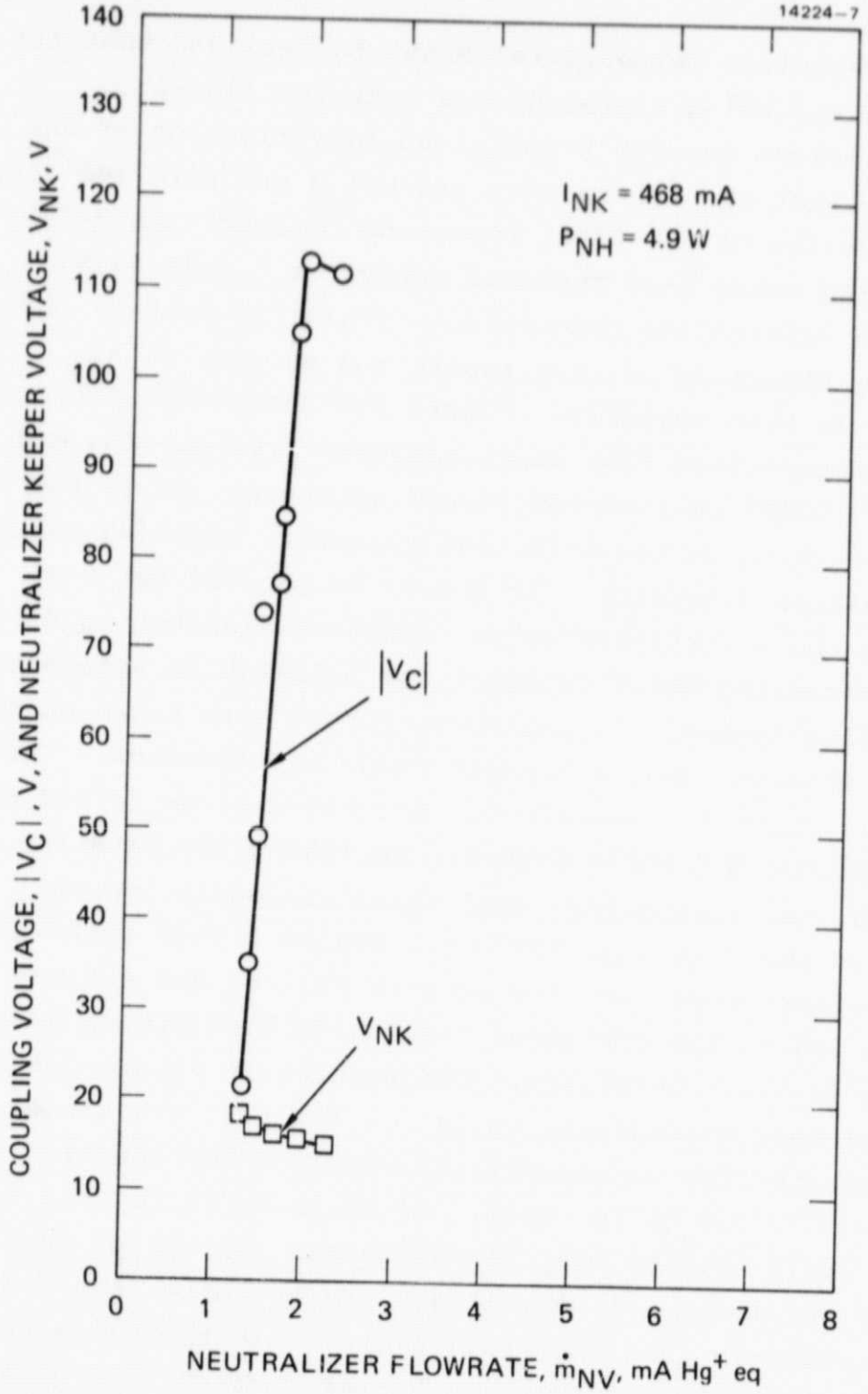

Figure D-3. Neutralizer-keeper voltage, V_{NK}, and copuling voltage, V_C, versus neutralizer-vaporizer flowrate (P_{NH} = 4.9 W).

(based on vaporizer temperature) might be real and that the neutralizer was being operated at a very low flowrate.

The previous results prompted an investigation of the possibility that the neutralizer was being run with low flowrates. A review of the final report on Contract NAS 3-18917 ("Engineering Model 8-cm Thruster Subsystem," June 1978) produced an interesting observation. This can best be shown by reproducing Figure 28 of that report and showing it as Figure D-4 in this appendix. Figure D-4 shows that there is a region of neutralizer flow where satisfactory coupling did not exist for a 0.127-cm-diameter keeper aperture. If we had a similar condition on the life test thruster, coupling should occur at higher flowrates. It should be pointed out that increasing the neutralizer-keeper aperture diameter to 0.18 cm on the Engineering Model Thruster was believed to eliminate this poor-coupling region. In any case, curves were taken on the life test thruster over a broader range of flowrates. These results are shown in Figure D-5. A curve similar to the shape shown in Figure D-4 was obtained. In taking the data in Figure D-5, the neutralizer (and thruster) operation was unstable in the 2 to 4 mA (Hg^+ eq.) region. This instability was also experienced when the data in Figures D-2 and D-3 were taken and led to the erroneous conclusion that flooding was occurring in the neutralizer. The results in Figure D-5 show that the keeper voltage was quite low and that the slope of the keeper-voltage/flow characteristic obtained for coupling voltage less than 30 V was quite small. As small as it is, the control loop was still able to control the keeper voltage at that value necessary for low coupling voltage. Furthermore, the flowrate required was only 1-mA (Hg^+ eq.) higher than the value used at the start of the cyclic test. A keeper current of 620 mA was required for coupling at this flowrate, but after four days of operation at these new values coupling occurred at I_{NK} = 550 mA. No further changes in parameters were implemented.

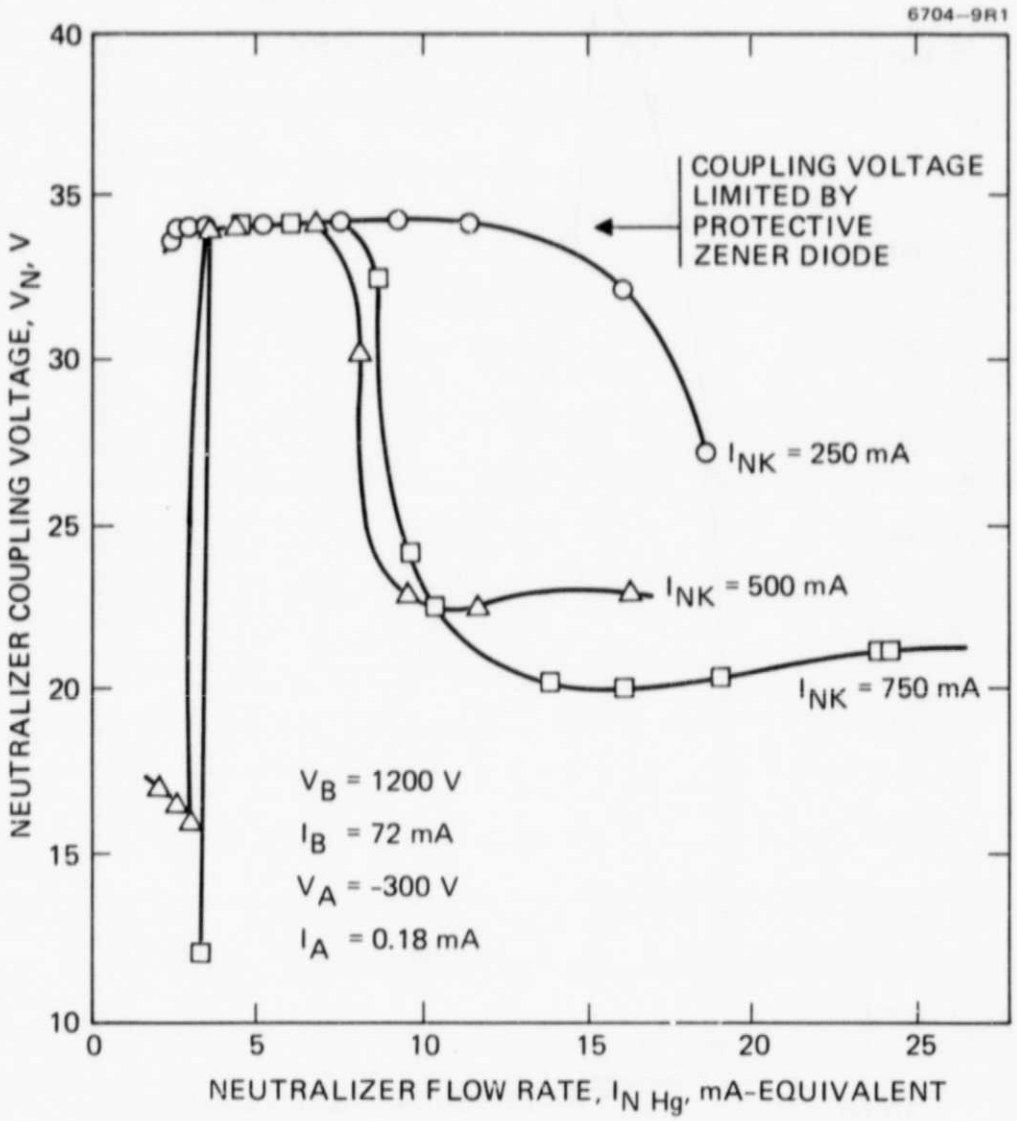

Figure D-4. Neutralizer coupling characteristics with keeper aperture diameter of 0.127 cm for Engineering Model Thruster (from Final Report of Contract NAS 3-18917, June 1978).

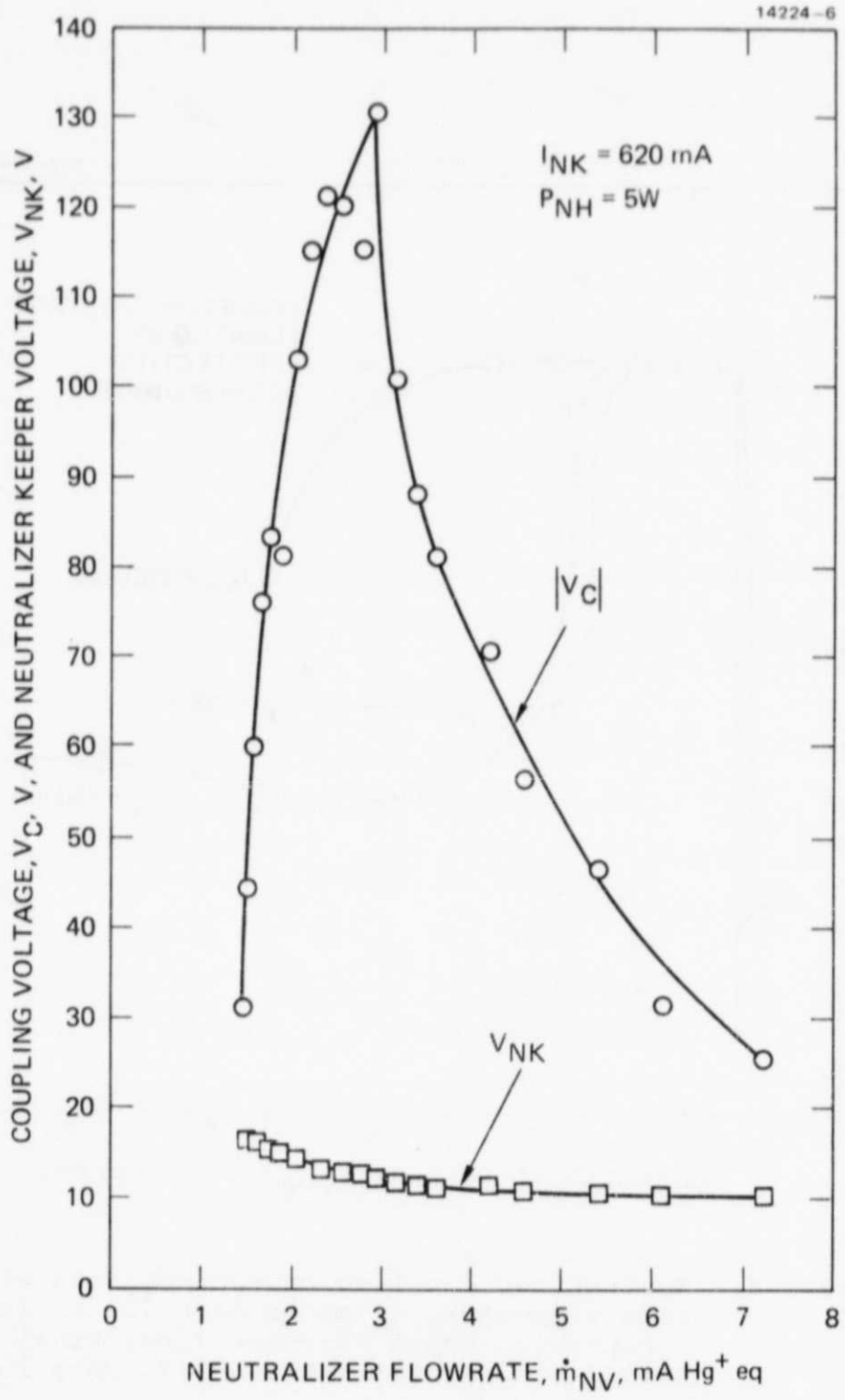

Figure D-5. Neutralizer-keeper voltage, V_{NK}, and coupling voltage, V_C, as a function of neutralizer vaporizer flowrate, in $_{NV}$.

When this study was made in February 1983, several possible explanations for this change in neutralizer performance were presented. These were the following:

- A decrease in keeper aperture
- Excessive amount of mercury near the neutralizer
- A better conditioned cathode required less mercury flow to maintain a constant keeper voltage.

At the time the neutralizer data was taken, a decrease in the neutralizer keeper aperture was not considered to be reasonable; however, post-test analysis revealed that the keeper aperture did indeed decrease from 0.070 in. (0.178 cm) to 0.56 inches (0.143 cm). It is now believed that the change in neutralizer performance was largely due to the decrease in the neutralizer keeper aperture and a better conditioned cathode.

APPENDIX E

POST TEST EXAMINATION

On December 14, 1983 the 8-cm thruster S/N 903 was removed from the HRL Cyclic Lifetest Facility after having successfully completed 652 "on-off" cycles and 9,489 hours of accumulated "beam-on-time". Subsequent to its removal, personnel from HRL and NASA-LeRC performed individual visual observations of the thrust system at various stages of its (partial) disassembly.

The examination of the thruster following its removal from the life test facility took place in two segments. The first segment of disassembly performed was the removal of the ground screen, shell and anode, ion optics, neutralizer keeper, cathode cup pole piece, and baffle. This level of thruster disassembly was limited to the degree necessary to view critical components and to perform non-destructive measurements, with the intent of preserving the option to assemble and retest. The thruster was then reassembled and more operational data taken. After tests indicated that a vapor leak was present in the isolator of the cathode-isolator-vaporizer (C-I-V) assembly, the second segment of disassembly took place. In addition to the disassembly made initially, the thruster was removed from the gimbal and the C-I-V was removed from the thruster backplate. The results, which included electrical measurements, magnetic measurements, physical measurements, and photographs, are presented in the following paragraphs.

A. CHRONOLOGY

The removal and post-test examination of the lifetest thrust system was conducted using a specific chronology that was established by mutual agreement between HRL and LeRC personnel. The intent, of course, was to minimize any changes to the after-test state of the thruster, preserving as much diagnostic information as possible. For completeness, the chronology of the

events is described below. For clarity, and to facilitate their interpretation, the analysis results that are presented in the next section are cataloged according to component or subassembly.

The first step in the post-test examination involved removal of the side-port window in the HRL Lifetest Facility. This provided access to the interior of the vacuum chamber and enabled a 12-in.-square mirror to be placed inside and near the thruster (for closer visual observation of the ion-extraction assembly). Next, the top end-bell of the vacuum chamber was removed, and the thrust system and mounting hardware were lifted out of the chamber (geometry shown in Figure E-1). The assembly was photographed in situ. The next step involved removing the thruster system (Thruster, Gimbal Assembly, and Beam-Shield Unit) from the mounting hardware and remounting the system on a vertical support structure. It was then transported to the HRL Mercury Room for examination and disassembly (the vertical orientation of the thruster system was carefully maintained).

At this point the gimbal covers were removed, and each team member inspected the exterior of the thruster and beam-shield unit, ion-extraction assembly, neutralizer keeper, and gimbal housing. The vertical orientation of the thruster was preserved, and mirrors and magnifying glasses were used to facilitate visual inspection. Photographs were also taken.

Next, the beam shield and outer shell were removed, providing access to the exterior of the discharge chamber, neutralizer assembly, and the ion-extraction electrodes and mounting hardware. Both individual visual observations and photographs were obtained at this point. A gaussmeter was used to survey the magnets, and a low-power (7-30X) microscope was used to examine the juncture between the neutralizer feedline and vaporizer. The ion-extraction assembly was removed in a manner such that the plane of the electrodes remained in the same horizontal orientation as existed during the test. The discharge

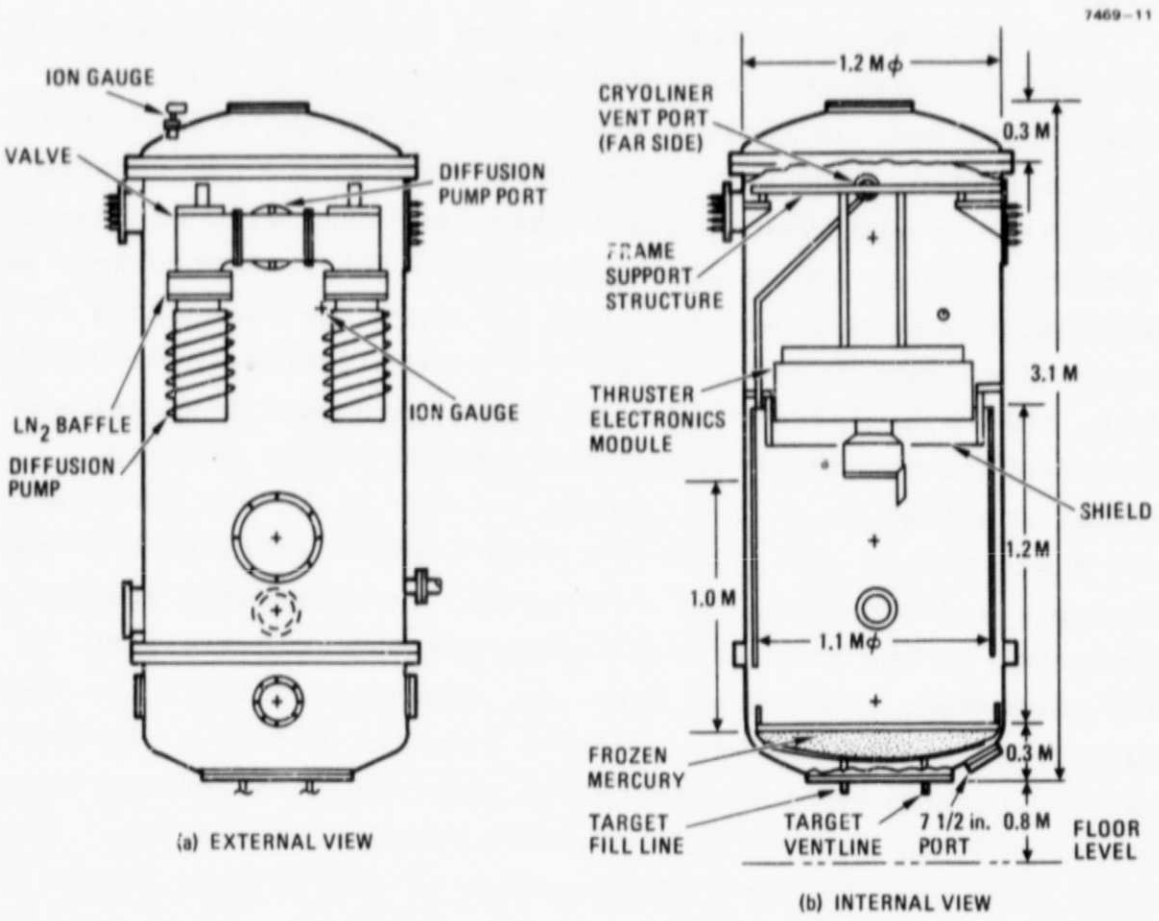

Figure E-1. Vacuum lifetest facility.

side of the screen electrode was examined and photographed, and two foreign objects that were found resting on the accel electrode were collected. Next, the interior of the discharge chamber was observed using a mirror.

The discharge chamber was removed (while maintaining its vertical orientation), and visual observations of the anode, insulators, and the region between the anode and chamber wall were performed. The thruster-mounting structure was rotated 90° to provide an end view of the neutralizer assembly, discharge-chamber endwall, and cathode polepiece/baffle. Photographs were obtained and plug gages were used to check the dimensions of the neutralizer-keeper aperture and the neutralizer-cathode orifice. Next, the neutralizer-keeper was removed to permit visual and photographic documentation of the cathode heater and tip. Closer examination of the cathode orifice plate was performed, and a micrometer and depth gage were used to estimate the orifice-plate dimensions. At this point, the discharge chamber was remounted to the endwall and a complete magnetic-field survey was performed. Following this, the discharge chamber, cathode polepiece, and baffle were removed from the endwall. Both visual and photographic documentation were obtained for the cathode keeper and the cathode side of the polepiece and baffle. Plug gages were used to check the diameter of the cathode keeper and orifice.

Next, the ion-extraction assembly was turned over, permitting visual observation and photographic documentation of the downstream side of the accelerator electrode. Resistance/open-circuit measurements were performed for various components; samples removed from the beam shield and ion-extraction assembly were checked to determine whether or not they were magnetic. Plug and feeler gages were used to measure the screen and accel aperture diameters and the interelectrode spacing.

B. EXAMINATION RESULTS OF FIRST DISASSEMBLY

After removing the side-port window, the thruster system and interior of the vacuum chamber were accessible for visual observations, which were facilitated by inserting a mirror inside the chamber to view the ion-extraction and neutralizer assemblies. The thruster, beam shield, electronics module, and vacuum chamber were noted to be extremely "clean". No mercury (either in droplet or finely divided form) was visible, except on the annular shield indicated in Figure E-1. The top side of this surface was covered with large-size mercury drops, which were vacuumed up before removing the thruster from the facility. The beam shield was also free of mercury, but what appeared to be back-sputtered material was evident on its surface.

A photograph showing the appearance of the thruster and electronics module is presented as Figure E-2 (the annular shield discussed above had been removed prior to taking the photo). The cleanliness of the thrust system is evident in the photograph, which also gives some indication of the appearance of the interior of the vacuum chamber. A closeup of the thruster system is presented as Figure E-3, which illustrates to an even greater degree the cleanliness of both the thruster and electronics module. The interior side of the beam shield is also visible in this photo. Figure E-4 is a photograph of the interior of the electronics module, showing the appearance of the propellant tank, gimbal enclosure, power-electronics unit, and interconnecting cables and feedlines.

Having obtained the photos described above, the thruster was removed from the electronics module, and both units were transported to the HRL Mercury Room for further examination on the subassembly and component levels.

M14979

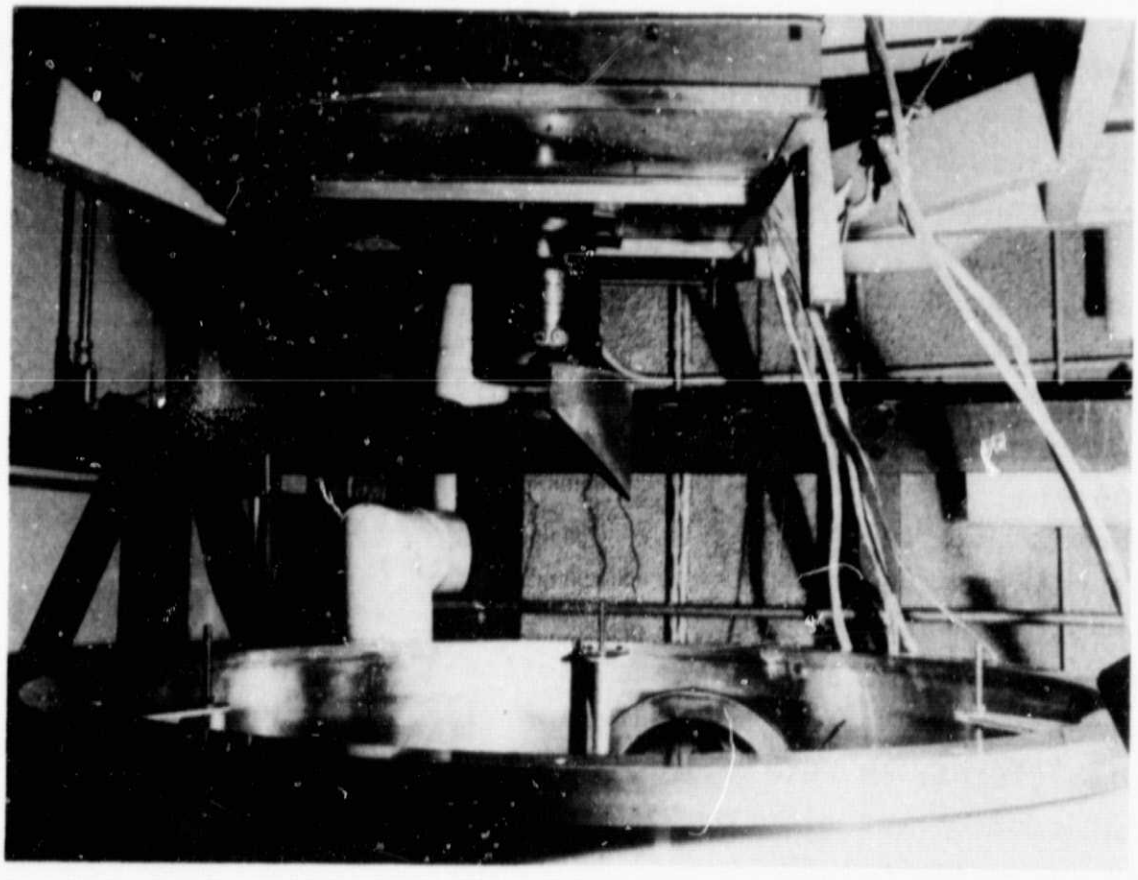

Figure E-2. Post-test appearance of the thruster and electronics module.

M14980

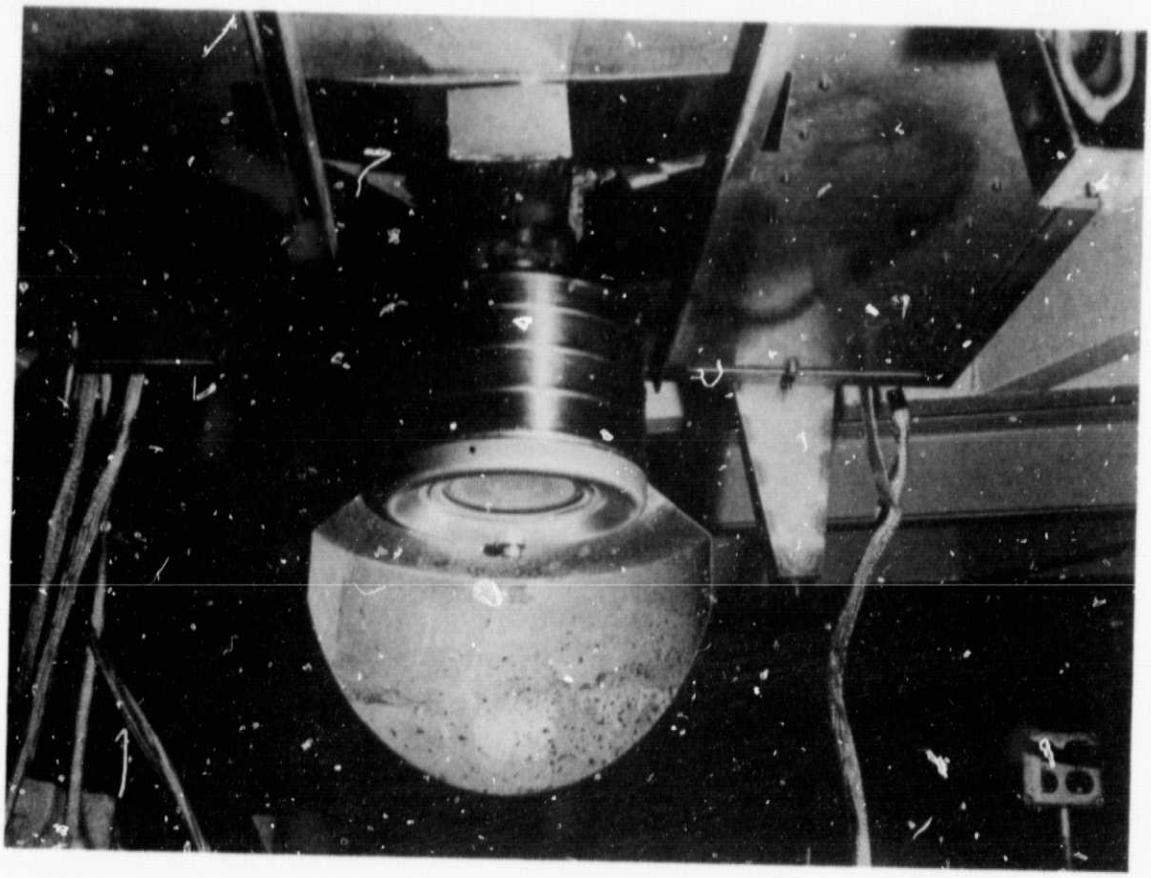

Figure E-3. Post-test appearance thruster.

M14978

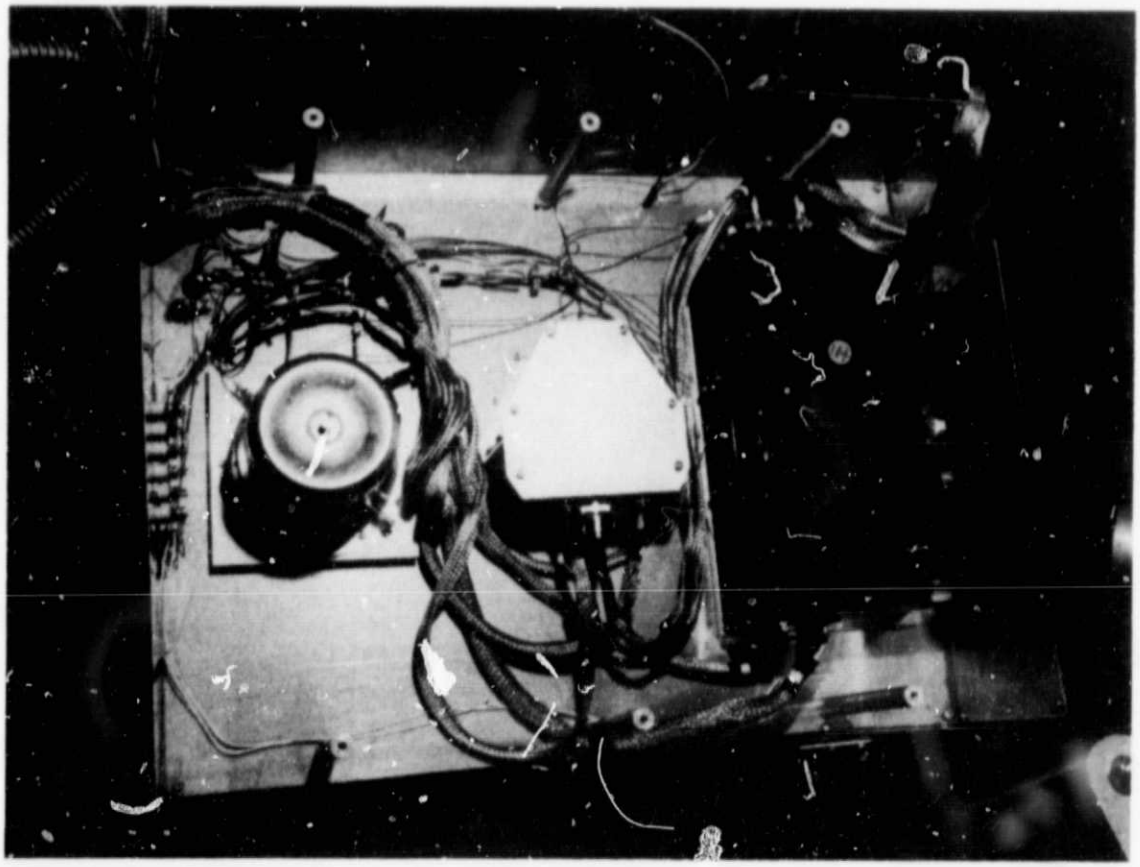

Figure E-4. Post-test appearance of electronic module with cover removed.

1. Ion-Extraction Assembly

At the conclusion of the lifetest, the ion-extraction assembly developed a 3-Ω short. Therefore, we monitored the screen-accel resistance periodically throughout the removal and examination in an attempt to determine the cause of the short, and we maintained the assembly in the test orientation during much of the documentation effort.

a. Accel and Screen Electrodes

Figure E-5 is a photograph of the accelerator electrode that was obtained while viewing the thruster from below (thruster pointed down, as it was during the test). Both the accel grid and the ground-screen mask are "clean", with only a few smudges visible on the mask (apparently the result of handling during the removal step). The outer three "rows" of accel apertures are seen to have a notched appearance, with the pattern symmetrical about the thruster axis. Some evidence of charge-exchange-ion erosion is evident, particularly near the center of the electrode. Upon close inspection, the reader can distinguish an aperture near the center which has undergone erosion through its web and an aperture in the region adjacent to the neutralizer that has a peculiar elongated shape. There are four locations where mercury droplets can be seen through the accel apertures. The electrode features described above are even more apparent in the closeup of Figure E-6. A closeup of the accel grid that was taken after removing the ion-extraction from the thruster is presented in Figure E-7 (same orientation as in Figures E-5 and E-6).

Figures E-8 and E-9 present blowups of Figure E-7 that illustrate the general pattern of the charge-exchange erosion near the center of the grids (although not clearly evident in these blowups, the triangular erosion sites defined by three adjacent apertures have eroded all the way through the accel

M14990

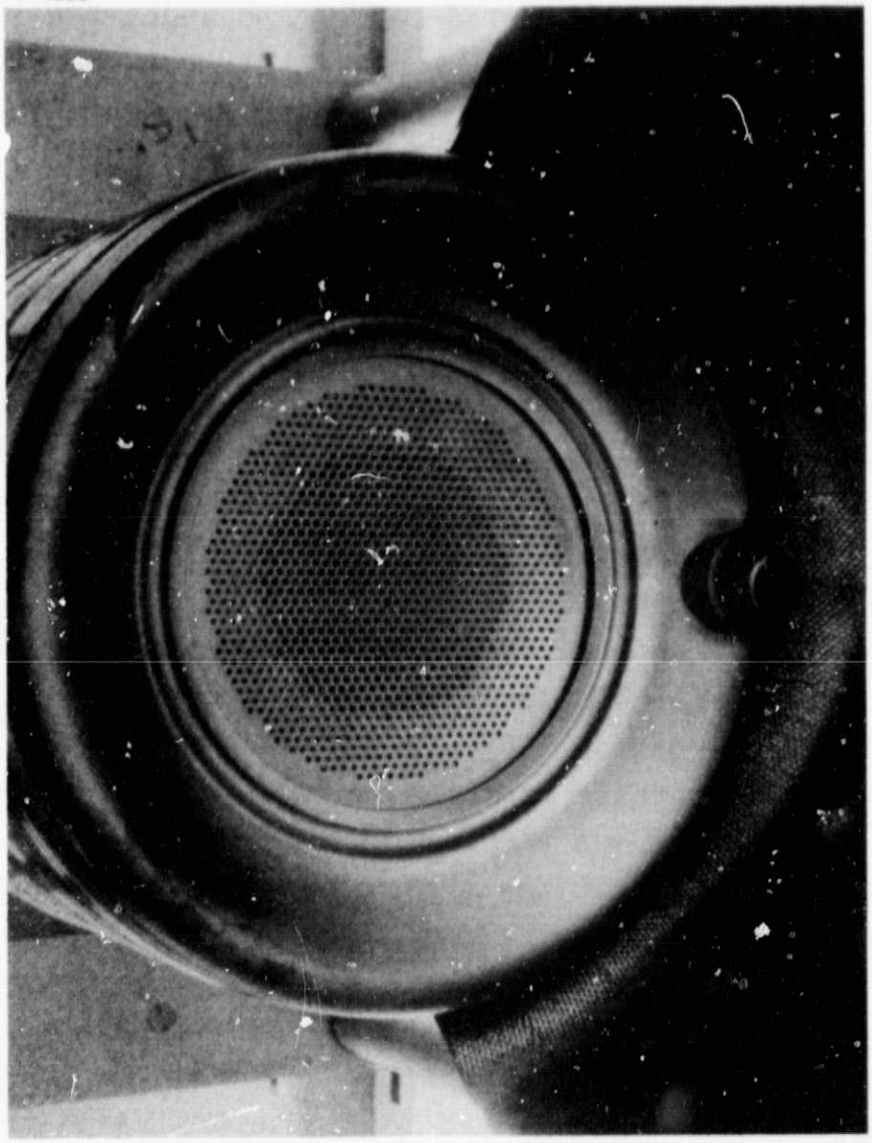

Figure E-5. Post-test appearance at accel grid.

M14997

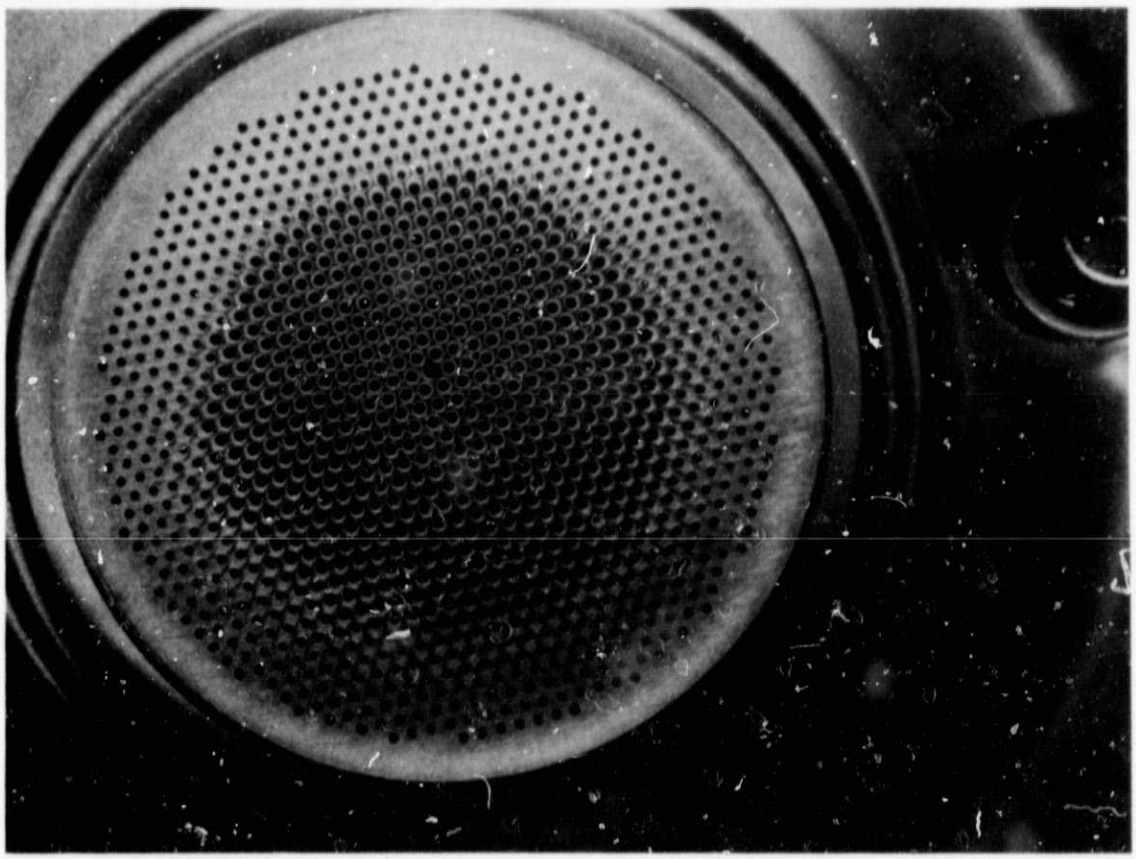

Figure E-6. Post-test appearance of accel grid (closeup).

M14987

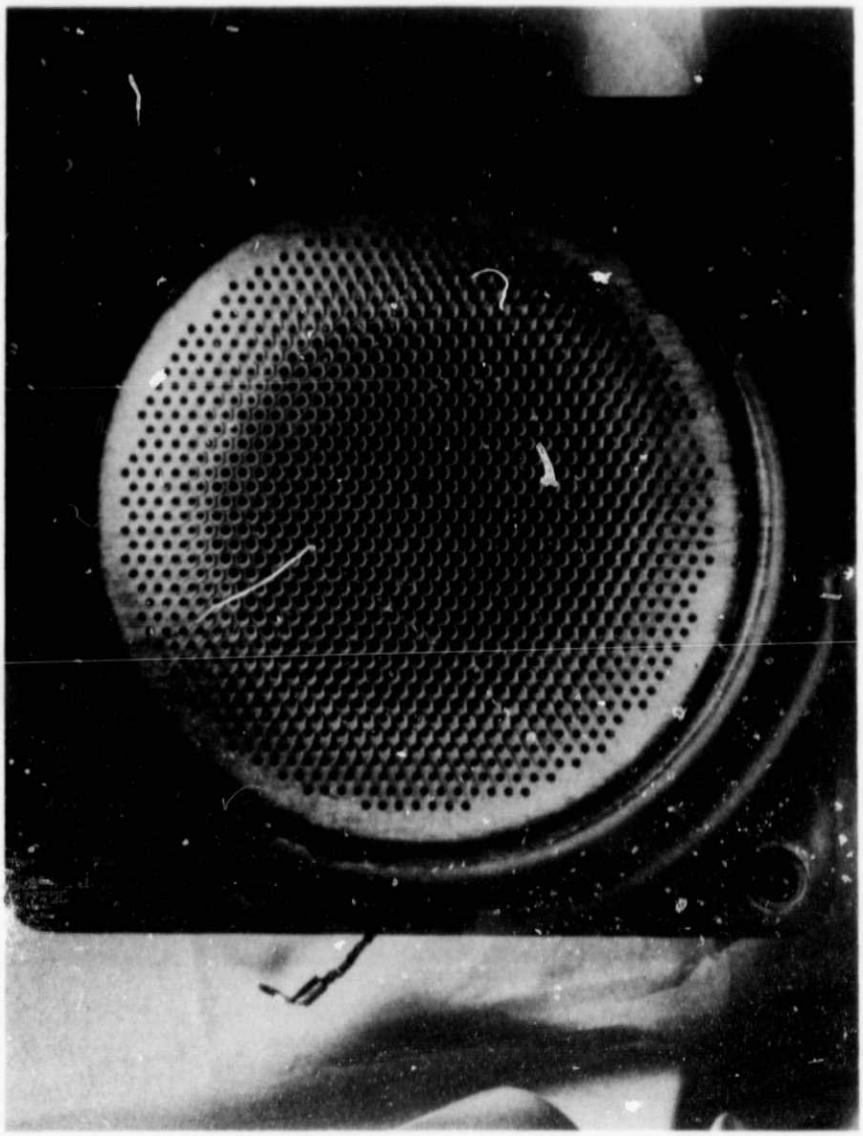

Figure E-7. Post-test appearance of accel grid after removal from thruster.

M14985

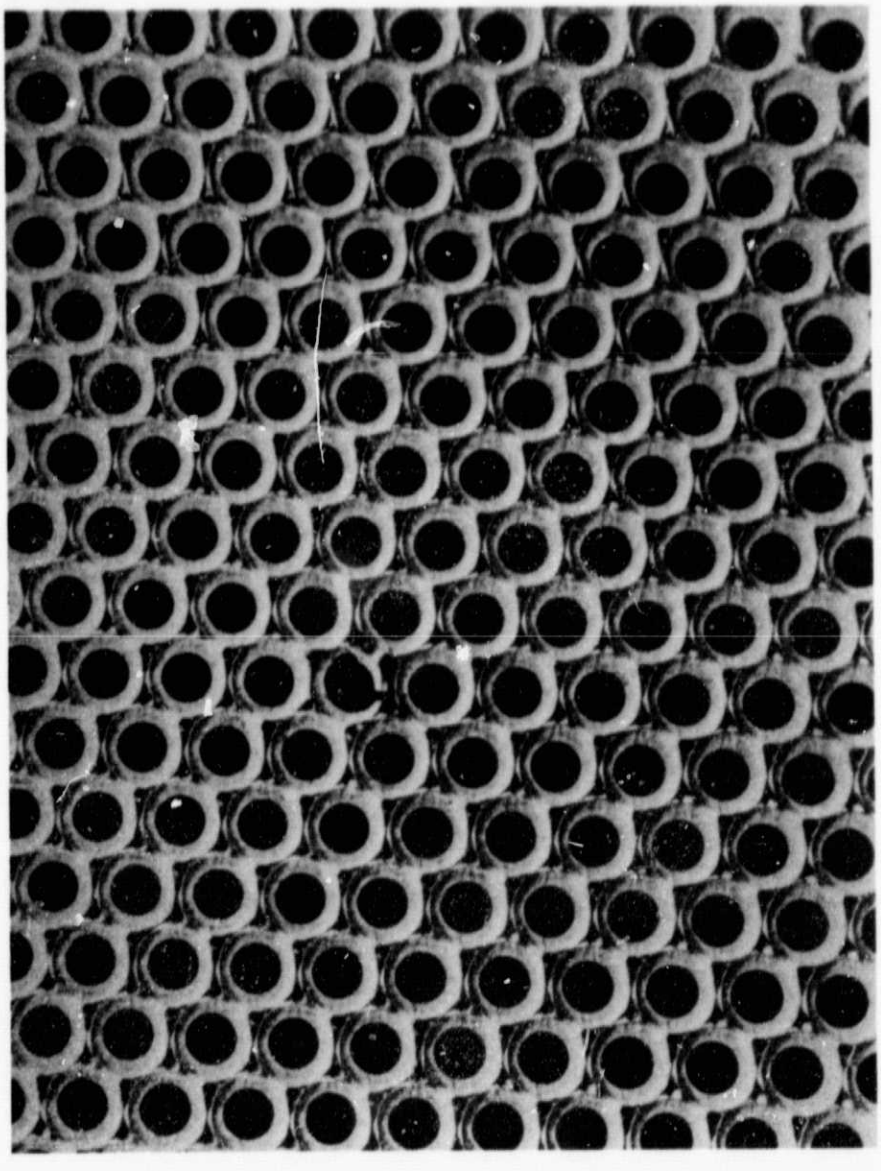

Figure E-8. Enlarged view of accel grid.

M14985

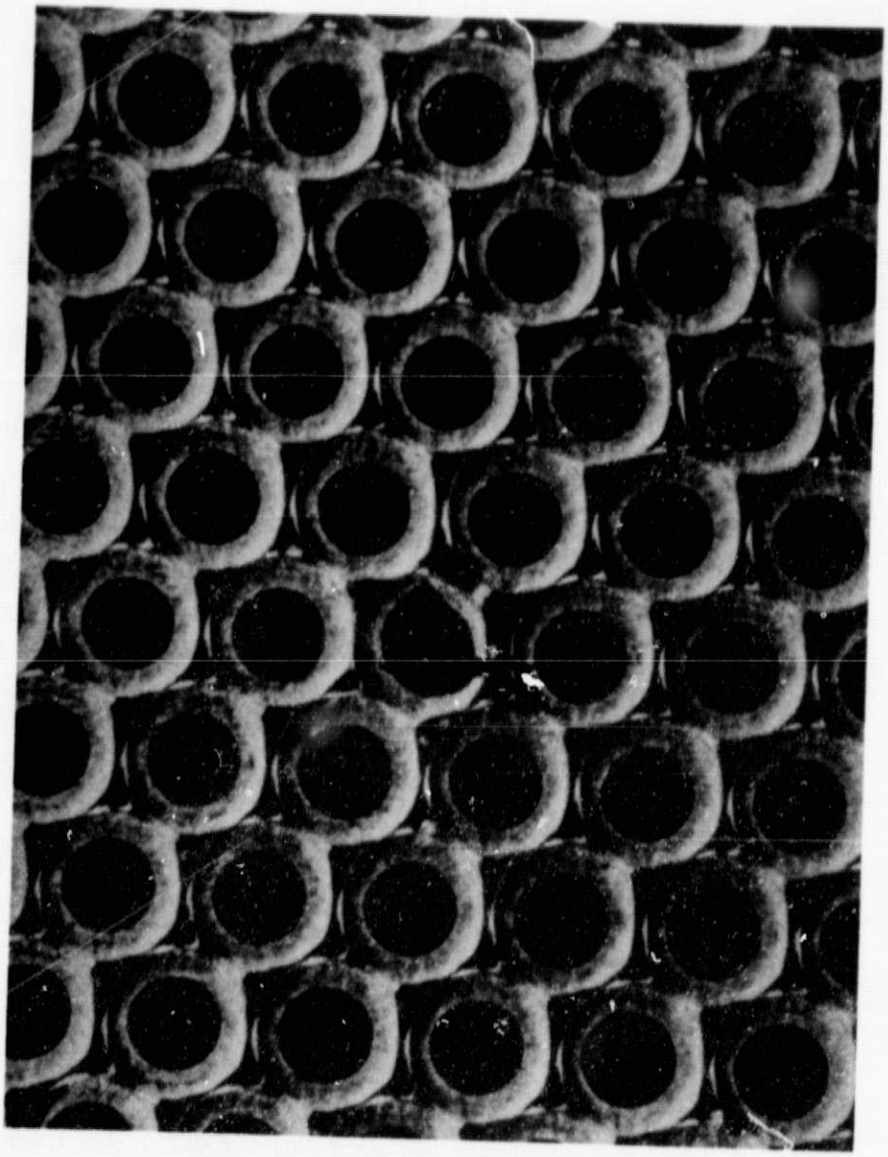

Figure E-9. Enlarged view of accel grid.

grid). These figures also provide additional detail on the eroded web near the center of the grid. Figure E-10 is a blowup showing the notching that occurs near the beam edge and the peculiar appearance of the aperture adjacent to the neutralizer (3 o'clock position, fourth aperture from the edge).

Figure E-11 is a photograph taken from the screen side of the ion-extraction assembly, showing the damaged accel aperture near the center of the electrode. Close examination of the adjacent screen aperture shows a buildup of material, apparently caused by deposition of material sputtered from the accel grid. Also, the small white spots that appear just below the top edges of some of screen apertures are those locations where the accel grid was eroded all the way through. Figures E-12, E-13, and E-14 are additional photos showing the appearance of the accel grid (taken from the screen-grid side). Figure E-15 is a photo taken from the same orientation, showing a peculiar "crater" near the (bottom) edge of one of the central screen apertures. Figure E-16 shows details of the accel-aperture notching that was prevalent near the edge of the aperture pattern. The accel aperture in the center of this photo can be seen to be bridged by a slender piece of material -- one of the foreign objects that was collected.

b. Aperture and Interelectrode Spacing Measurements

The diameters of select screen and accel apertures were measured using plug gages (1-mil graduations), and the results are presented in Figures E-17 and E-18 (in parentheses), along with similar measurements that were performed during the assembly of the ion-extraction assembly. Interelectrode-spacing measurements were performed using L-shaped feeler gages, and the results are presented in Figure E-19 (in parentheses), along with similar measurements that were performed prior to the test. Integrating the accel-aperture dimensions over the extent of the aperture pattern gives an open area of 10.0 cm^2, which represents a 9.2% increase over the nominal pre-test value of 9.16 cm^2.

M14984

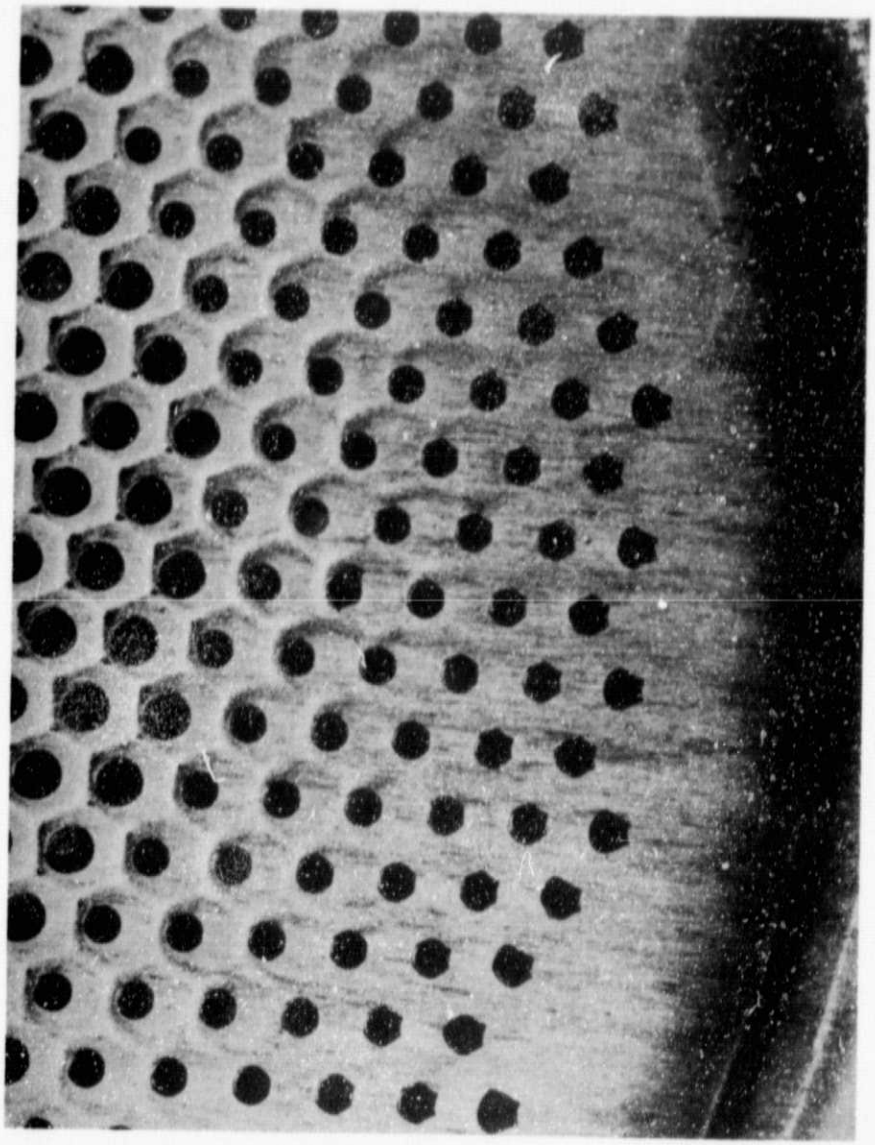

Figure E-10. Edge holes of accel grid.

M14994

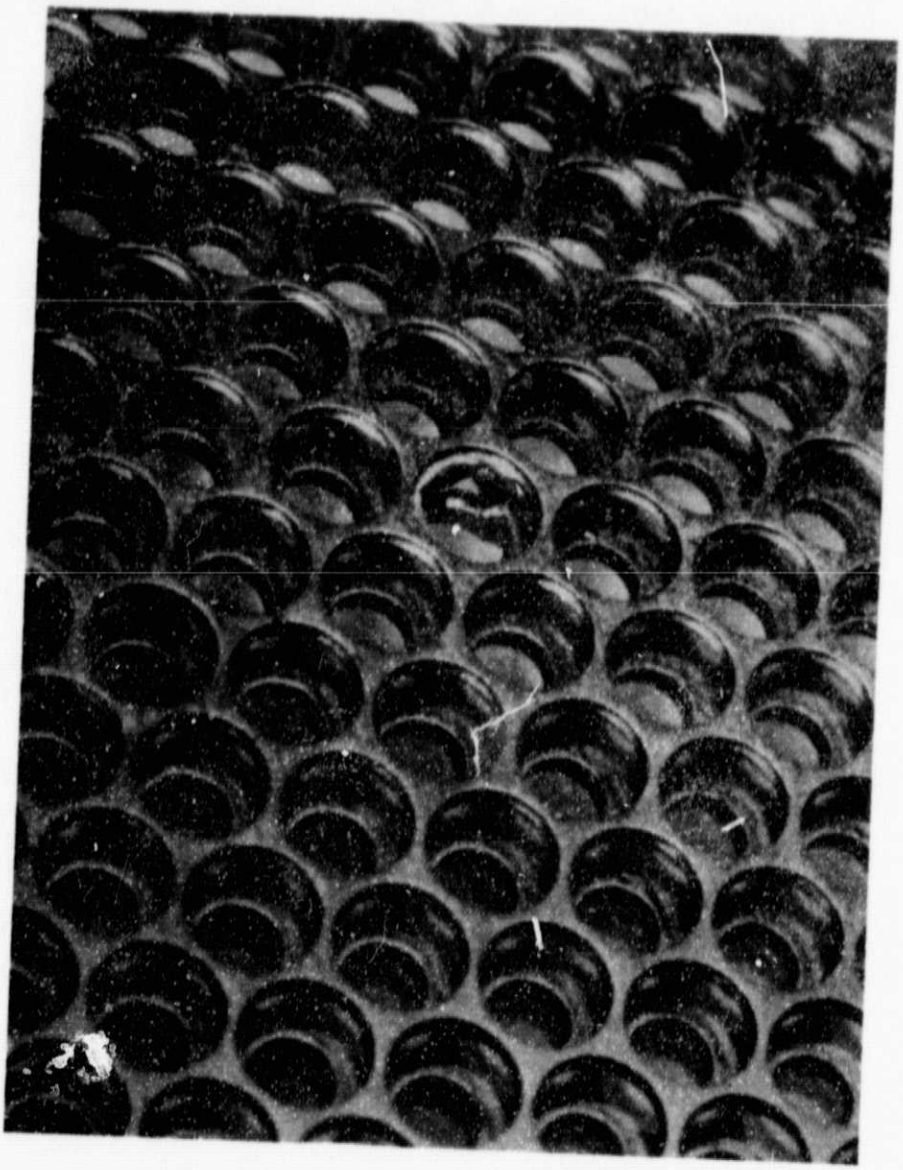

Figure E-11. Screen side of ion-extraction assembly.

M15008

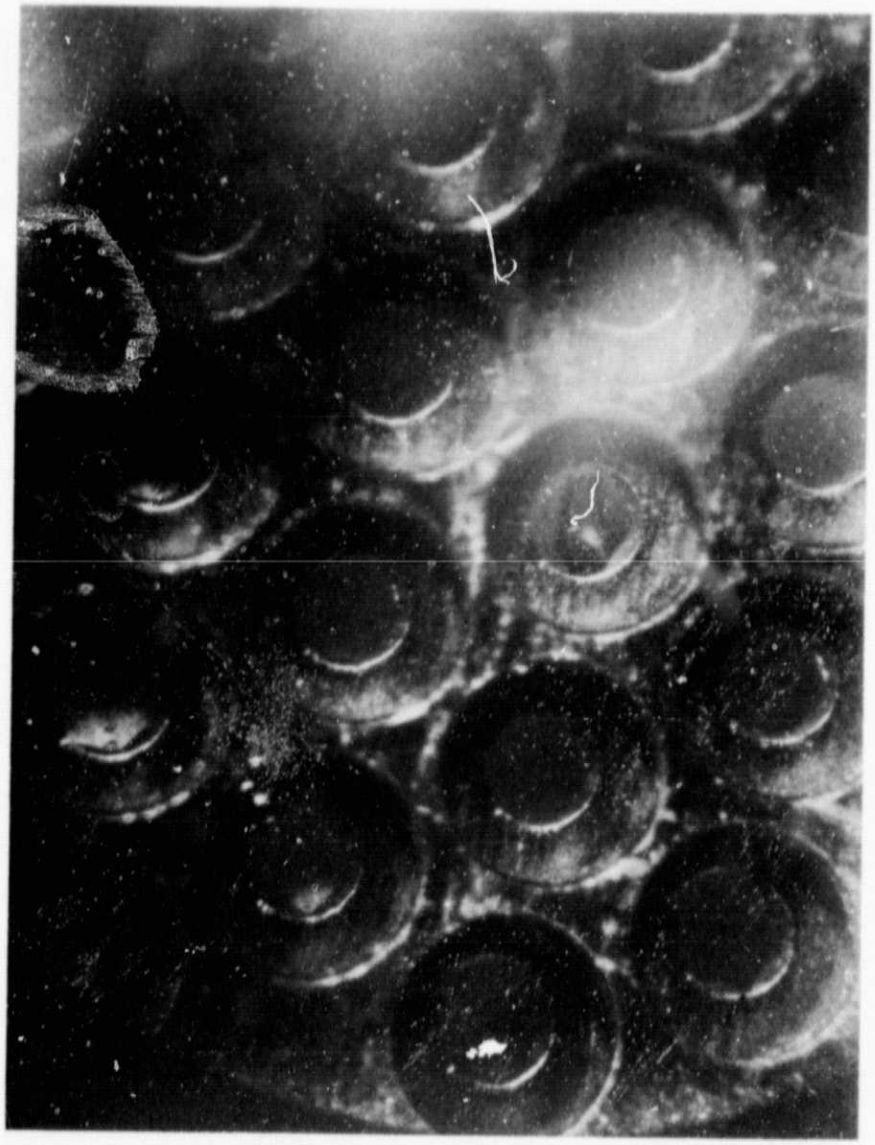

Figure E-12. Screen side of ion-extraction assembly.

M15009

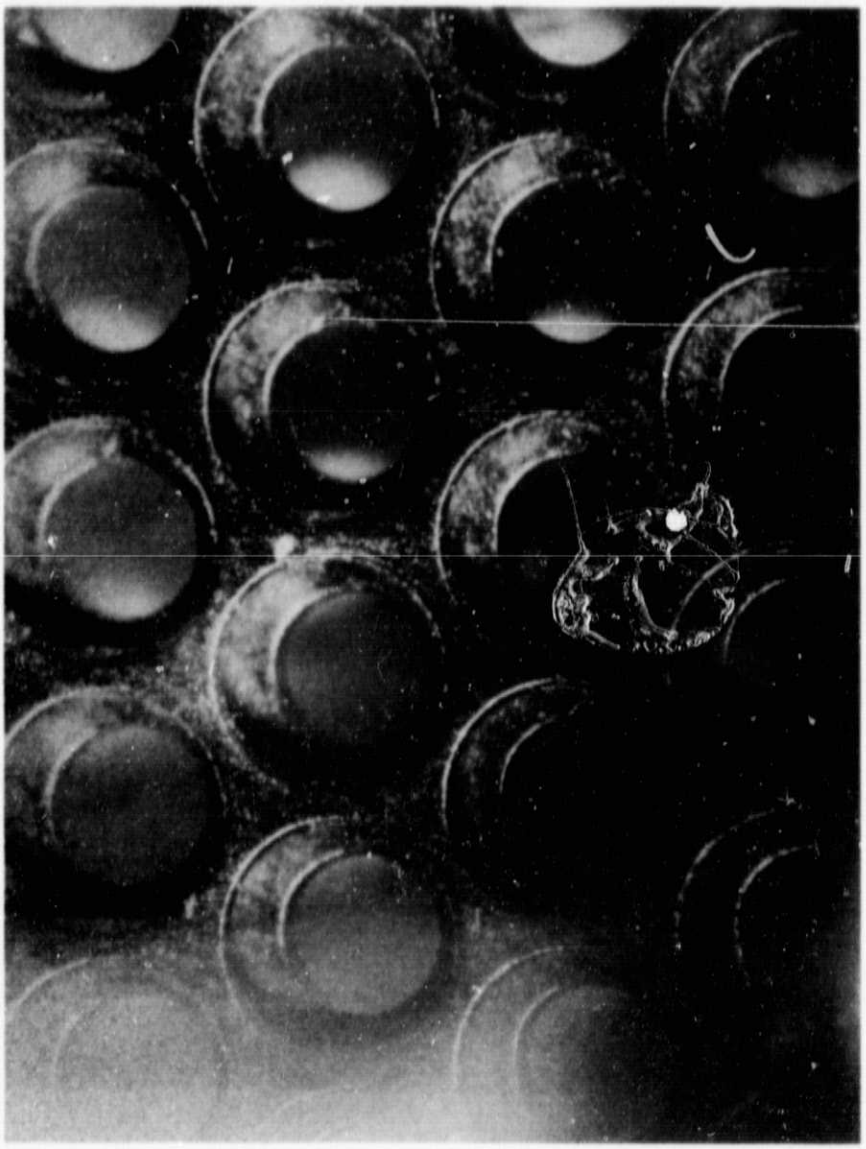

Figure E-13. Screen side of ion-extraction assembly.

M15007

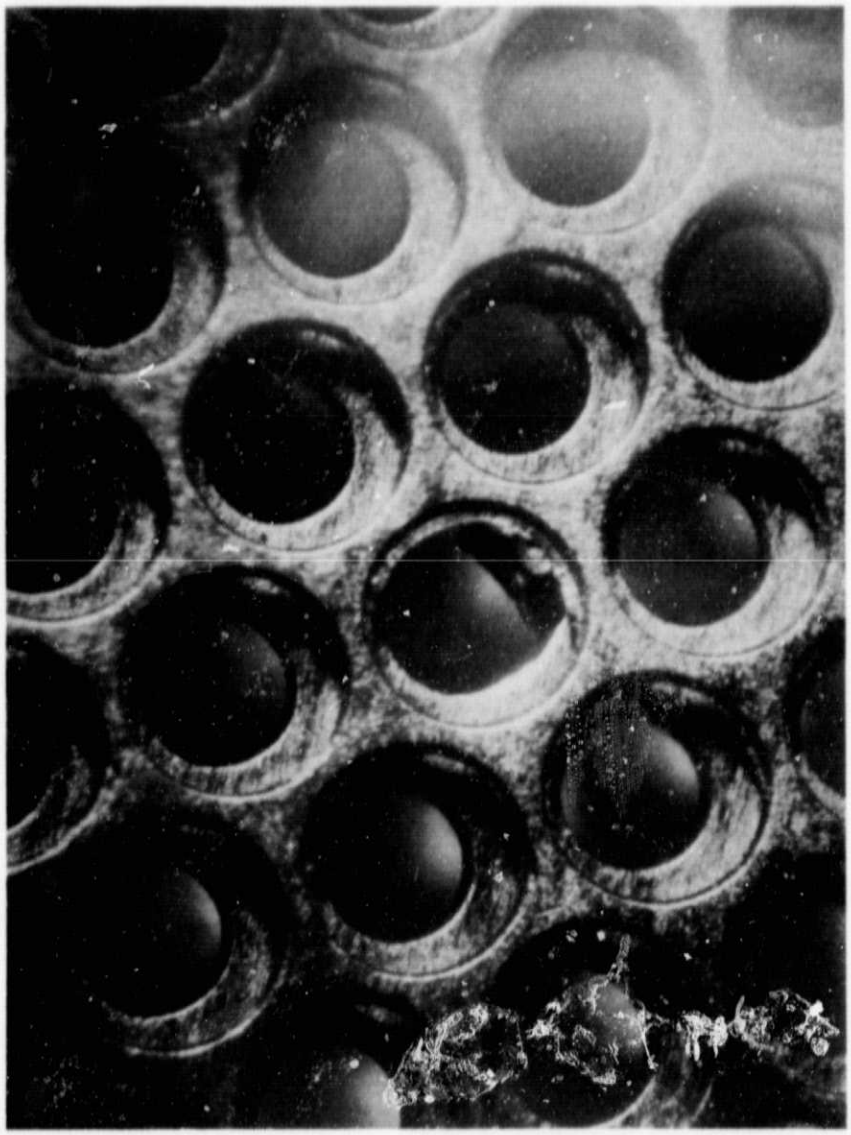

Figure E-14. Screen side of ion-extraction assembly.

M15009

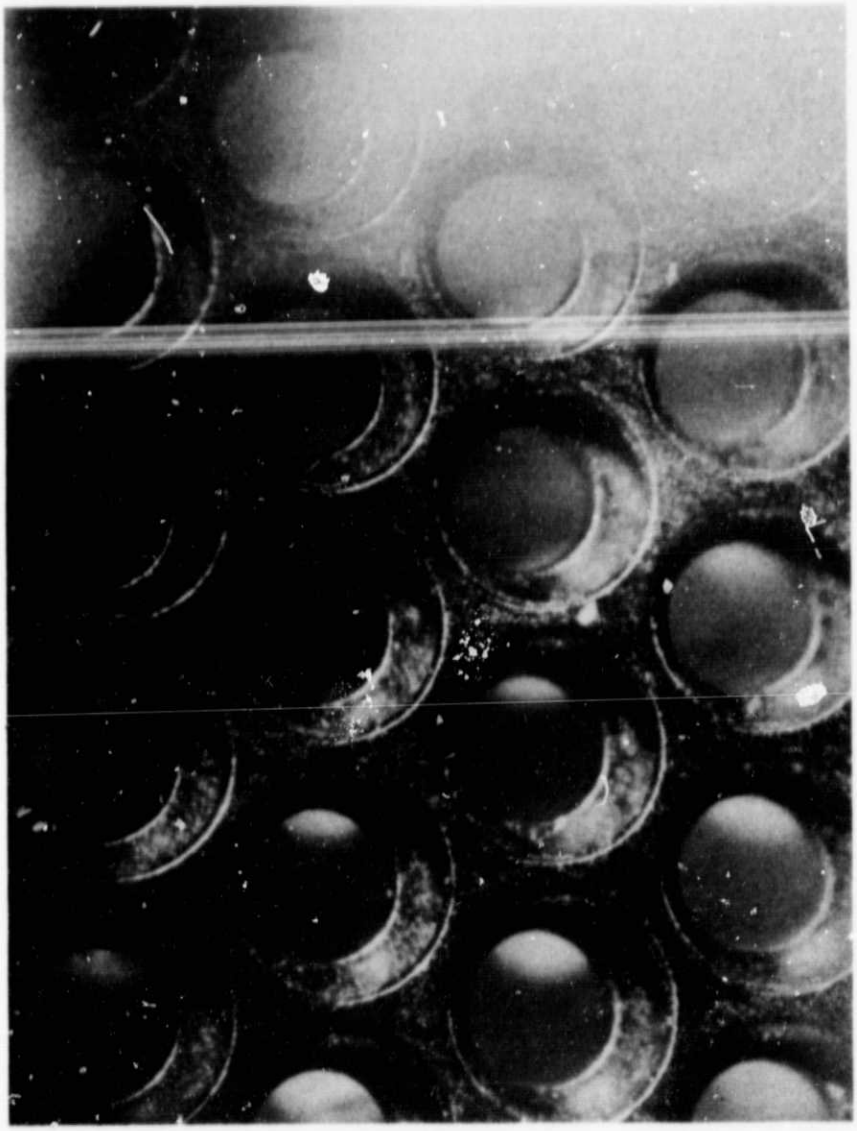

Figure E-15. Screen-side of ion-extraction assembly showing "crater".

C-2

M15006

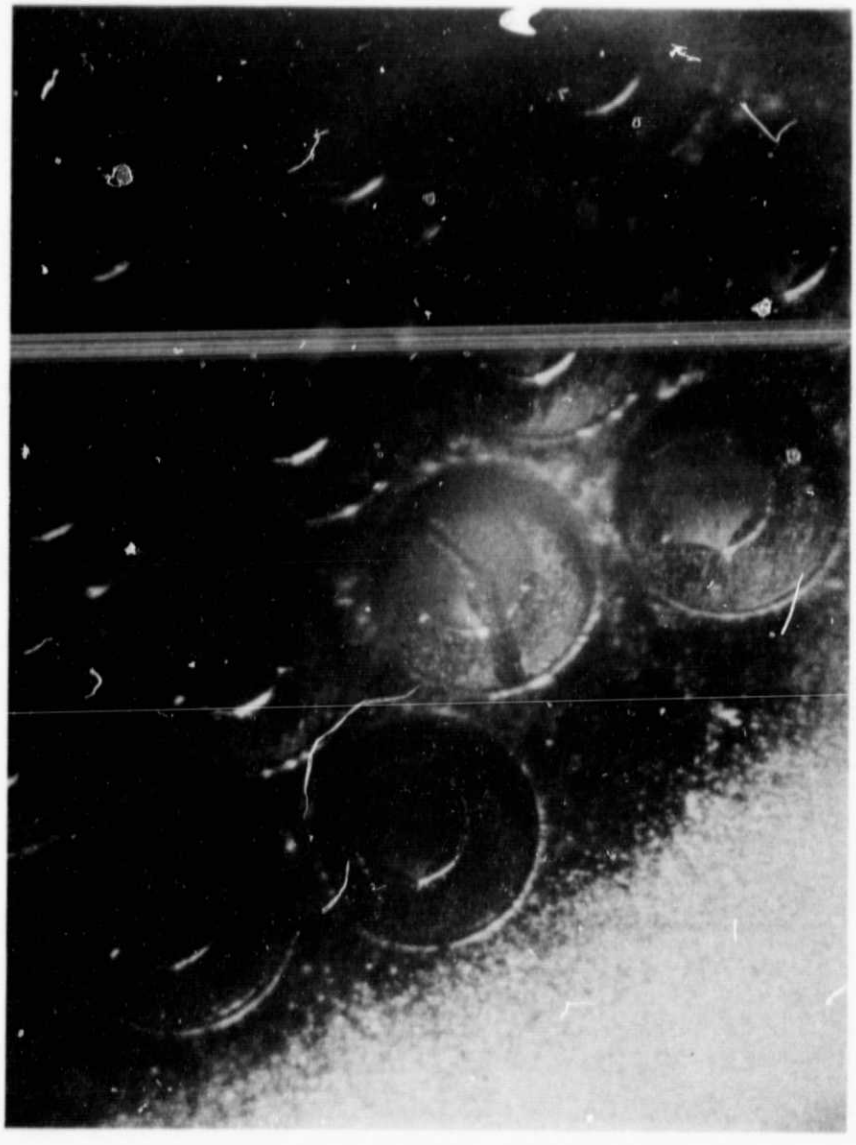

Figure E-16. Screen side of ion-extraction assembly showing accel notching.

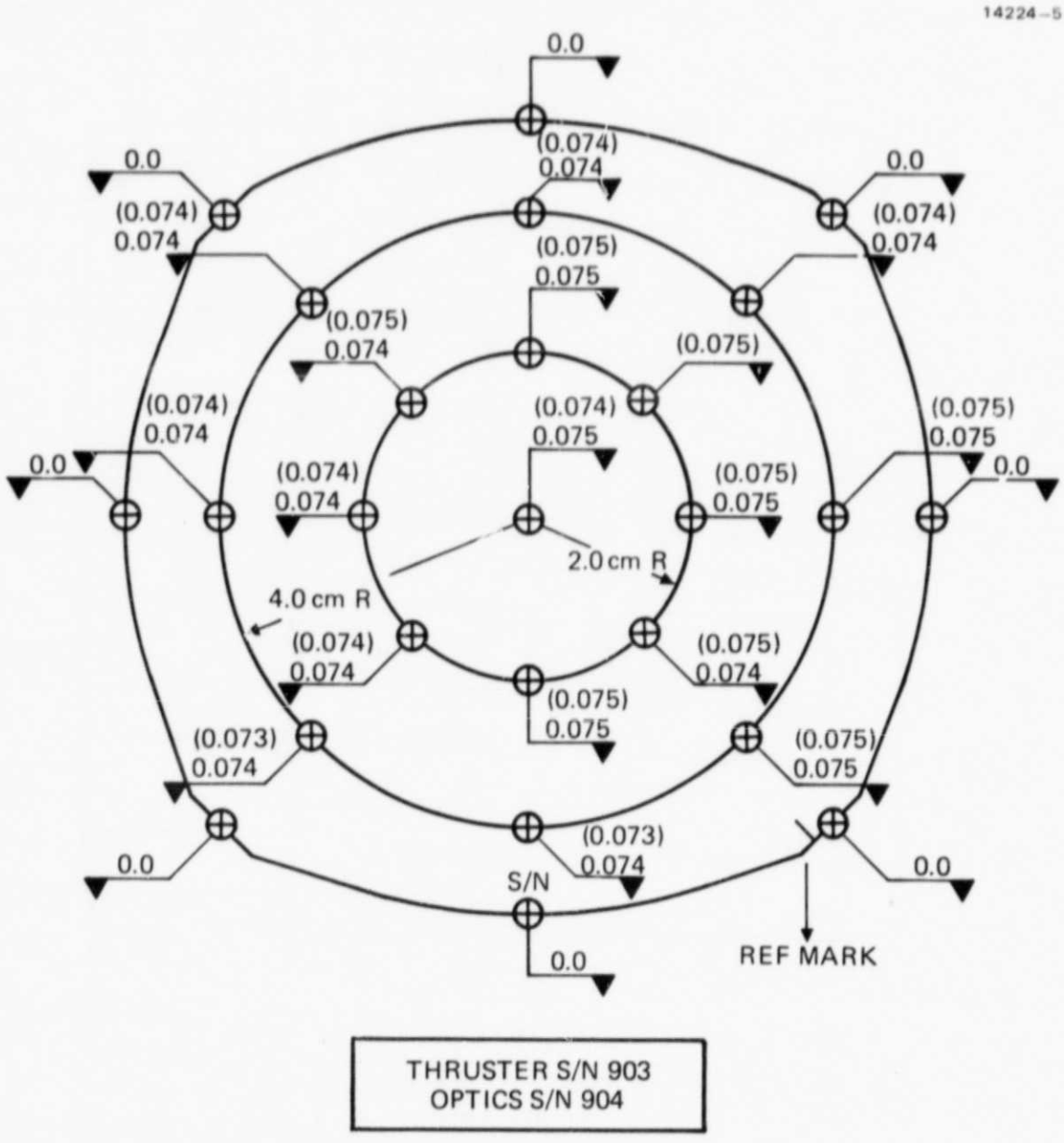

THRUSTER S/N 903
OPTICS S/N 904

Figure E-17. Pre-test and post-test screen aperture dimensions (inches). Post-test values in parenthesis.

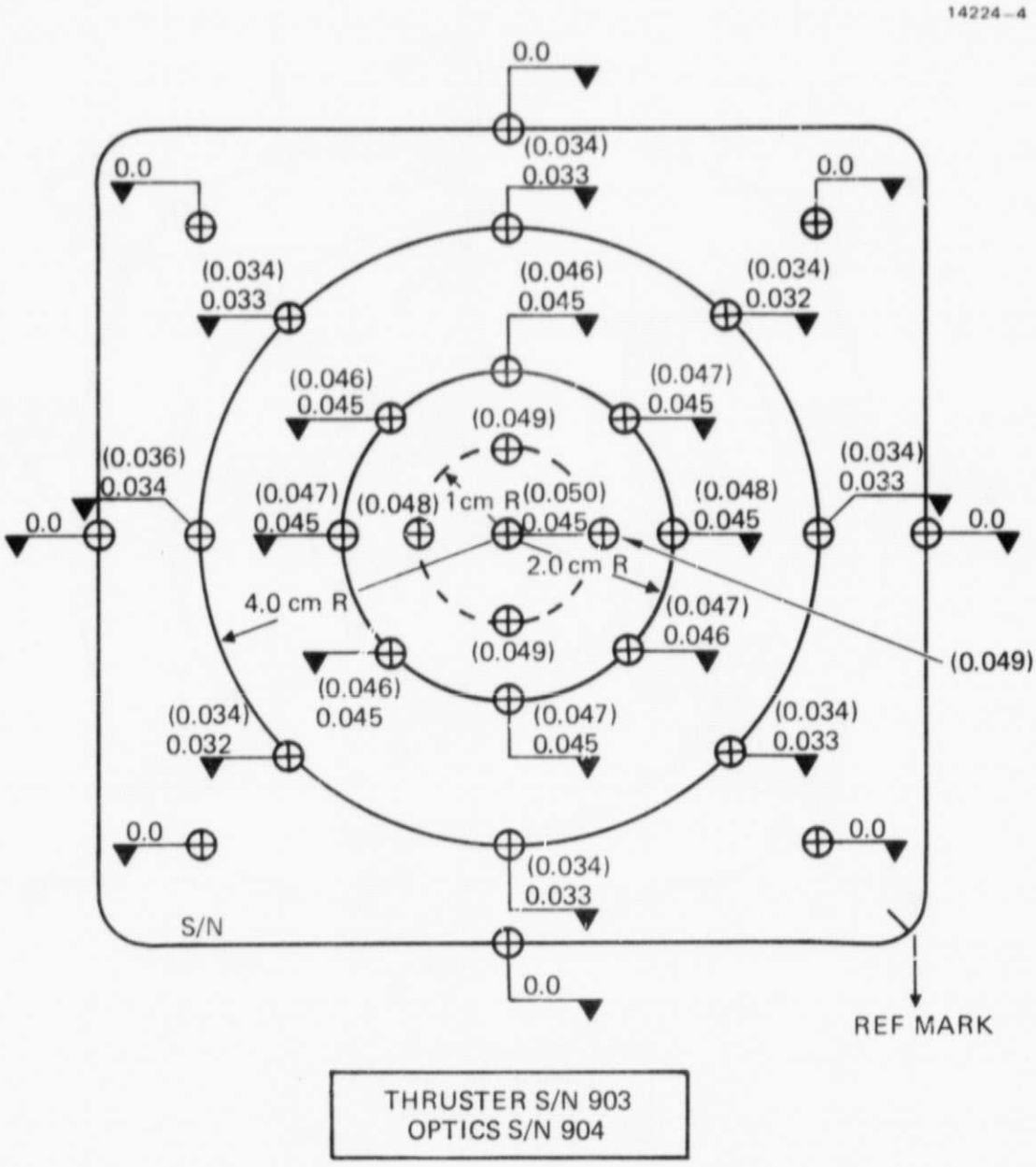

Figure E-18. Pre-test and post-test accel dimensions (inches). Post-test values in parenthesis.

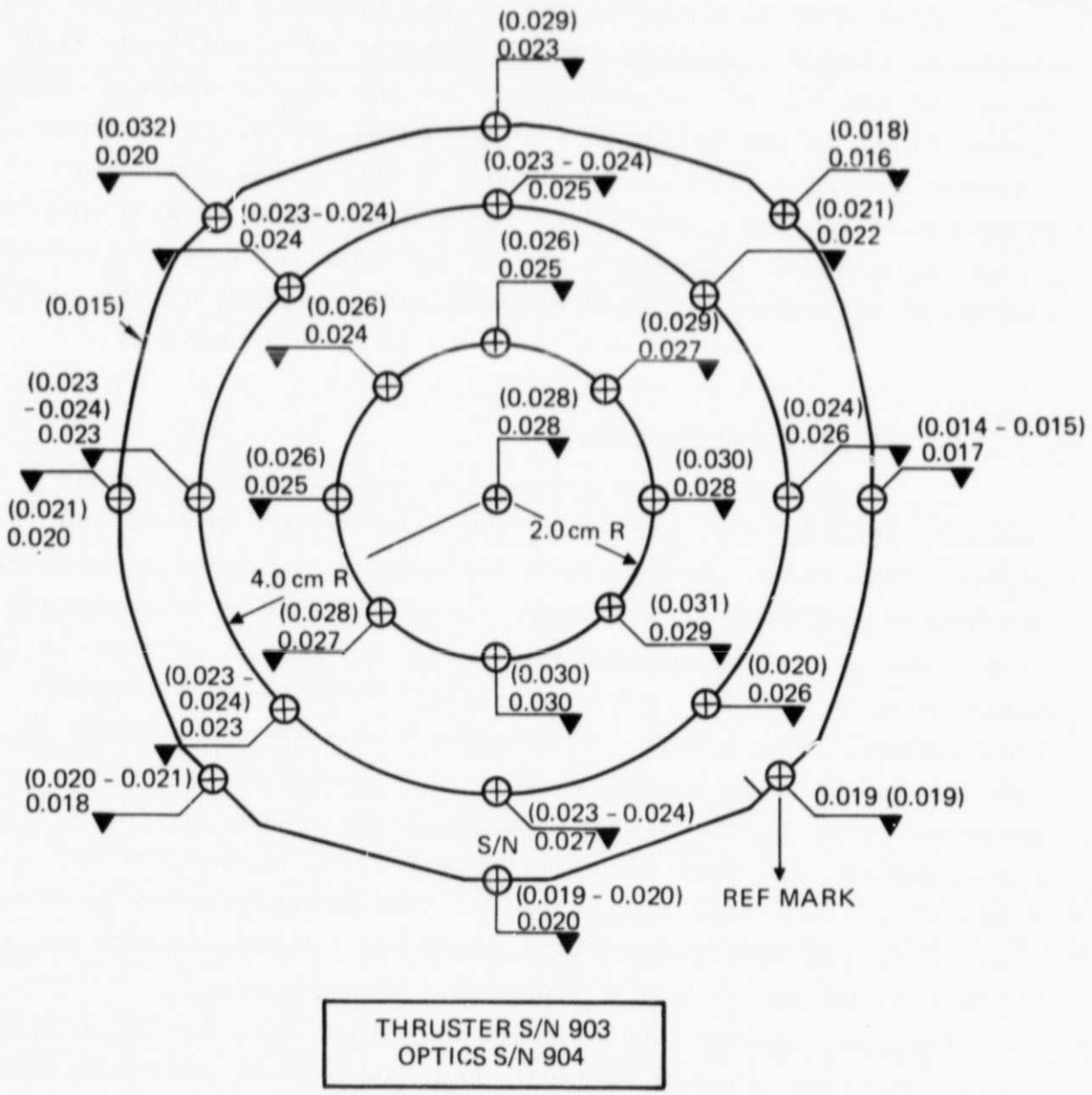

Figure E-19. Pre-test and post-test screen accel spacing (inches). Post-test values in parenthesis.

2. Discharge Chamber

Figure E-20 is a photograph of the exterior surface of the discharge chamber, showing the high degree of cleanliness that characterized all of the components of the thrust system. Additional views of the exterior are presented below, in the neutralizer section. Figure E-21 shows a photo that was taken after the discharge chamber was removed from the endwall and shows the general appearance of the upstream side of the screen electrode and anode. Although not clearly evident in the photo, the anode insulators had a very clean (white) appearance.

a. Baffle and Polepiece

Figure E-22 is a closeup of the discharge-chamber endwall, showing the details of the cathode, polepiece, and baffle. The flame-sprayed surfaces show no evidence of sputter erosion or deposition, and there is no evidence of discoloration. The appearance of the baffle is considered normal; it is centered with respect to the polepiece, with all the support legs intact. The screen covering the flow-diversion ports is intact, and nothing abnormal about the discharge cathode is apparent. The baffle diameter and thickness were measured using a micrometer, and were found to be 0.811 in. (2.060 cm) and 0.025 in. (0.064 cm), respectively. The corresponding fabrication specifications are 0.813 ± 0.002 in. (2.065 ± 0.005 cm) and 0.030 ± 0.003 in. (0.076 ± 0.008 cm), respectively.

The only abnormality evident in Figure E-22 is the delamination of flame-sprayed material that is evident on the outside (left) edge of the polepiece. Additional views of the endwall assembly are presented in Figures E-23 and E-24.

The appearance of the upstream side of the baffle and its support legs is illustrated in the photo of Figure E-25. No unusual features are apparent. The diameter of the baffle-support legs was measured at several locations using a micrometer and was found to be 0.044 in. (0.124 cm) (fabrication specifications are 0.050 ± 0.002 in. or 0.127 ± 0.005 cm).

M15006

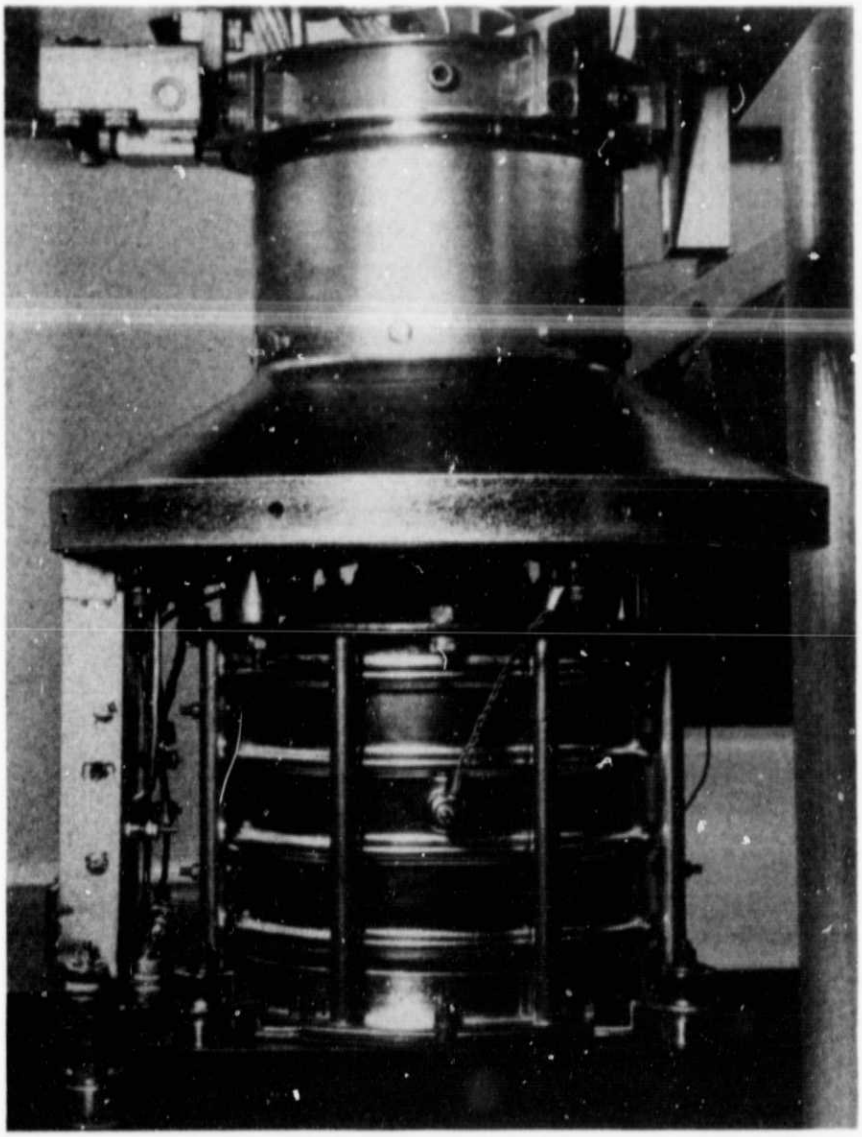

Figure E-20. Post-test appearance of discharge chamber.

M14991

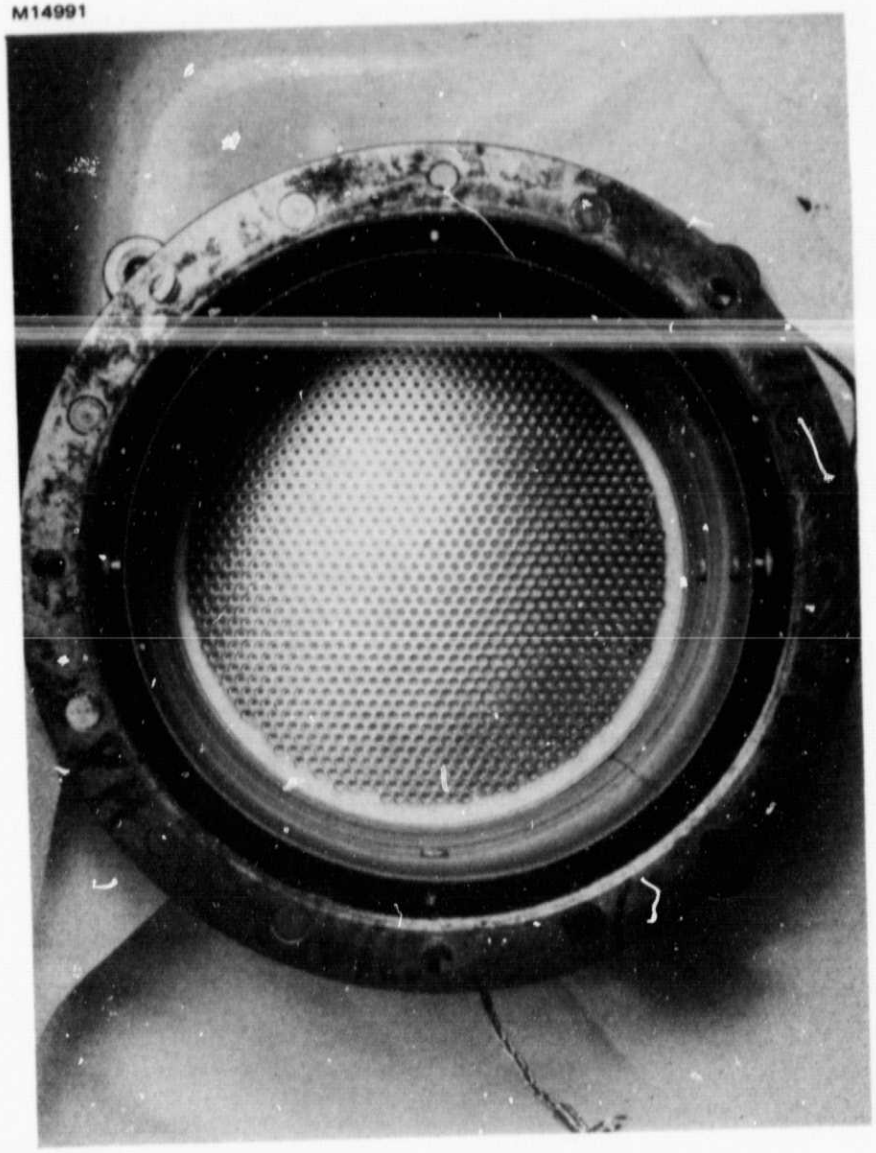

Figure E-21. Post-test appearance at discharge chamber interior.

M14981

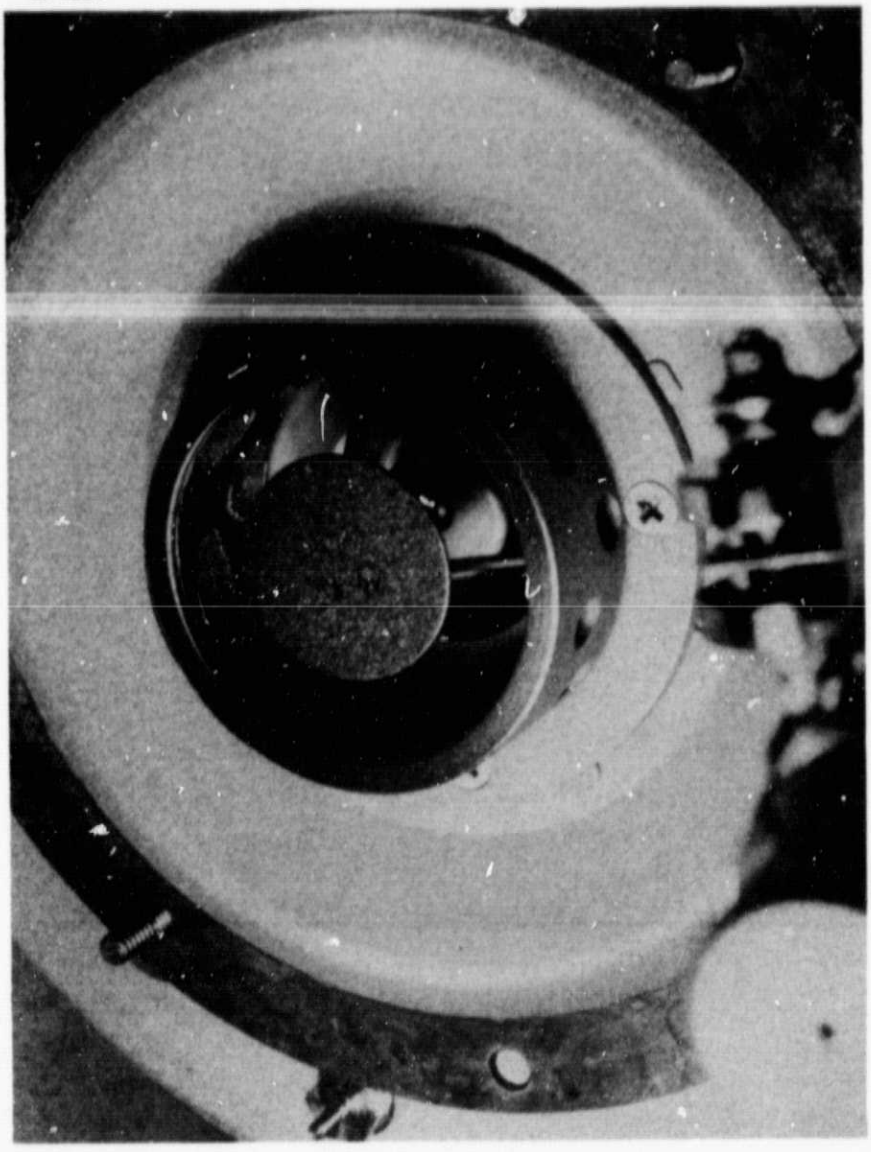

Figure E-22. Post-test appearance of discharge chamber endwall, cathode cup pole piece and baffle.

M14983

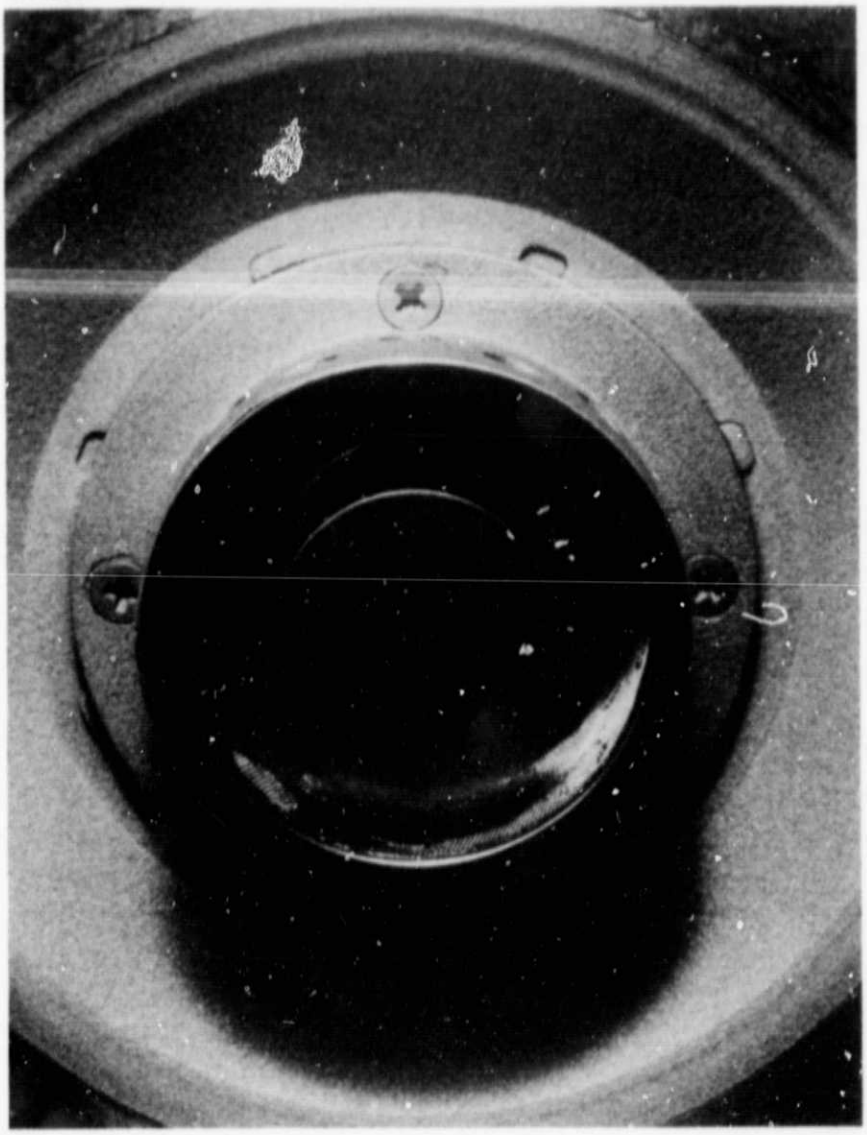

Figure E-23. Post-test end-wall assembly.

M14982

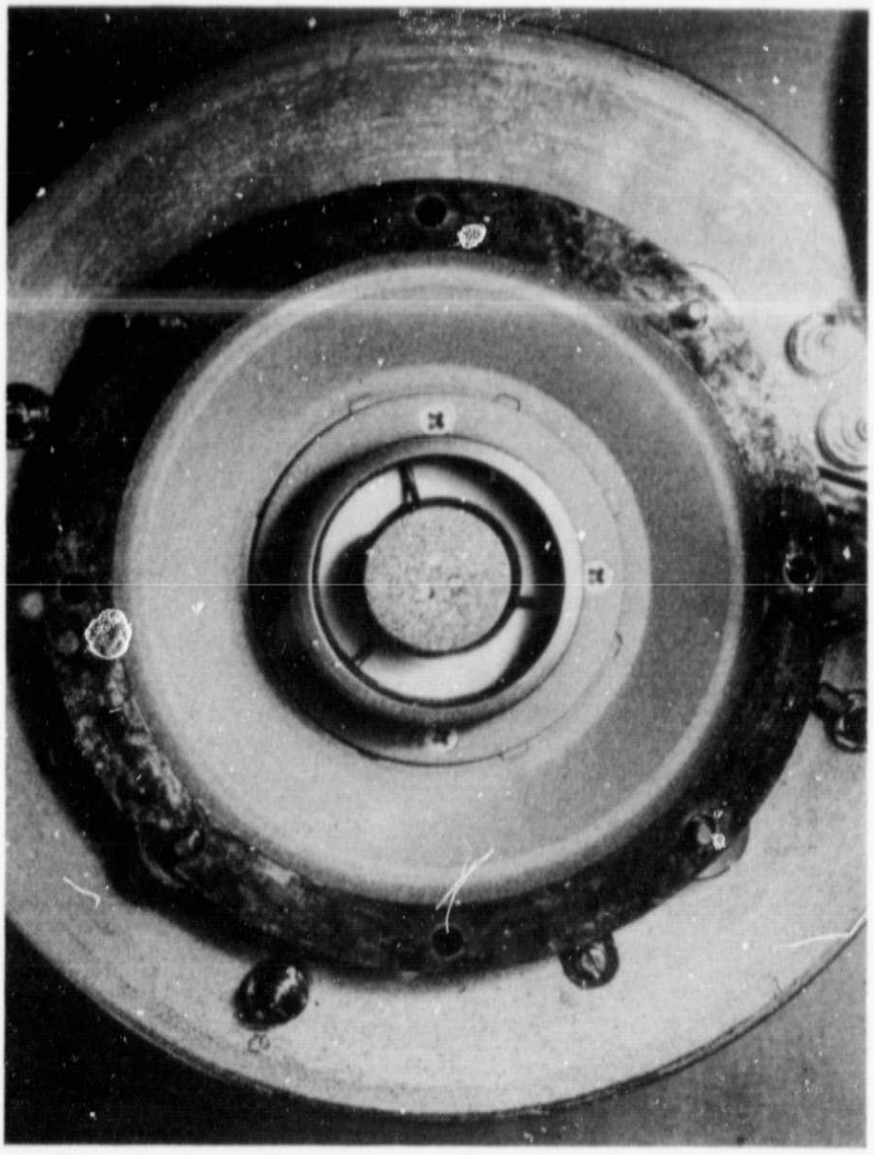

Figure E-24. Post-test end-wall assembly.

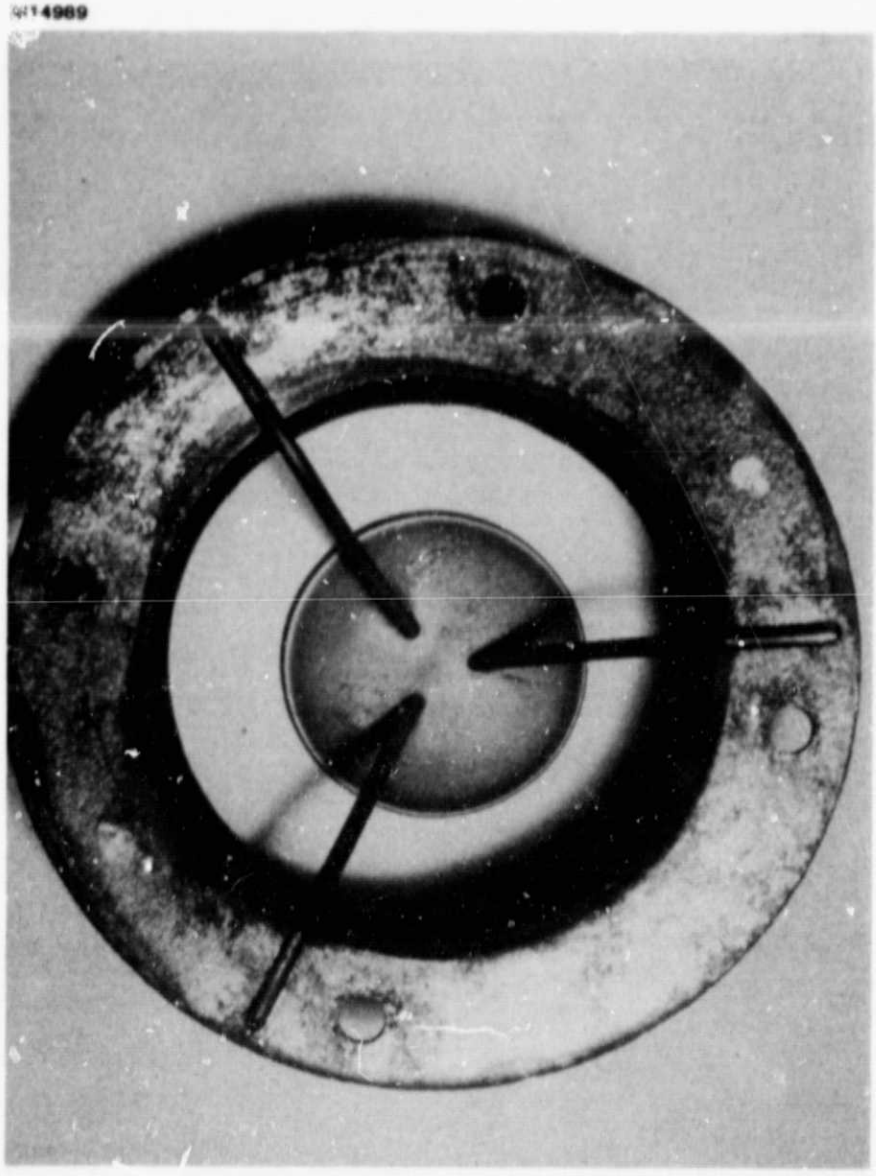

Figure E-25. Post-test appearance of upstream side of baffle assembly.

b. Discharge Cathode and Keeper

Figure E-26 is a closeup of the cathode keeper, showing that the cathode orifice is symmetrical with respect to the keeper aperture. The location of the baffle supports is evident from the three radial markings that extend out to the endwall. The only unusual feature apparent in Figure E-26 is the "amalgamated" appearance of the Philips-head screws that attach the cathode-vaporizer assembly to the endwall. Figure E-27 is a closeup of the cathode-keeper aperture and demonstrates the symmetry and "normal" appearance of the cathode orifice.

Plug gages were used to estimate the diameter of the cathode and keeper apertures, which were found to be $0.009 \leq d_o \leq 0.010$ in. ($0.023 \leq d_o \leq 0.025$ cm) and $d_{ck} = 0.098$ in. (0.249 cm), respectively. These dimensions compare very favorably with nominal fabrication values of 0.010 in. and 0.099 in., + 0.002, − 0.001 in., respectively.

c. Magnetic-Field

A gaussmeter was used to survey the exterior magnetic field prior to disassembly of the discharge chamber and removal of the ion-extraction assembly. All magnet polarities were the same, and magnetic-field values of 45-55 gauss were measured along the length of the magnets. With the ion-extraction assembly removed, detailed field measurments were conducted within the discharge chamber. Although similar detailed measurements were not performed during the assembly of thruster S/N 903, the post-test measurements are similar to those conducted during the assembly of the flight-test thrusters. Axial-field measurements performed on thruster S/N 903 at the time of its assembly are presented in Figure E-28, along with the post-test measurements (shown in parentheses). The largest difference in the axial (B_z) component for the two sets of data is 6 percent. The axial location of the maximum in the magnetic-field data is the same for both sets of measurements.

M14986

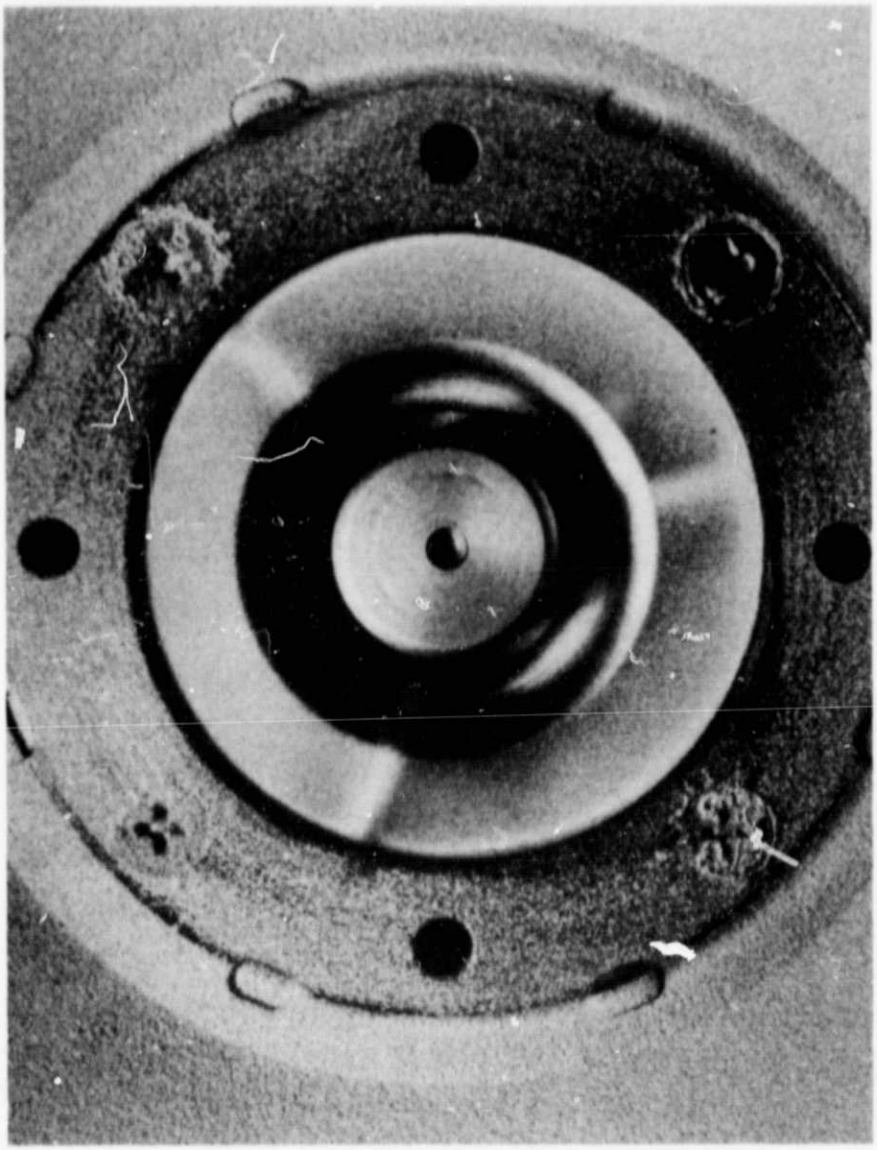

Figure E-26. Post-test appearance of cathode keeper.

M14998

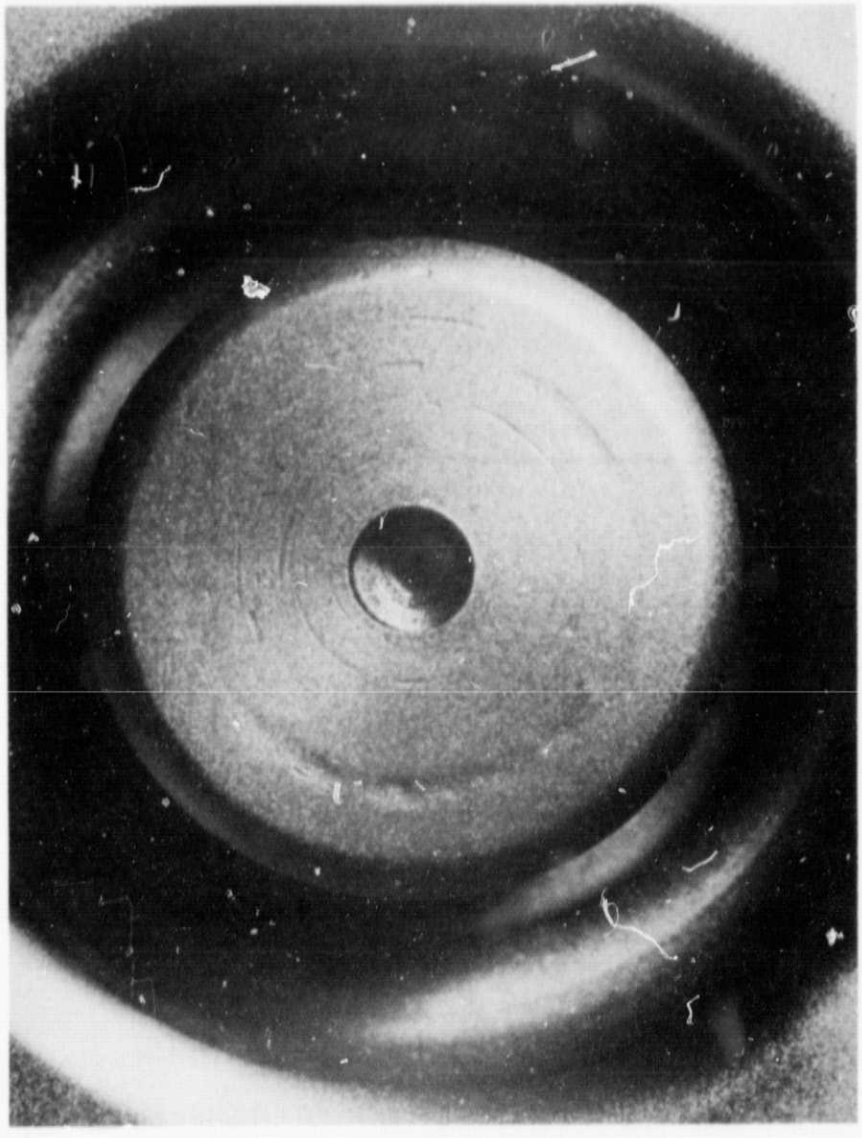

Figure E-27. Post-test appearance of cathode keeper.

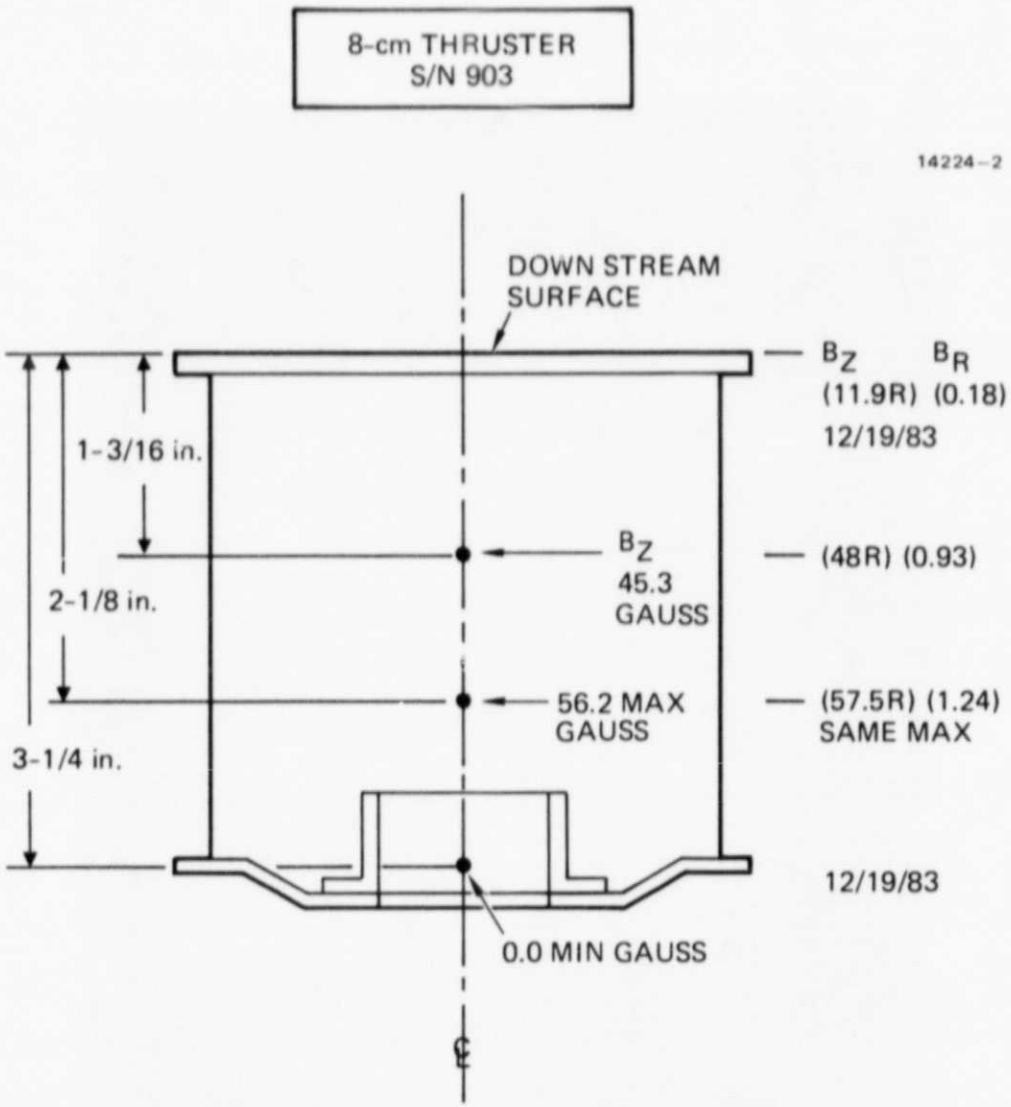

NOTE: MAGNETS INSERTED NORTH POLE TO OPTIC (DOWN STREAM) SIDE.

ASSEMBLY CONSISTS OF THRUSTER SHELL ASSY WITH ANODE, END PLATE AND CATHODE POLE (OPTICS REMOVED).

Figure E-28. Pre-test and Post-test magnetic field measurements. Post-test values in parenthesis.

3. Neutralizer Assembly

Figure E-29 shows the appearance of the neutralizer assembly. The only abnormality noted was the appearance of the braided keeper lead, which was discolored and suggested an excessive keeper current was drawn at some point after assembly. The keeper lead was the only electrical lead that was discolored, and the contrast between it and the other current conductors was quite noticeable (cf the neutralizer keeper and heater leads of Figure E-29. Figure E-30 is a closeup of the neutralizer-feedline transition, showing that the braze joint is "drawn in", but there is no evidence of a crack at the juncture. The discoloration of the keeper lead is also apparent in this photo.

A closeup of the downstream side of the neutralizer keeper is presented in Figure E-31, showing good alignment of the cathode and keeper apertures. The keeper has an unusual appearance (in comparison to Figure E-27, which we attribute to the buildup of (as yet not determined) material. Measurements of the keeper aperture showed the diameter to be d_{nk} = 0.056 in. (0.142 cm), which indicates the hole decreased in size (the nominal fabrication value is 0.070 ± 0.001 in. or 0.178 ± 0.003 cm, apparently as a result of sputter deposition of material from the cathode orifice plate.

Figures E-32 and E-33 show the appearance of the neutralizer cathode after removing the keeper. The flame-sprayed alumina was "snow-white", and only a few very-fine cracks were evident. The cathode orifice plate did show signs of significant erosion, however, and the cylindrical throat region of the orifice plate was no longer visible. The shape and dimensions of a newly fabricated component are presented in Figure E-34a. Figure E-34b presents the results of measurements performed using a micrometer and plug gages to determine the indicated dimensions of the orifice plate, and upon comparison, it is apparent that the neutralizer orifice has undergone substantial erosion.

M15003

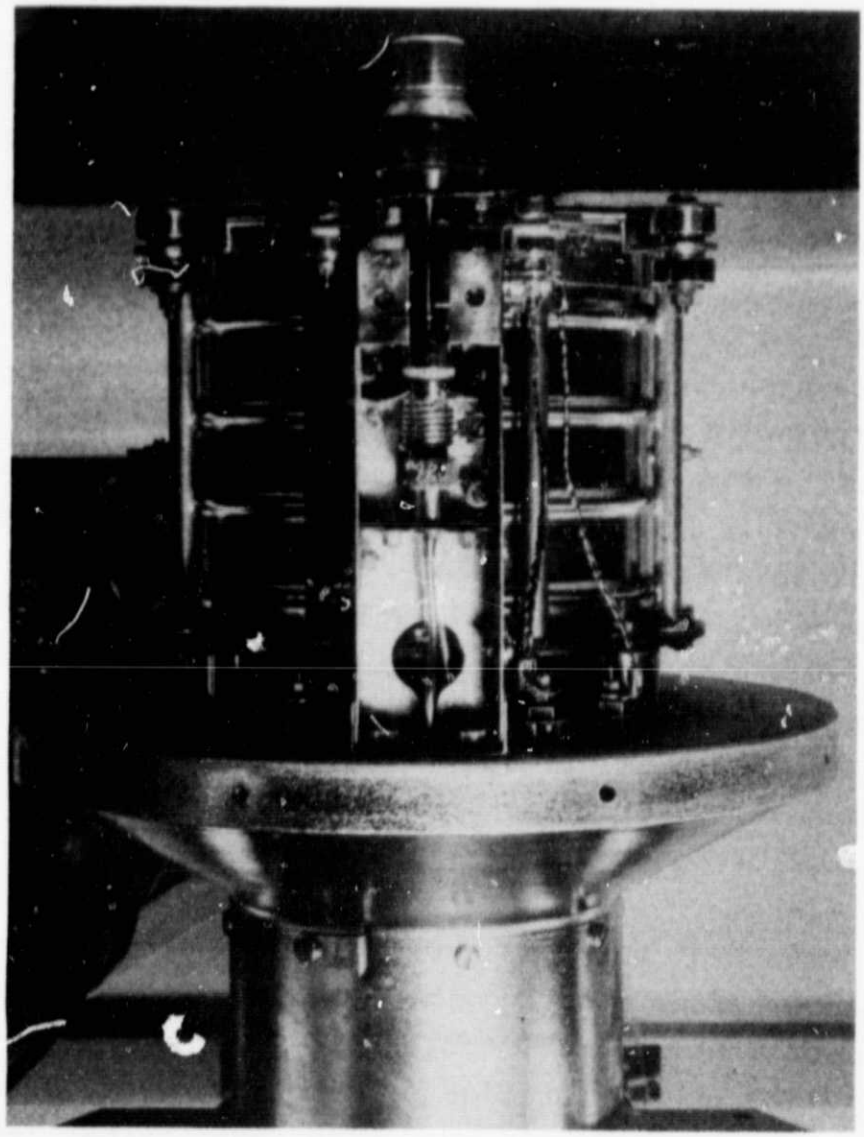

Figure E-29. Post-test appearance of neutralizer assembly.

M15002

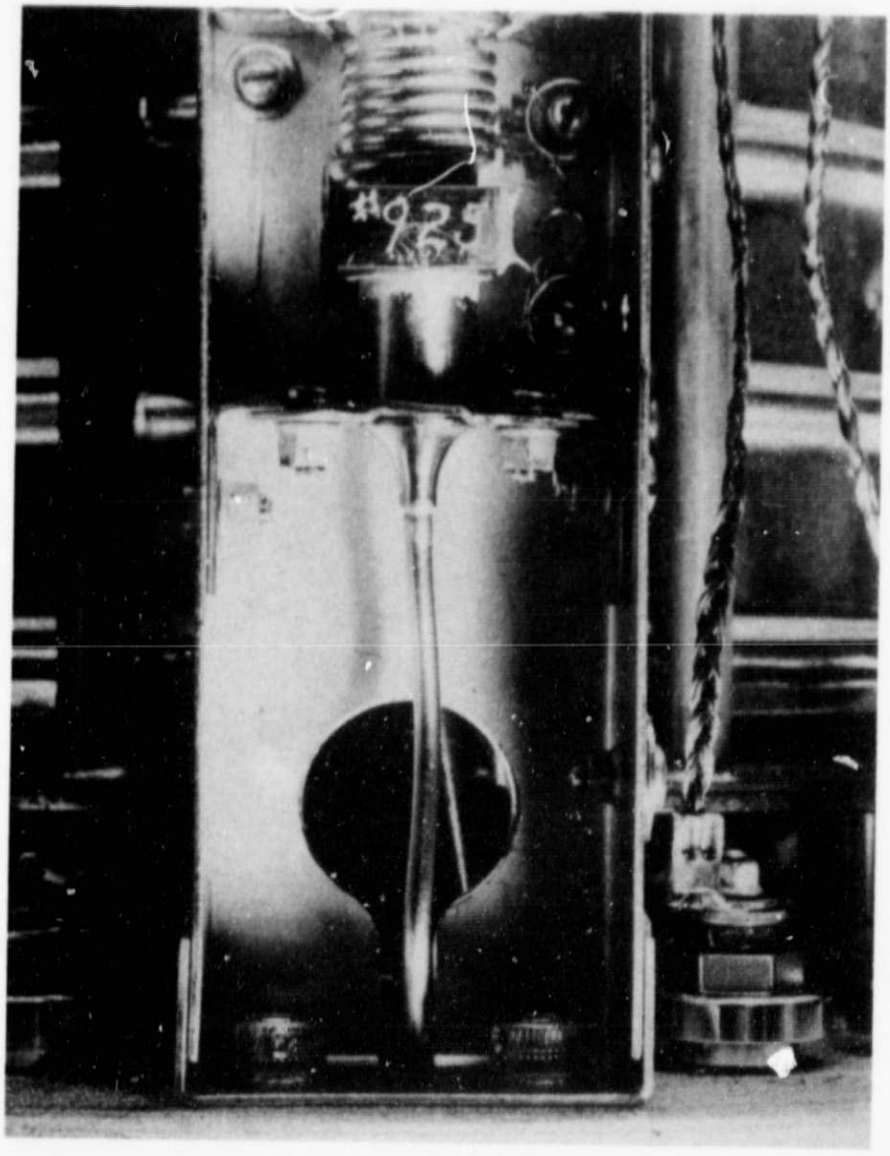

Figure E-30. Post-test appearance of neutralizer feedline transitions.

M14993

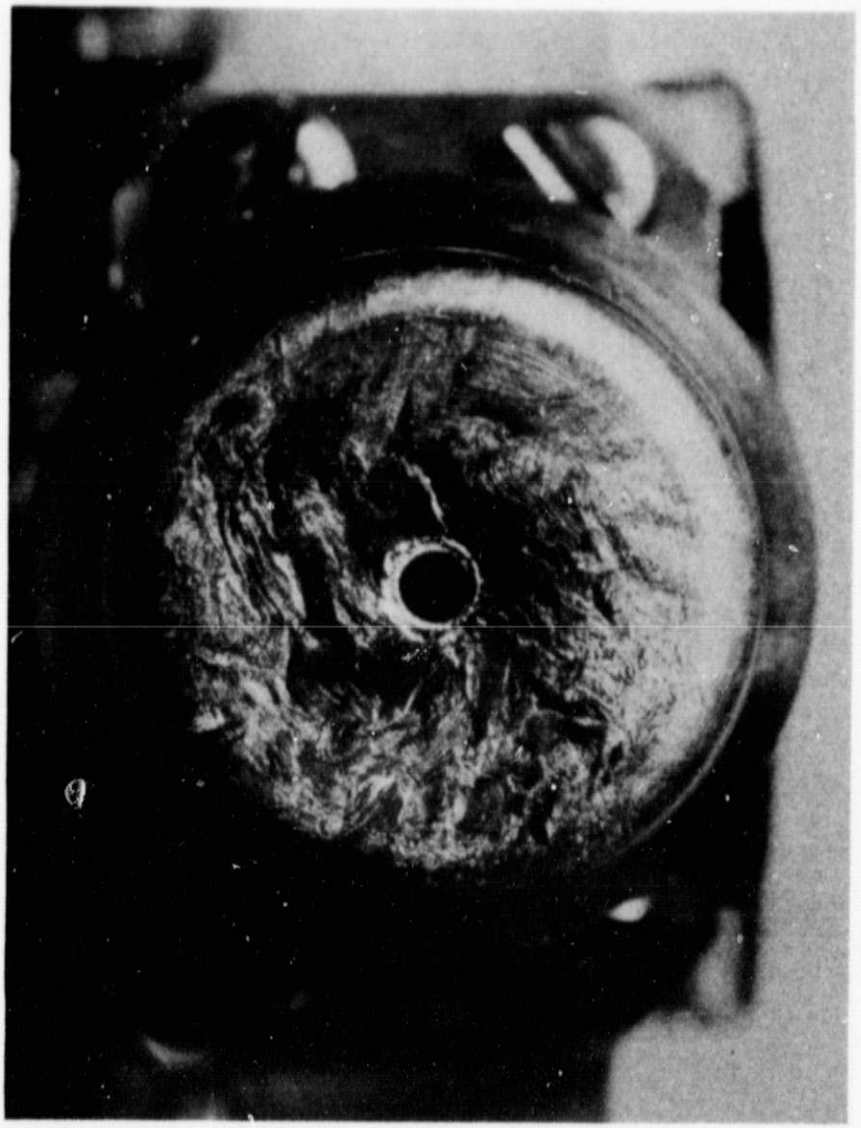

Figure E-31. Post-test appearance of neutralizer keeper.

M14995

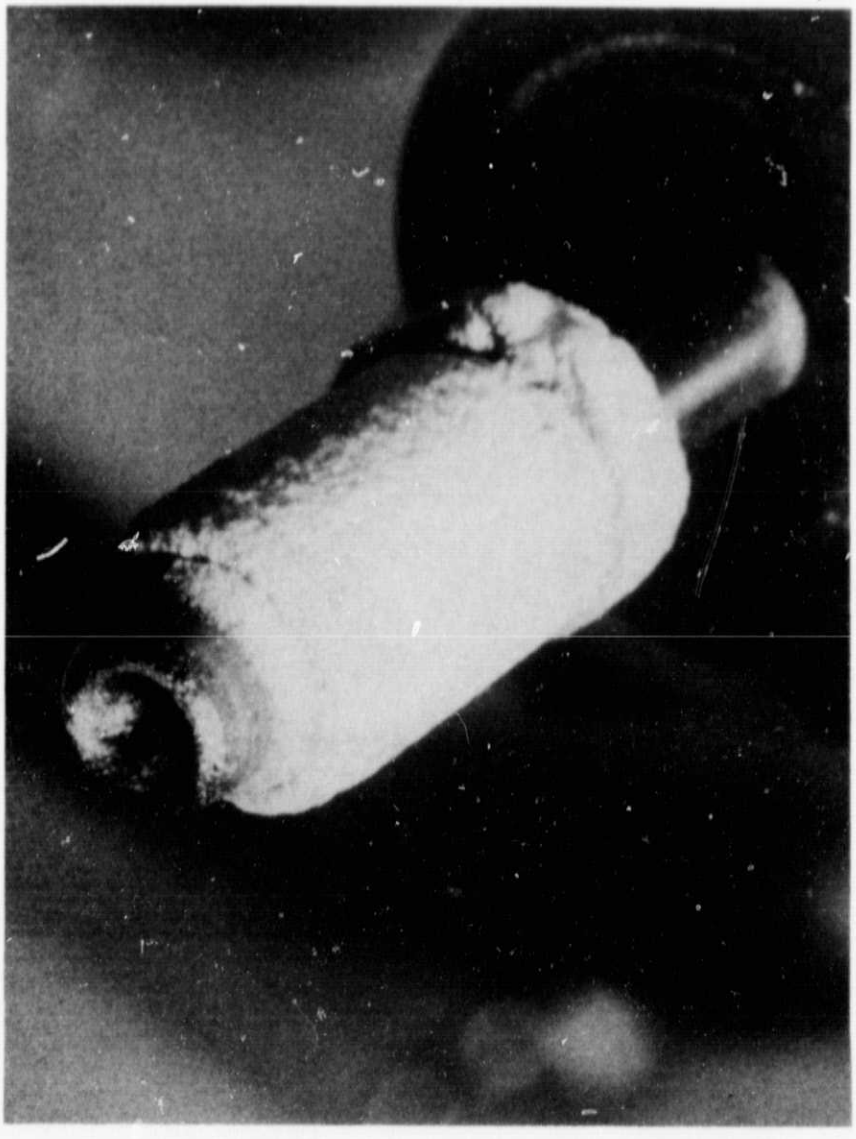

Figure E-32. Post-test appearance of neutralizer cathode.

M14996

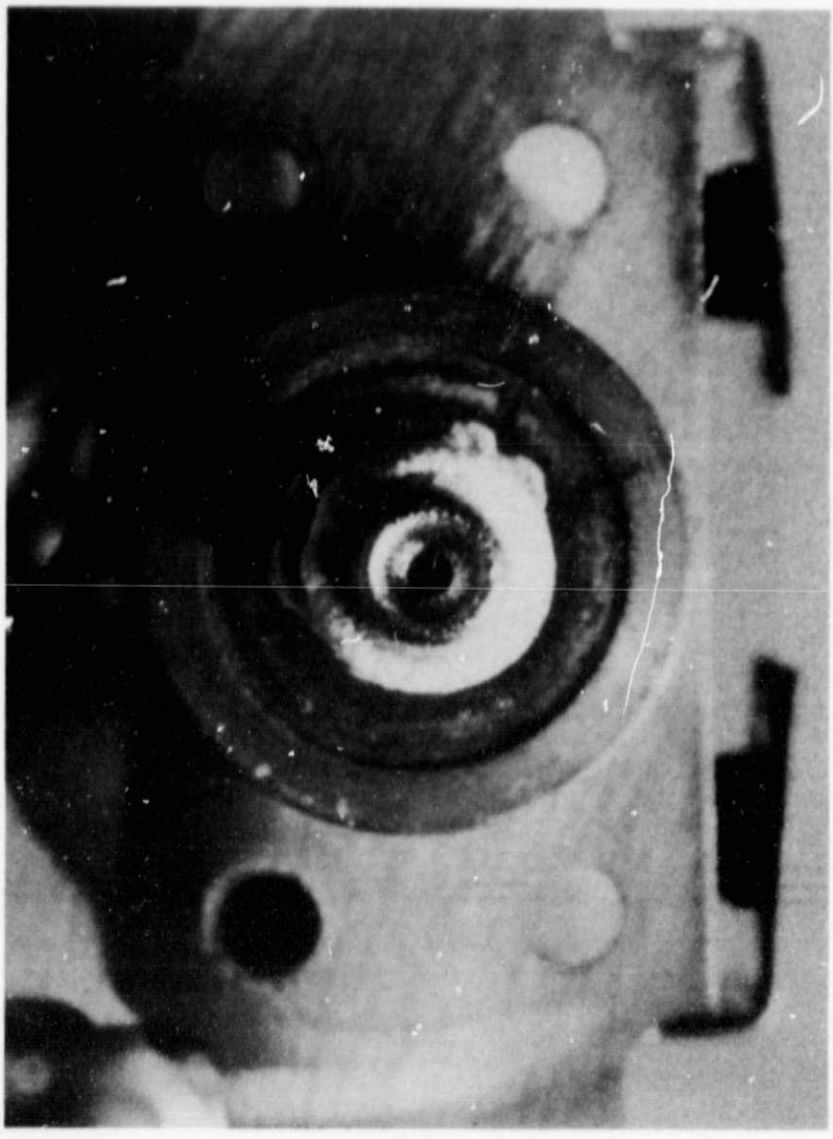

Figure E-33. Post-test appearance of neutralizer cathode.

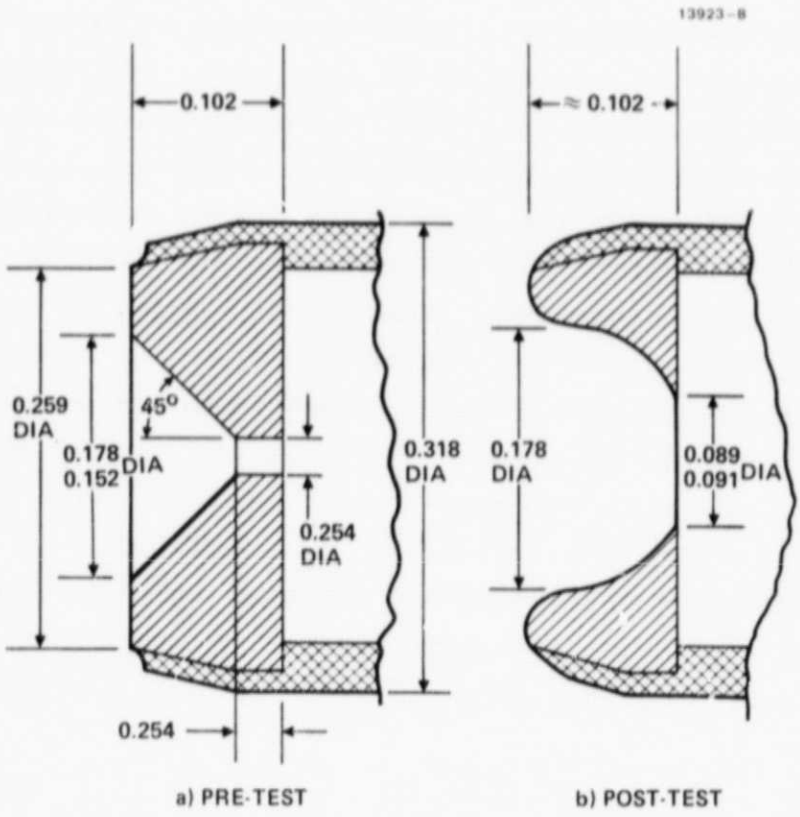

Figure E-34. Cross-section of neutralizer cathode orifice (dimensions in cm).

4. Beam Shield

Figure E-35 is a photo of the exterior side of the beam shield. Although there is some discoloration evident, the only departure from the appearance of a newly fabricated beam shield is the existence of several locations where is appears that the composite "weave" is beginning to separate. The general consensus of opinion was that this separation may have resulted from the pre-lifetest vibration test.

Figure E-36 shows the appearance of the interior side of the beam shield, which does not indicate any clearly defined region of beam interception. There does appear to be a divergent pattern emanating from the region near the neutralizer orifice, but the source of the discoloration is unclear. There is also evidence of material buildup in the region of the beam shield that separates the two cylindrical regions. It appears that in some places the buildup of material has come off, leaving relatively "clean" weave material behind. The black spots nearer the edge of the shield are thought to be produced when sputtered material (gray) flakes off the surface.

5. Gimbal

Figures E-37 and E-38 show the gimbal unit with its covers removed for inspection. The appearance is "normal", with no noticeable discoloration. There was no indication of propellant having leaked from any of the feedline connections. Figure E-39 shows the connector side of the gimbal. The 14-pin male connector was somewhat discolored, both on its exterior and the pins themselves. Several tiny mercury droplets were noticed in the cutout region that houses the gimbal pivot.

M14992

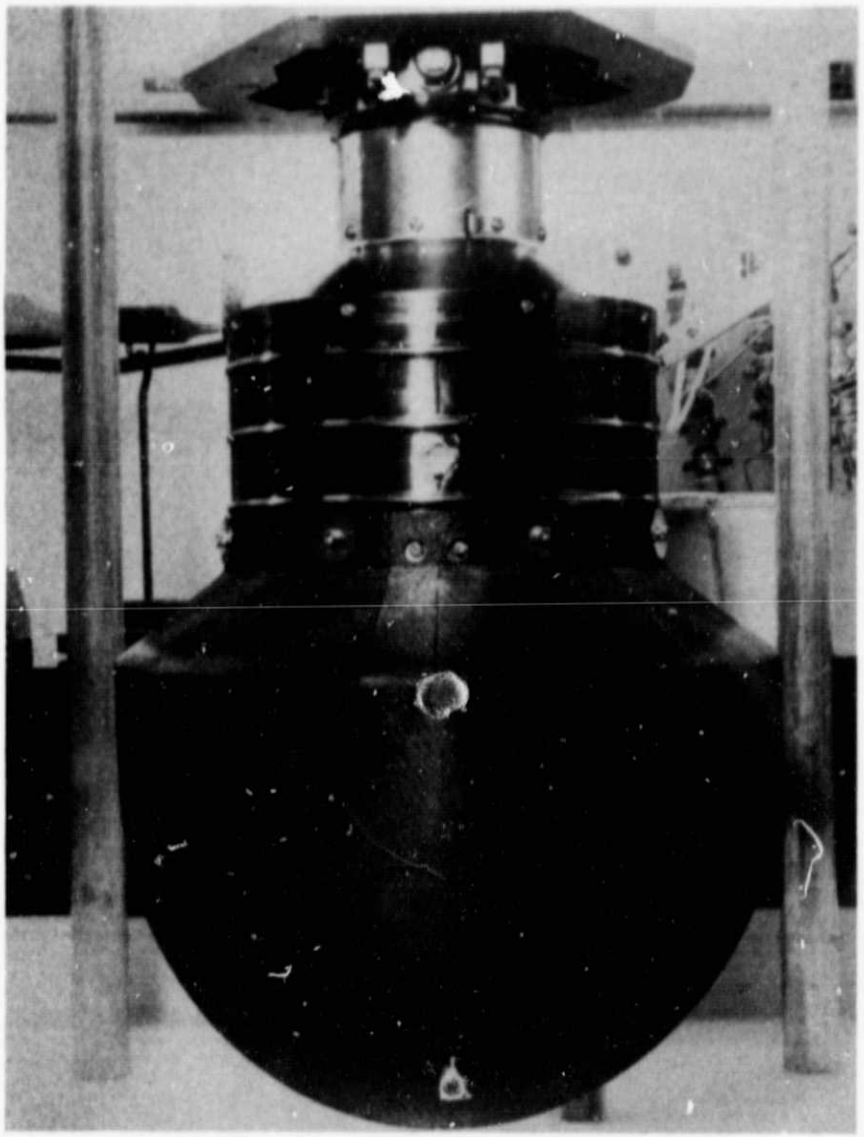

Figure E-35. Post-test appearance of back side of beam shield.

M14968

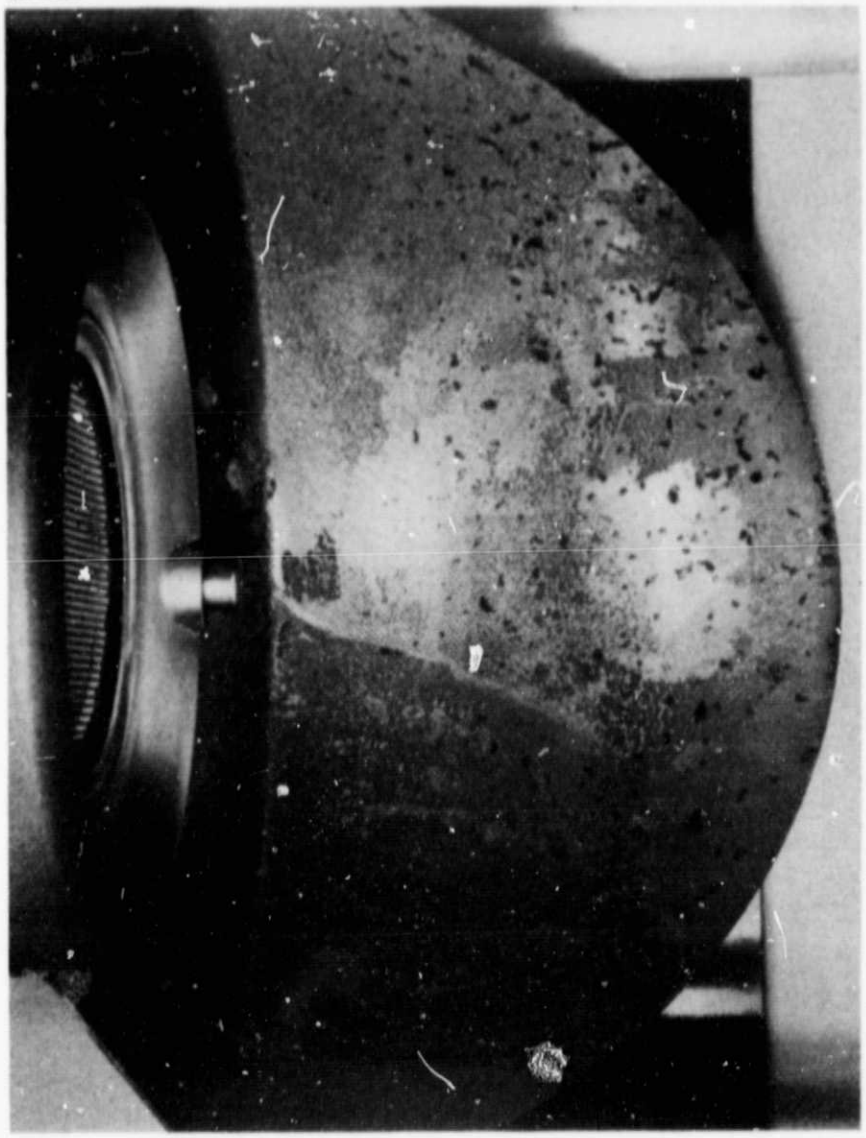

Figure E-36. Post-test appearance of interior side of beam shield.

M15001

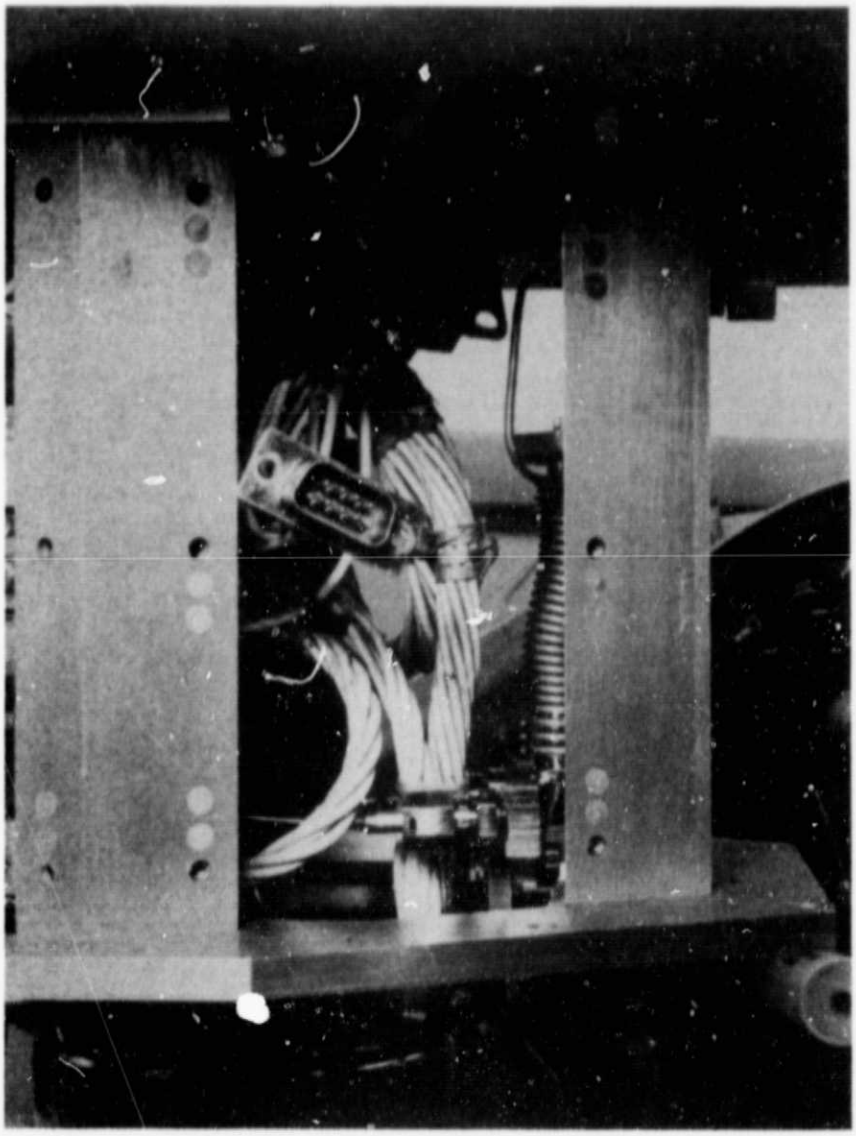

Figure E-37. Post-test appearance of gimbal with covers removed.

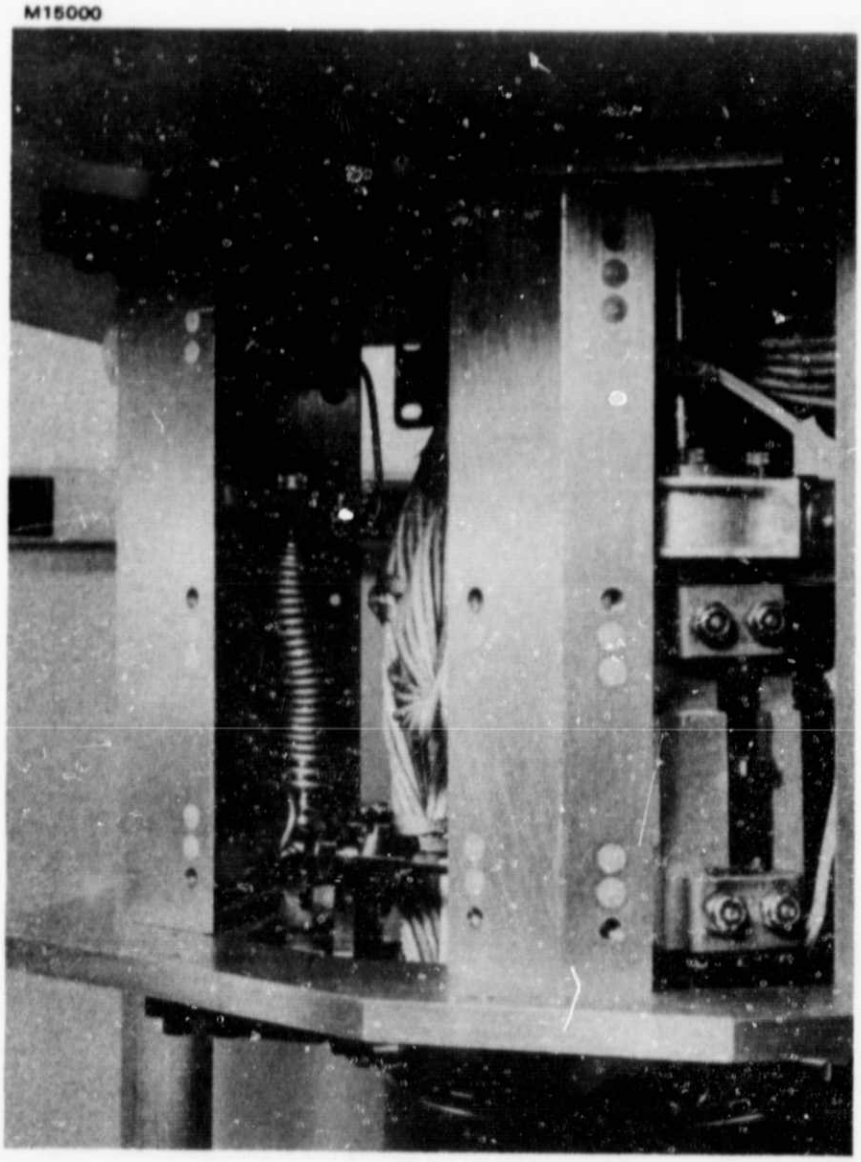

Figure E-38. Post-test appearance of gimbal with covers removed.

M14999

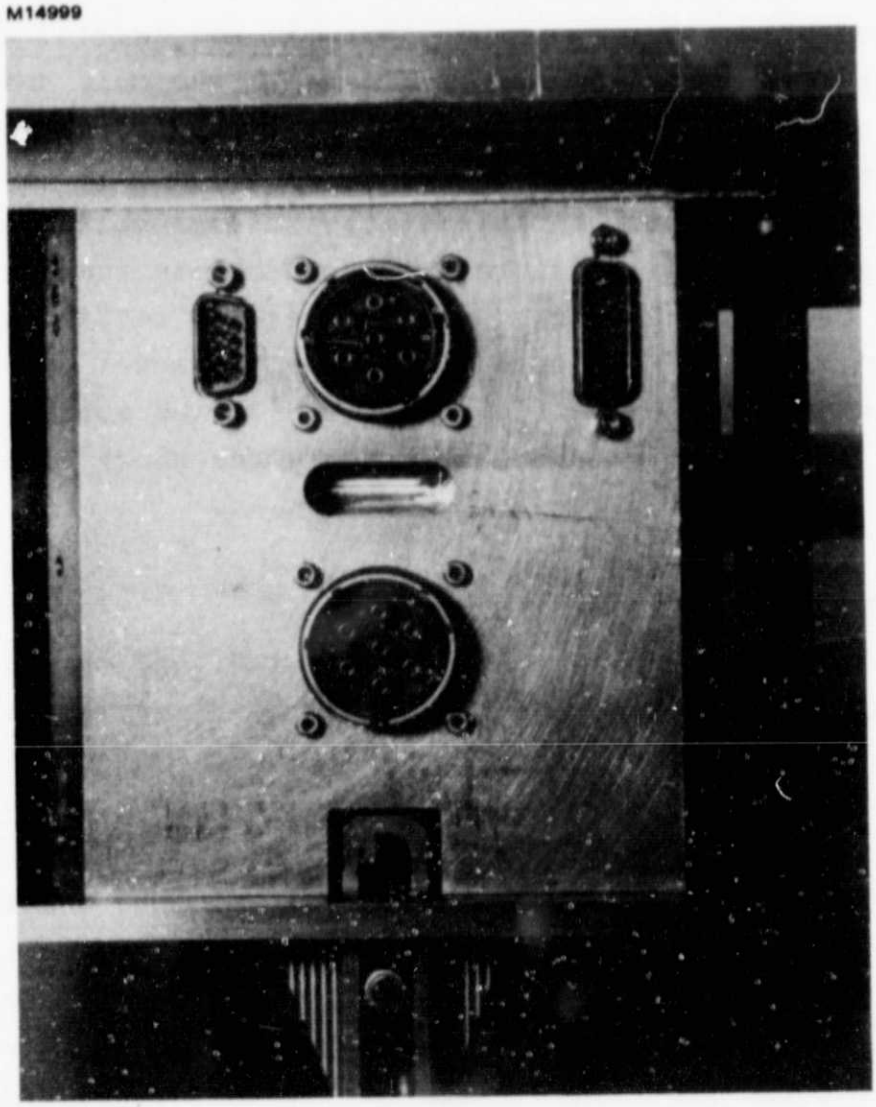

Figure E-39. Post-test appearance of gimbal connectors.

6. Resistance Measurements

Various resistance/open-circuit measurements were conducted at various stages during the disassembly and examination, and the results are summarized in Table E-1. The only anomalous finding was the resistance between screen and accel electrodes. These electrodes were shorted at the conclusion of the test and during the early part of the post-test disassembly and analysis. We removed the large, visible mercury droplets that were observed between the electrodes, and we also retrieved two pieces of material that were resting on the accel grid. None of these actions eliminated the short, but during subsequent handling of the ion-extraction assembly the short cleared itself.

7. Propellant Tank and Feedlines

The propellant tank, propellant valve, and pressure transducer were removed from the thrust system as an integral assembly. We were unable to detect any "sloshing" of residual propellant in the tank. Consequently, the amount (if any) of mercury remaining in the tank is very small.

The possibility of a liquid-propellant leak was investigated by pressurizing the inlet to the propellant manifold to a pressure of up to 100 psig (using ultra-pure argon), and then squirting alcohol on the feedlines, connections, and welds upstream of the vaporizers. No "bubbles" were detected, suggesting the absence of a liquid leak (assuming there was no mercury in the feedlines). We checked the torque of the neutralizer feedlines and found it to be less than the value called out in the assembly IPD. The advancement of the resistoflex nuts required to bring the tourque into specifications was measured and determined to be relatively small (see Table E-2).

Table E-1. Resistance Measurements

Description	Test Voltage V	Resistance Ω
Beam Shield surface	0	4-5 K
Neutralizer Keeper	500	5-6 M
Accel-to-screen	500	∞
	1000	2800 M
	1200	0
	500	2500 M
	600	2500 M
	800	2100 M
	1000	3200 M
	1100	0
	0	5.5
Anode-to-shell	100	∞
Cathode Keeper	500	5-6 M
Cathode-to-ground screen	0	20,000 M

Table E-2. Resistoflex Fittings

	Gap Between Nut and Manifold	
	Discharge-Cathode inches	Neutralizer inches
First measurement	0.045	0.049
Torque to 48 in-lbs	0.042	0.046

8. Sample Analysis

A total of six pieces of material was removed from the beam shield and from between the screen and accel electrodes. The small samples were placed in plastic containers, and a $Sm-Co_5$ magnet was used to determine whether or not the samples were magnetic. Table E-3 presents a summary of the results, indicating where the samples were obtained, and showing that only two of the samples that were removed from the beam shield were (slightly) magnetic. No magnetic attraction was observed on the samples that were found resting on the accel electrode.

This concluded the analysis of the first disassembly. The thruster was reassembled and underwent further testing. The mercury feedlines were disconnected from the manifold and individual burrettes were connected to the discharge and neutralizer vaporizers. A series of tests were made that determined the following:

- Neutralizer vaporizer flowrate was normal.
- Discharge vaporizer flowrate was excessive.
- New gridset had minor effect on mercury utilization.
- Ionization gage pressure measurements indicated that the region surrounding cathode isolator had a mercury pressure 30 times higher than other 8 cm thrusters.

The second disassembly took place after the ionization gage pressure measurements indicated that a mercury vapor leak appeared to be in the cathode isolator. The C-I-V assembly was removed from the thruster and is shown in Figure E-40 with the isolator shield in place. A ball of material can be seen next to the left screw on the flange that is brazed to the isolator. Closeups of the ball are shown in Figure E-41 and E-42. The material appeared to be granular and copper in color. Removing the shield, also disclosed a similar type of material at the downstream end of the isolator. This material followed the

Table E-3. Comparison of Beam Shield Samples

Sample No.	Location	Magnetic
1	Beam shield	No
2	Beam shield	No
3	Inside of mark (ground screen)	Yes
4	Beam shield	Yes
5	Between grids	No
6	Between grids	No

No - No attraction to SmCo market
Yes - Slight attraction to SmCo market

M15926

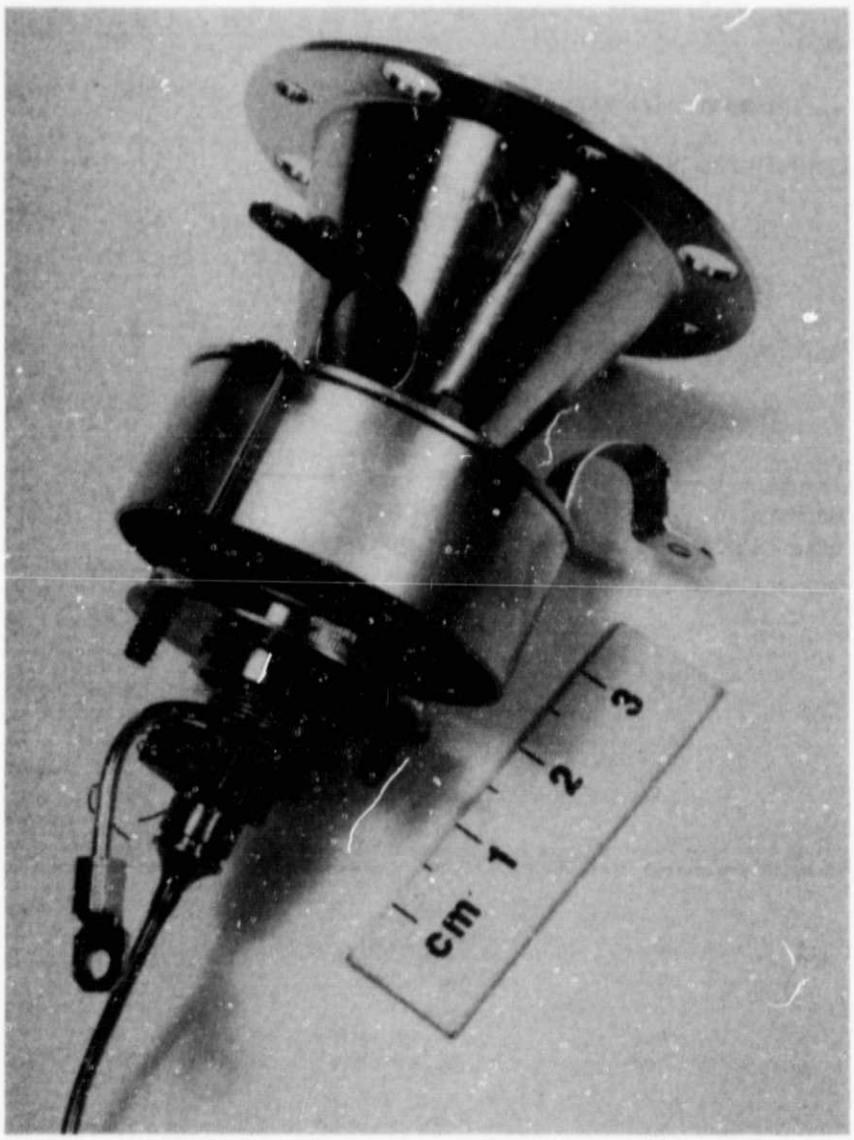

Figure E-40. Post-test C-I-V assembly.

M15928

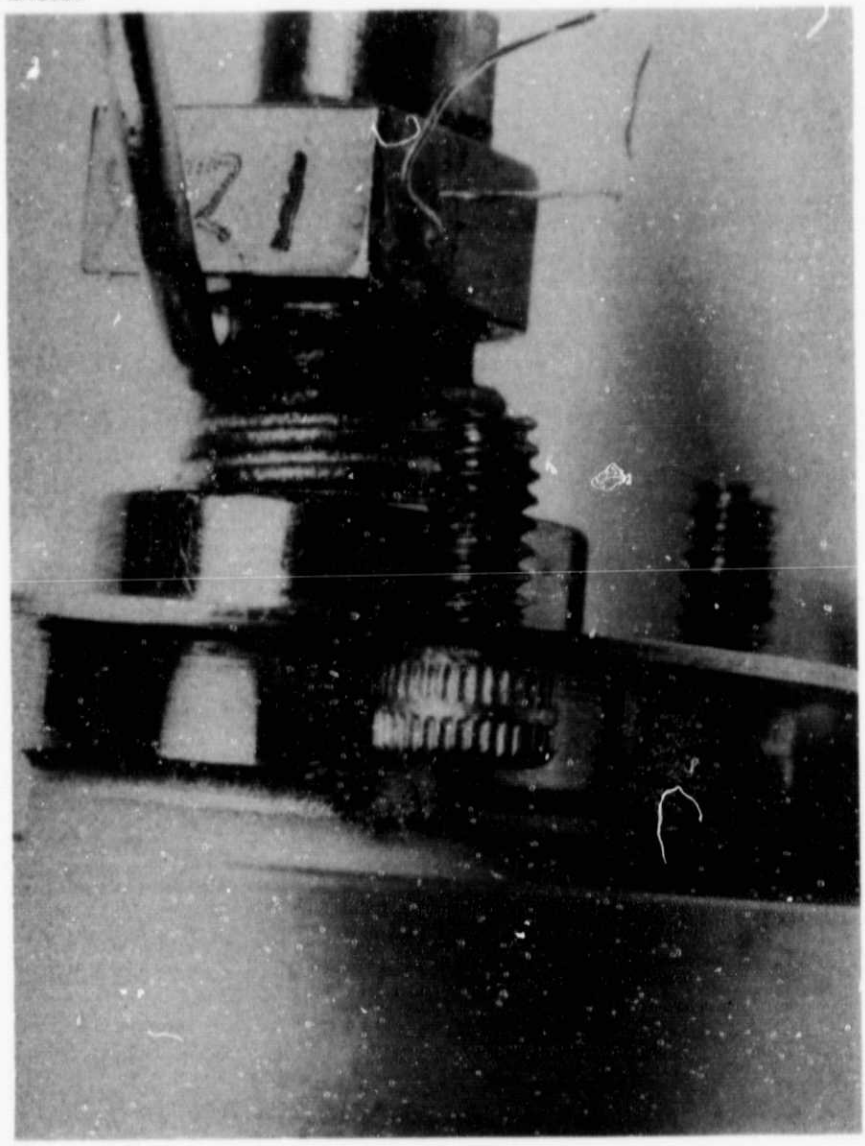

Figure E-41. C-I-V with ball of material on braze joint.

M15927

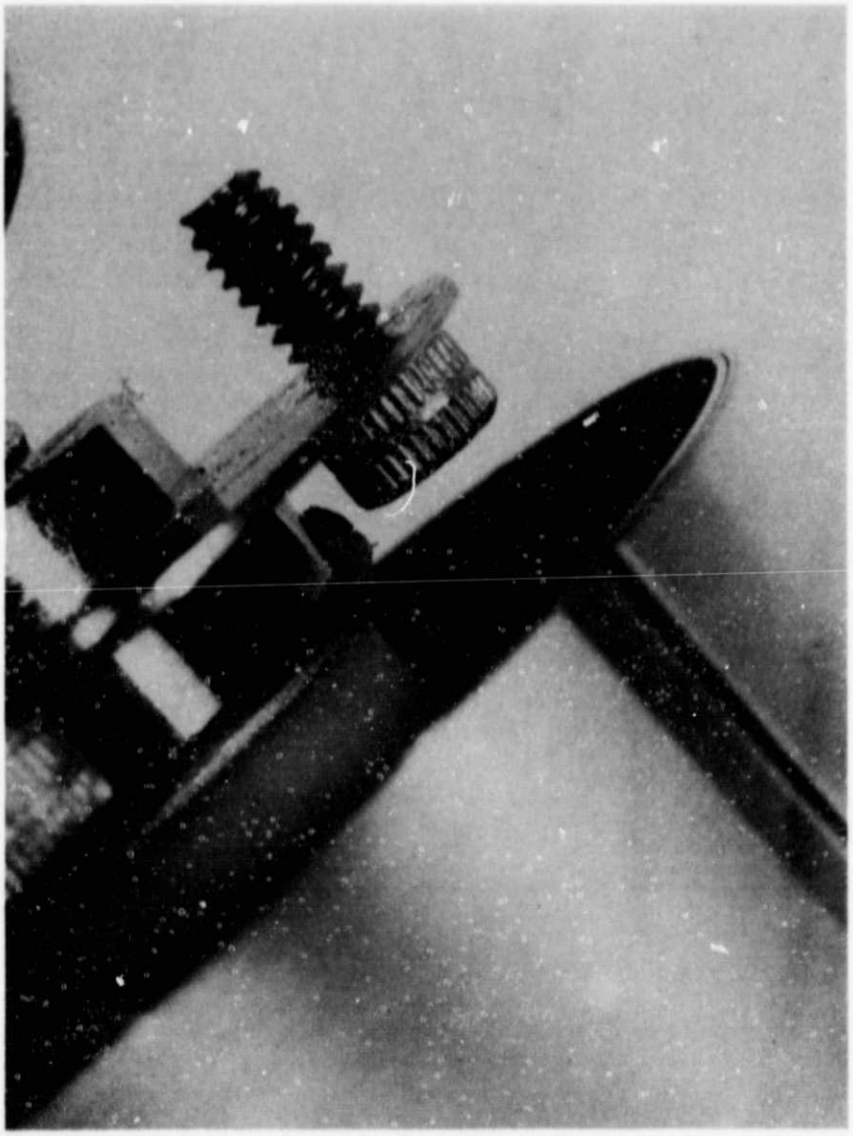

Figure E-42. C-I-V with ball of material on braze joint.

braze material for about 1/4 of the circumference of the braze joint as shown in Figure E-43. Except for the ball of material at the upstream end of the isolator and the material on of the joint circumference of the isolator at the downstream end, the braze looked normal.

Bubble checks made showed that both of the regions of the foreign material leaked. The region with the ball of material had the largest leak since it had to be sealed with epoxy before the smaller leak could be detected. After cleaning and sealing both regions with epoxy, the assembly was checked with a leak detector and found to be leak tight. The thruster was tested after this cathode isolator assembly was installed. The results of the test are listed in Table E-4; also listed in Table E-4 are the performance acceptance test results made prior to the start of the cyclic endurance test. It can be seen that the thruster performance has nearly attained the original PAT values. The discharge utilizations are identical; i.e., $\eta_{dish} = 0.83$. There is a slight difference in the discharge energies.

C. SUMMARY

The overall, general appearance of thruster S/N 903, its electronics module, and the interior of the Lifetest Facility was extremely "clean" (subsequent exposure to air and handling have degraded this appearance somewhat). In fact, even experienced ion-thruster technologists might be surprised, after viewing the thrust system, to learn that it had undergone over 9,000 hr of testing. The discharge chamber showed no obvious signs of erosion, deposition, or flaking' and its physical and magnetic properties were essentially unchanged, compared with those measured or specified at the time of its fabrication and assembly. There was no conclusive indication of a propellant leak, either in liquid or vapor form in the first disassembly, and there was no residual mercury detected around the propellant tank.

M15924

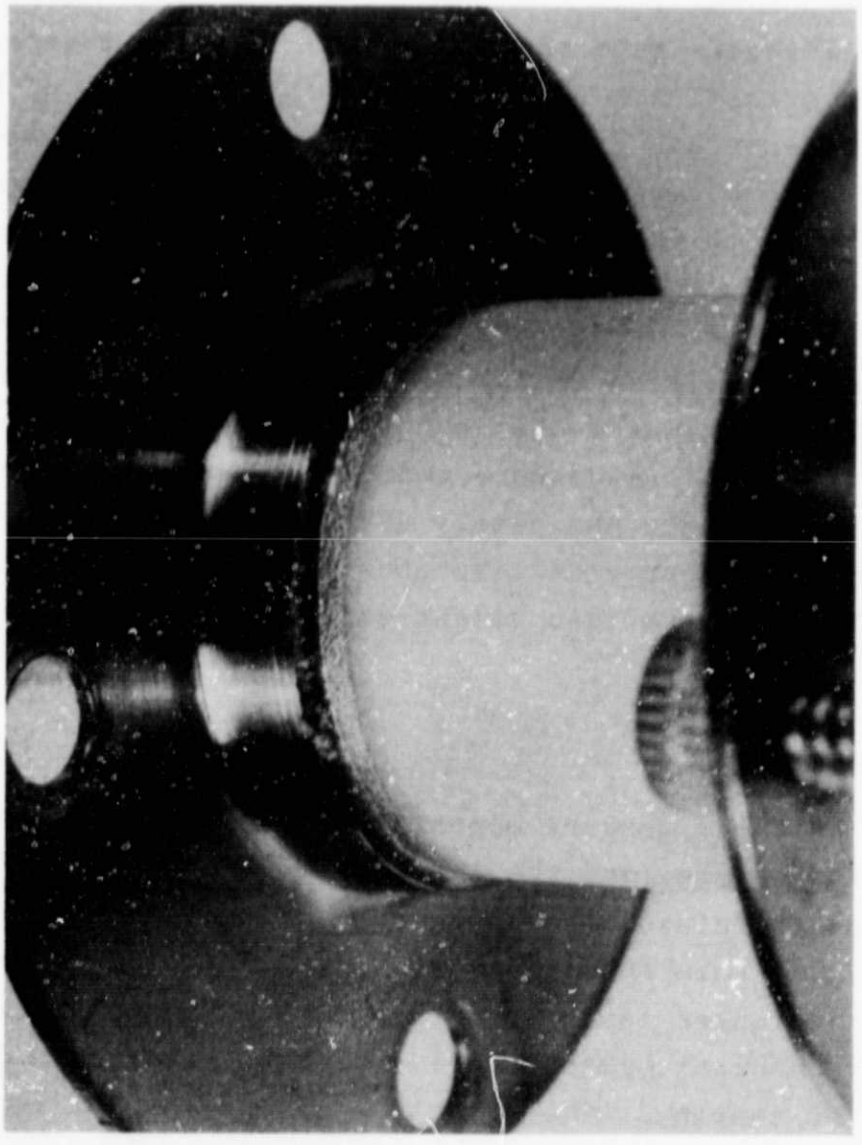

Figure E-43. Downstream isolator braze joint with foreign material.

Table E-4. Thruster Operating Values

Date Description	4/30/84 Sealed Isolator	12/4/80 First PAT
V_D,V	41.0	39.7
I_D,mA	417	386
V_{DK} V	13.2	12.7
I_{DK} mA	78	60
V_δ,V	27.0	27.0
V_{DH}, V	2.19	2.31
I_{DH}, A	1.16	1.16
V_{DV}, V	4.56	4.52
I_{DV}, A	1.56	1.64
V_{NK}, V	14.4	15.6
I_{NK}, mA	559	500
V_{NH}, V	2.98	2.85
I_{NH}, A	1.32	1.30
V_{NV}, V	2.05	2.30
I_{NV}, A	0.62	0.72
V_S, V	1164	1200
V_B, V	1186	1228
I_S, mA	72.0	72.0
V_A, -V	300	300
I_A, mA	0.21	0.23
V_C, -V	19.5	11.9
T_{DV}, °C	274	266
$\dot{m}_{DV}$, mA-Hg^+	87.25	86.4
T_{NV},°C	283	280
$\dot{m}_{DV}$, mA-Hg^+	6.23	4.98
$\dot{m}_{NV}$, mA-Hg^+	93.5	91.4
η_{Hg}	0.77	0.79
η_{Dish}	0.83	0.83
εi, eV/ion	252	223
P_{TOTAL}, W	127.9	128.7

After minimal (careful) handling of the ion-extraction assembly, the short between the screen and accel electrodes (that was present at the conclusion of the test) disappeared and reappeared. Both liquid mercury, as well as two pieces of (as yet unknown) material, were observed in the interelectrode gap. It is believed that the short was caused by the material buildup in the gap between the screen and accel grids at one of the apertures.

The orifice plate of the neutralizer cathode had undergone substantial erosion. The aperture diameter has increased from the nominal fabrication specifications of 0.010 in. (0.025 cm) to a measured post-test value of $0.035 < d_{nk} < 0.036$ in. The throat of the orifice (originally cylindrical in shape) has eroded to a shape that appeared to be a very thin; geometry that could result in a rapid increase in aperture diameter if erosion continued.

The accel electrode of the ion-extraction assembly has undergone substantial erosion caused by charge-exchange ions. In the center of the electrode, the familiar triangular-shaped pits that form in the regions bounded by three adjacent apertures had eroded all the way through. The diameter of the accel apertures has increased to about 0.048 in. (0.122 cm) in the large-aperture region. The enlarged apertures result in a calculated increase in open area of about 9 percent. If the open area of the triangular pits is considered, this value will be slightly higher. The increase in the open area of the accelerator electrode undoubtedly produced a corresponding increase in neutral loss and a reduction in propellant-utilization efficiency, leading to higher-than-normal production of charge-exchange ions and consumption of propellant.

One of the accel apertures near the center of the electrode underwent erosion of its web in such a way that can only be interpreted as the result of direct impingement. It is believed that this erosion led to the buildup of material to create a grid short. The cause of the beamlet defocusing that would lead to such an observed erosion pattern was not determined. We cannot rule out the possibility of partial blockage of the adjacent screen aperture as the cause of the defocusing.

The three outermost rows of accel apertures have a notched shape. At one location near the edge of the accelerator-aperture pattern, an aperture has a peculiar out-of-round geometry.

The second disassembly and leak check of the isolator revealed two localized leaks in the regions of the abnormal braze material. Patching of these leaks and subsequent thruster testing restored the thruster performance to the original performance acceptance test values. The leak in the isolator caused the lower than expected mercury utilization.